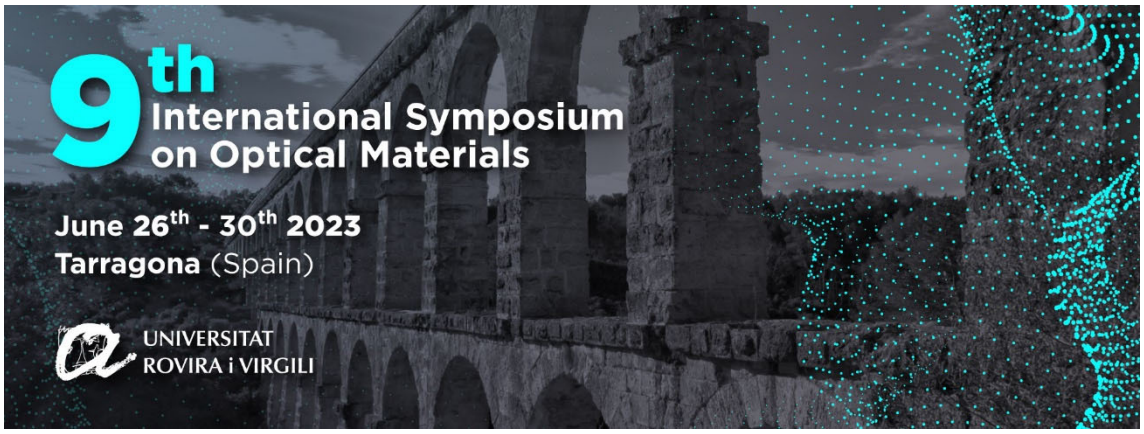

PROGRAM OF THE 9th INTERNATIONAL SYMPOSIUM ON OPTICAL MATERIALS, IS-OM'9

26th June, Monday

8:00 h Registration

9:00 h Opening welcome

9:30 h Luisa BAUSÁ. **Plenary**

Controlling the spatial coherence and subwavelength waveguiding of rare earth quantum emitters by plasmonic nanostructures

10:30 h Coffee break

11:15 h Amina BENSALAH-LEDOUX. Invited

Chirality at the molecular scale: materials and spectroscopy

11:40 h ~~Ismail MEKKAOUI. Oral~~ CANCELLED

~~*Fluorescence time decay of 1,2-Indanedione-arginine and applications*~~

11:55 h Natalia JURGA. Oral

Designing photon upconversion nanoparticles showing luminescence in whole human blood

12:10 h Akira YOSHIKAWA. Invited

Crucible-free bulk crystal growth of oxide single crystals using OCCC method

12:35 h Kacper PROKOP. Oral

Structural and spectroscopic properties studies of perovskite-type cubic Nd3+-doped $M_3Y(PO4)_3$ ($M = Sr^{2+}$ or Ba^{2+}) solid-solution

12:50 h Lukasz DUDA. Oral

Organic dye-doped systems based on different matrices: properties and potential applications

13:05 h Lunch on-site

14:30 h Kheirreddine LEBBOU. Invited

Recent progress on GAGG (Ce,Mg) single crystal growth and their performance for high energy physics

14:55 h Andrey TURSHATOV. Invited

Tracer-based sorting with lanthanide-activated phosphors for plastics recycling

15:20 h N. SARUKURA. Invited

Spectral Imaging of cultural assets using newly developed fluoride ultraviolet optics

~~**15:45 h** A. DIKSHIT. Oral~~ CANCELLED

~~*TCAD assessment of hybrid perovskite solar cell incorporating NiOx as HTL and TiO2 as ETL*~~

18:30 h. Welcome reception

27th June, Tuesday

8:00 h Registration

9:00 h Muhammad Ali BUTT. Invited

HYPHa project - A voyage of developing a low-cost integrated photonic platform

9:25 h Eva MIHÓKOVÁ. Invited

Lead halide perovskite nanocomposites for fast timing detectors

9:50 h Yuui YOKOTA. Invited

High pressure annealing effects on optical and scintillation properties for $Gd_3(Ga,Al)_5O_{12}$:Ce scintillator single crystal

10:15 h Georges BOULON. Oral

Investigations on the electric-dipole allowed $4f^25d \rightarrow 4f^3$ broadband emission of Nd^{3+}-doped $20Al(PO_3)_3$-80LiF glass for potential VUV scintillator of neutron detection

10:30 h Coffee break

11:15 h Rei SASAKI. Oral

Growth and scintillation properties of $LaCl_3$/6LiCl /$SrCl_2$ ternary eutectic for thermal neutron detection

11:30 h Karol BARTOSIEWICZ. Oral

Correlation between Sc concentration and $Lu_3(Al,Sc,Ga)_5O_{12}$:Pr single crystal lattice distortion, atom distribution, Raman, luminescence, and scintillation properties

11:45 h Christophe DUJARDIN. Oral

Nanoporous scintillators for radioactive gas detection

12:00 h Mohamed MEHNAOUI. Oral

Structural and optical properties of dysprosium-doped calcium-oxyapatites $Ca_{10-2x}Dy_xLi_x(PO_4)_6O_2$ ($0 \leq x \leq 1$)

12:15 h Melvin John EMPIZO. Oral

Ce^{3+} centers in scintillating lithium fluorophosphate glasses

12:30 h Keito SHINOHARA. Oral

Pr^{3+} ion energy levels and decay times of scintillating fluoride glasses

12:45 h Masao YOSHINO. Oral

Growth, scintillation properties, pulse shape discrimination capability of (Ca,Sr)I_2:Eu scintillator

13:00 h Lunch on-site

14:30 h Tomasz GRYZYB. Oral

The use of Er^{3+} ions as sensitizers in upconverting nanoparticles: from synthesis to biological applications

14:45 h Nicolás PAZOS-PEREZ. Oral

Tuning the optical properties of gold nanostars

15:00 h Dominika PRZYBYLSKA. Oral

Core@shell structure with highly doped Nd^{3+} sensitizing ions for temperature sensing and bioimaging

15:15 h Agata SZCZESZAK. Oral

Inorganic nanoparticles based on rare earth elements for advanced applications

15:30 h Eugenio CANTELAR. Oral

Er^{3+}-doped CaF_2 nanocubes: Synthesis and optical characterization

15:45 h Jakub PAWLOW. Oral

Structural and spectroscopic properties of nano-crystalline Nd3+-doped $GdPO_4$ obtained by ionic liquid and oleic acid-assisted methods

18:00 h. Excursion

28th June, Wednesday

9:00 h Malgorzata GUZIK. Oral

New transparent optical ceramics based on isotropic and anisotropic oxide structures - challenges and perspectives

9:15 h Shekhar GUHA. Oral

Anisotropic thermo-mechanical properties of $BaGa_2GeS(e)_6$ crystals

9:30 h Valentin PETROV. **Plenary**

Acentric Barium chalcogenides for nonlinear optics in the mid-IR

10:30 h Coffee break

11:15 h Maria Jesús PASCUAL. Invited

Proccesing of rare-earth-doped nanostructured glass-ceramics for enhanced photoluminiscence

11:40 h I. LóPEZ. Invited

Second harmonic generation in femtosecond laser-induced damage structures in Nd:YAG crystals

12:05 h Makoto NAKAJIMA. Invited

Terahertz time domain ellipsometry and its application in wide-bandgap semiconductors characterization

12:30 h Luis SCALVI. Oral

Thin film deposition of organic-inorganic quinoline-tin dioxide pn-junction for optoelectronic devices

12:45 h Masood GHOTBI. Invited

BIBO: an effective nonlinear crystal for femtosecond optical parametric oscillators

13:10 h Lunch on-site

FREE TIME

29th June, Thursday

9:00 h Ionut Gabriel BALASA. Invited

Rare earth-diamond hybrid structures for optical quantum technologies

9:25 h Laura MERCADÉ. Invited

Silicon optomechanical crystal cavities for microwave signal processing and biosensing

9:50 h Luca GUERRINI. Invited

Chemosensing of low molecular weight biothiols via surface-enhanced Raman spectroscopy (SERS)

10:15 h Hendrik SWART. Oral

Laser-induced heating decimated luminescence nanothermometry using robust LaOF:Yb^{3+},Er^{3+} upconversion nanophosphor

10:30 h Coffee break

11:15 h Víctor LAVÍN. Oral

New strategies for efficient optical pressure & temperature sensors

11:30 h Anastasia BABKINA. Oral

Highly luminescent borogermanate glass with mixed perovskite $CsPb(Br,I)_3$ and $(Cs,Rb)Pb(Br,I)_3$ nanocrystals: properties and applications

11:45 h Anna KOZLOWSKA. Oral

Tailoring the optical and photometric properties of light sources based on dual-layer ceramics

12:00 h Yashashchandra DWIVEDI. Oral

Optical modulation and humidity sensing performance of Tb:Ce complex inhibited polymeric nanofibres

12:15 h Luis SCALVI. Oral

Ultraviolet excitation of persistent photoconductivity, close to room temperature, in composites of reduced graphene oxide and tin dioxide

12:30 h Yuriy ZORENKO. Oral

Recent developments of composite scintillators and LED converters based on the epitaxial structures of oxide compounds

~~**12:45 h** Ashutosh Kumar DIKSHIT. Oral~~ CANCELLED

~~*Effect of ZnO Nanorods on Nontoxic Pervoskite solar cell*~~

13:00 h Lunch on-site

14:30 h - 16:00 h POSTER SESSION

19:30 h. Gala dinner

30th June, Friday

9:00 h Mamoru KITAURA. Invited

Local structures of Tm ions in $Ca_2Al_2SiO_7$:Eu,Tm long persistent phosphorescence phosphor studied by X-ray fluorescence holography and positron annihilation lifetime spectroscopy

9:25 h Kei KAMADA. Invited

A novel $CeCl_3$/NaCl/$SrCl_2$ ternary eutectic scintillator for fast and high resolution radiation imaging applications

9:50 h Shunsuke KUROSAWA. Invited

Luminescent Properties of Ce-doped Garnet Transparent Ceramics Prepared by the Spark Plasma Sintering Process

10:15 h Yusuke URANO. Oral

Scintillation Properties of Tl-doped $Cs_3(Cu, Li)_2I_5$ Crystals for Cosmic Dark Matter Search

10:30 h Coffee break

11:15 h Daisuke MATSUKURA. Oral

Demonstration of Dose Rate Monitoring System with Garnet-Type Scintillators

11:30 h Sami SLIMI. Oral

Structure and luminescence properties of Dy^{3+} doped $Li_3Ba_2Gd_3(WO_4)_8$ tungstate for applications in wLEDs

11:45 h Giulio GORNI. Oral

Toward white light emission from Bi and V codoped borosilicate glasses upon UV excitation

12 h Closing ceremony

LIST OF POSTERS

1 *Dual green-red emission of Mn-doped Li_2O-ZnO-GeO_2 glass-ceramics*
Anastasiia Babkina

2 *Localized-enhancement of 1L MoS_2 photoluminescence on ferroelectric domain walls*
Joan Javier Ronquillo Tutiven

3 *Modelling of spectral response of electrically biased suspended graphene over variable trench depth*
Kamila Leśniewska-Matys

4 *Surface waveguides with modal shaping in Nd:YAG crystal for sensing applications: design and fabrication with femtosecond laser pulses*
Víctor Arroyo Heras

5 *Material aspects of Yb:CNGG lasers*
Carlos Zaldo

6 *Optical and Scintillation Properties of Pr^{3+}-Doped (La, Y)$_2Si_2O_7$ Single Crystals*
Yuka Abe

7 *Luminescence and scintillation properties of Tb,Ce co-doped (Gd,La)$_2Si_2O_7$ for radiation imaging*
Rikito Murakami

8 *Crystal Growth and Optical Properties of Ce-doped (Gd, Y, Tb)$_3Ga_3Al_2O_{12}$ Scintillators for X-ray Imaging*
Kazuya Omuro

9 *Excitonic luminescence in (Lu,Y)$_2SiO_5$:Ce^{3+} single crystals*
Vladimir Pankratov

10 *Influence of swift heavy ions on structural and luminescent properties of several important optical and scintillator materials*
Viktorija Pankratova

11 *Optical and luminescence investigation of barium borate doped with Ce^{3+} under ultraviolet (UV) excitation for scintillating glasses*
Masahiro Yamashita

12 *Optical thermometry properties of a novel quaternary tungstate $Li_3Ba_2Gd_3(WO_4)_8$: Ho, Tm*
Sami Slimi

13 *New nanoprobe designs for bioimaging and contactless luminescence thermometry*
Carlos Zaldo

14 *Fabrication of surface relief gratings (SRGs) in hydrogen bonded polymer-dye complexes and their replication for security features*
Łukasz Duda

15 *Photoluminescence and Raman spectroscopy of Ce^{3+} doped $Y_3Al_5O_{12}$ single crystalline films LPE grown onto $Y_3Al_5O_{12}$ and $Lu_3Al_5O_{12}$ substrates*
Anton Markovskyi

16 *Optimization of photolithography process using negative tone resist towards obtaining high-quality photonic structures*
Jakub Pawłów

17 *Fabrication of Mach-Zehnder interferometer structures based on low-cost SiO_2:TiO_2 optical platform for integrated photonics applications*
Kacper Prokop

18 *Transmission measurements of GaAsP layers grown from the vapour phase by heteroepitaxy*
Valentin Petrov

19 *Second harmonic microscopy of femtosecond laser micro-modifications in BBO crystal*
Nuria Sevilla-Sierra

20 *Application of hard metal (Al, Cu, Cr) masks for dry etching of sol-gel-derived silica-titania photonic structures*
Łukasz Duda

~~**21** *Structural and optical properties of nd3+ doped $Sr_6Y(PO_4)_5$ phosphor*~~
~~**Abdessalem Badri**~~ CANCELLED

	26 June		27 June		28 June		29 June		30 June
	MONDAY		**TUESDAY**		**WEDNESDAY**		**THURSDAY**		**FRIDAY**
8 h	**registration**	**8 h**	**registration**						
9 h	**Opening welcome**	**9 h**	A. BUTT / Invited	**9 h**	M. GUZIK / Oral	**9 h**	I. BALASA / Invited	**9 h**	M. KITAURA / Invited
9:30 h	Plenary: Prof. Luisa BAUSÁ	**9:25 h**	E. MIHÓKOVÁ / Invited	**9:15 h**	S. GUHA / Oral	**9:25 h**	L. MERCADÉ / Invited	**9:25 h**	K. KAMADA / Invited
10:30 h	**Coffee break**	**9:50 h**	Y. YOKOTA / Invited	**9:30 h**	Plenary: Dr. Valentin PETROV	**9:50 h**	L. GUERRINI / Invited	**9:50 h**	S. KUROSAWA / Invited
11:15 h	A. BENSALAH-LEDOUX /Invited	**10:15 h**	G. BOULON / Oral	**10:30 h**	**Coffee break**	**10:15 h**	H. SWART / Oral	**10:15 h**	Y. URANO / Oral
11:40	~~I. MEKKAOUI / Oral~~	**10:30 h**	**Coffee break**	**11:15 h**	M.J. PASCUAL / Invited	**10:30 h**	**Coffee break**	**10:30 h**	**Coffee break**
11:55 h	N. JURGA / Oral	**11:15 h**	R. SASAKI / Oral	**11:40 h**	I. LóPEZ / Invited	**11:15 h**	V. LAVÍN / Oral	**11:15 h**	D. MATSUKURA/ Oral
12:10 h	A. YOSHIKAWA / Invited	**11:30 h**	K. BARTOSIEWICZ / Oral	**12:05 h**	M. NAKAJIMA / invited	**11:30 h**	A. BABKINA / Oral	**11:30 h**	S. SLIMI / Oral
12:35 h	K.PROKOP /Oral	**11:45 h**	C. DUJARDIN / Oral	**12:30 h**	L. SCALVI / Oral	**11:45 h**	A. KOZLOWSKA / Oral	**11:45 h**	G. GORNI / Oral
12:50 h	L. DUDA /Oral	**12 h**	M. MEHNAOUI / Oral	**12:45 h**	M. GHOTBI / Invited	**12 h**	Y. DWIVEDI / Oral	**12 h**	Closing ceremony
13:05 h	**Lunch on-site**	**12:15 h**	M. EMPIZO / Oral	**13:10 h**	**Lunch on-site**	**12:15 h**	L. SCALVI / Oral		
14:30 h	K. LEBBOU/ Invited	**12:30 h**	K. SHINOHARA / Oral			**12:30 h**	Y. ZORENKO / Oral		
14:55 h	A. TURSHATOV / Invited	**12:45 h**	M. YOSHINO / Oral			**12:45 h**	~~A. DIKSHIT / Oral~~		
15:20 h	N. SARUKURA / Invited	**13 h**	**Lunch on-site**			**13 h**	**Lunch on-site**		
15:45 h	~~A. DIKSHIT / Oral~~	**14:30 h**	T. GRYZYB / Oral			**14:30 h**	POSTER SESSION		
16 h	end	**14:45 h**	N. PAZOS-PEREZ / Oral		**FREE**	**16 h**	end		
		15:00 h	D. PRZYBYLSKA / Oral						
		15:15 h	A. SZCZESZAK / Oral						
		15:30 h	E. CANTELAR / Oral						
18:30	**WELCOME RECEPTION**	**15:45 h**	J. PAWLOW / Oral			**19:30 h**	**GALA DINNER**		
		16 h	end						
		18	**EXCURSION**						

Ultraviolet excitation of persistent photoconductivity, close to room temperature, in composites of reduced graphene oxide and tin dioxide

André L. ALMEIDA, [a,b] Lucas P. FONSECA, [a] Lucas M. MARTINS, [b] Luis V A SCALVI [a]

[a] *São Paulo State University, Lab of Electro-Optical Experiments on Materials - Physics Dept-FC, Bauru, SP, Brazil* [b] *São Paulo State University, Chemistry Dept-FC, Bauru, SP, Brazil* luis.scalvi@unesp.br

Reduced graphene oxide (rGO) is reported with high electrical conductivity, with bandgap tuned in the range of 0.02 to 2.8 ev [1]. SnO_2/rGO devices deposited on Pt substrates constitute electrodes with the possibility gas detection [2]. In this work, rGO is synthesized by the method of Abdolhossseinzadeh et al. [3], and is combined with SnO_2 forming a composite, which is deposited on borosilicate glass substrates by spin coating, exhibiting very good electrical current stability in air, on the order of nA. Surprisingly, when the film is placed in vacuum (about 10^{-5} Torr), the current drops 2 orders of magnitude, decreasing slightly with lowering of temperature (in the range 150 – 300 K). It suggests that the material is preferentially adsorbing a reducing gas, which increases the amount of free electrons when exposed to air. Recently, the effect of ultraviolet light of a He-Cd laser (325nm) on this sort of film was reported, for similar samples but where the SnO_2 layer was slightly doped with 0.05at% of Er [4]. The general effect of the irradiating monochromatic light is to increase the conductivity about 6 orders of magnitude compared to the results in vacuum, changing from a current of 10 picoA, to a current of the order of 20 microA, under application of a voltage of 40 V. This experiment when performed at temperatures below room temperature leads the excitation with ultraviolet light to give rise to the phenomenon of persistent photoconductivity (PPC) even very close to room temperature. However, it is not clear the effect of the rare earth doping (Er^{3+}) on the PPC phenomena since the observable luminescence is green, unlike the Er^{3+} PL, preferentially in the near infrared. In this sense, we have built composites rGO/SnO_2 where the SnO_2 layer is not doped and the rGO proportion clearly affects the SnO_2 optical properties and the sample surface, as observed by optical transmittance and confocal microscopy images, leading to the presence of surface islands, for 3at% of rGO, which may contribute to optical confinement.

The strong response to ultraviolet light and the phenomenon of PPC indicates potential application in amplifiers, which could be adjusted by doping with rare-earths ions such as Eu^{3+} and Er^{3+}. The large difference in conductivity under light and in vacuum suggests application as sensors. Acknowledgements: FAPESP (Proc. 2018/09235-4 and 2022/08483-0)

References:

[1] Shen, Y; Yang, S.; Zhou, P.; Sun, Q.; Wang, P.; Li, J.; Chen, L.; Wang, X.; Ding, S.; Zhang, D.W.; *Carbon*, Vol. 62, **2013**, 157–164.

[2] C. Aydin, *J. Alloy Compd.*, Vol. 771, **2019**, 964-972.

[3] Abdolhosseinzadeh, S.; Asgharzadeh, H.; Kim, H.S.; *Sci. Rep.-UK*, Vol. 5, **2015**, 1-7

[4] Oliveira, L.S.; Fonseca, L. P.; Souza, R. D. ; Bueno, C. F.; Martins, L. M.; Scalvi, L. V.A.; *Current Appl. Phys.* Vol. 41, **2022**, 49–58

Second harmonic generation in femtosecond laser-induced damage structures in Nd:YAG crystals

[a] Ignacio Lopez-Quintas, [a] Nuria Sevilla-Sierra, [a] Javier R. Vázquez de Aldana

[a] Grupo de Investigación en Aplicaciones del Láser y Fotónica, Universidad de Salamanca, Pl. La Merced SN, 37008, Salamanca, Spain; ilopezquintas@usal.es

Ultrashort laser pulses in the femtosecond regime are widely used for 3D nano- and micro-structuring of transparent solids, allowing for high-precision local modification of the material (i.e., inducing refractive index changes). These modifications, in the form of damage tracks, are used to inscribe waveguides and other optical active elements in crystals, which can be integrated in photonic devices [1]. While the process of second harmonic generation (SHG) takes place exclusively in non-centrosymmetric materials, such as nonlinear crystals, it is known that a breakage in the symmetry can lead to an enhancement of the nonlinear susceptibility. Furthermore, in the case of focused beams, phase shift effects can also influence the nonlinear response of the material. Under this framework, we have investigated the nonlinear response of a modified centrosymmetric material, which, due to this symmetry, is not expected to generate second harmonic radiation. For that purpose, we have inscribed different structures using femtosecond laser pulses in the bulk of a Nd:YAG crystal (cubic system) and the nonlinear response of the sample was investigated using second harmonic generation microscopy (SHGM) [2,3]. This is the first time, to the best of our knowledge, that this technique has been applied to the analysis of damage tracks produced in an isotropic (centrosymmetric) crystalline material. The second harmonic signal is generated exclusively in the damage tracks, enabling the acquisition of high-resolution 3D images of the structures. The reported results are relevant, not only for the potential extension of the SHGM technique to other isotropic materials, or for their prospective application in the fabrication of photonic devices, but also because this is the first demonstration of bulk SHG in a modified Nd:YAG crystal.

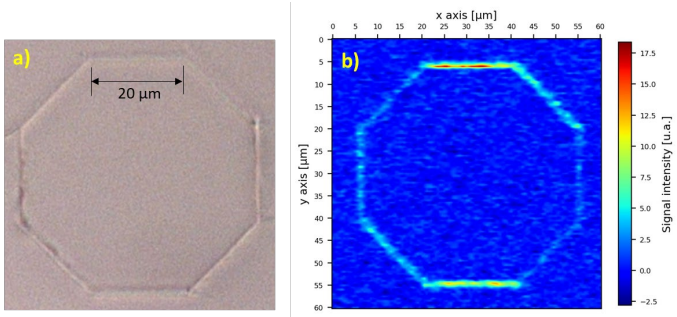

Figure 1. a) Optical image of the inscribed octagonal structure in the Nd:YAG crystal. Damage tracks are formed by focusing amplified NIR laser pulses in the crystal bulk. b) SHGM map of the structure obtained by focusing non-amplified 120 fs pulses at 800 nm. The SH signal (400 nm) is generated exclusively in the damage tracks.

References:

[1] Dong, N. et al., Femtosecond laser writing of multifunctional optical waveguides in a Nd:$YVO4^{+}$ KTP hybrid system. *Optics Letters*, 36, **2011**, 975.

[2] Aghigh A. et al., Second harmonic generation microscopy: a powerful tool for bio-imaging. *Biophysical Reviews*, 15, **2023**, 43-70.

[3] Yokota, H. et al., Optical second harmonic microscopy as a tool of material diagnosis. *Physics Research International*, 2012, **2012**, 704634.

Laser-induced heating decimated luminescence nanothermometry using robust LaOF:Yb^{3+}, Er^{3+} upconversion nanophosphor

Govind B. Nair[a], Sumedha Tamboli[a], S. J. Dhoble[b], H. C. Swart[a]

[a]Department of Physics, University of the Free State, Bloemfontein, South Africa.
[b]Department of Physics, R.T.M. Nagpur University, Nagpur 440033, India.
swarthc@ufs.ac.za

A microwave-assisted hydrothermal route was used to synthesize LaOF:0.05 Yb^{3+}, x Er^{3+} ($0.001 \leq x \leq 0.05$) upconversion nanoparticles (UCNPs). Luminescence nanothermometers based on LaOF:Yb^{3+},Er^{3+} UCNPs were also investigated. Laser-induced heating is a bothersome factor that can lead to the degradation of several temperature-sensing probes. One way to eliminate this influence on the thermal readouts is to identify the critical point of the laser power that produces undesirable effects on the probe and operate the laser excitation source at safe levels below this point. Unfortunately, most luminescent probes must be pumped by lasers operating at alarming power levels that can either disintegrate the probe or produce counterfactual results. The fluorescence intensity ratio (FIR) of the UCNPs was recorded using the visible (red) and near-infrared (NIR) regions, Fig 1(a) and (b), at different temperatures. The impact of laser-heating on the UCNPs was prevented by identifying the optimal operating conditions of the laser that could be used to record the FIRs without compromizing the integrity of the UCNPs. The behaviour of the UCNPs against the laser exposure time and power was analyzed to recognize the critical point of the laser power, below which laser-heating of the UCNPs was negligible. In this scenario, LaOF: Yb^{3+}, Er^{3+} UCNPs proved to be a highly sensitive and durable temperature sensing probe that can operate efficiently at low laser powers. Up to power densities below 18 W/cm^2, the laser-induced heating was easily nullified from the thermal readouts of this temperature sensor, thus, preventing the need for temperature calibrations in the measurements. The LaOF: Yb^{3+}, Er^{3+} UCNPs demonstrated consistent thermal readouts with impeccable accuracies at low laser power density (6.91 W/cm^2). These UCNPs exhibited remarkable durability and reusability over multiple thermal cycles. The impressive relative and absolute sensitivities, and noteworthy temperature resolution of the LaOF:Yb^{3+},Er^{3+} UCNPs indicates their potential for luminescence nanothermometry applications. This approach can be perceived as a benchmark for testing luminescent materials using nanothermometry.

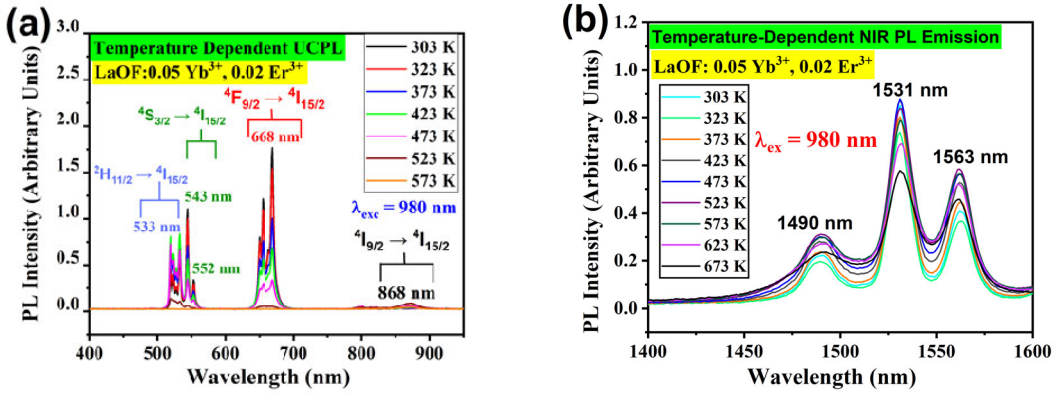

Fig. 1: Temperature-dependent PL spectra of LaOF:0.05 Yb^{3+},0.02 Er^{3+} UCNPs excited with a 980 nm diode laser: **(a)** UCPL, **(b)** NIR PL

Material aspects of Yb:CNGG lasers

María Dolores SERRANO, [a] Concepción CASCALES, [a] Nicolas TRCERA, [b] Pierre LAGARDE, [b] Carlos ZALDO, [a]

[a] Instituto de Ciencia de Materiales de Madrid. Consejo Superior de Investigaciones Científicas. c/ Sor Juana Inés de la Cruz 3. 28049 Madrid. Spain
[b] Synchrotron Soleil, 91192 Gif-sur-Yvette Cedex, France
cezaldo@icmm.csic.es

Recently, 31 fs laser pulses have been achieved by Kerr lens mode-locking of a 5 at% Yb doped $Ca_3(NbGa)_5O_{12}$ single crystal garnet, hereafter Yb:CNGG. [1] This achievement is associated with the occupancy of the octahedral (16*a*) and tetrahedral (24*d*) crystalline sites of the garnet simultaneously by Nb^{5+} and Ga^{3+}, what creates a great crystalline disorder nearby the dodecahedral Yb^{3+} (24*c*, also Ca^{2+} site) cation, thus its fluorescence is broadened as needed for short pulse laser operation.

CNGG melts at ≈1450 ºC, i.e. much lower than YAG (m.p. 1940 ºC), what eases its crystal growth. Platinum crucibles and air atmosphere can be used for the Czochralski growth of large crystal sizes. [2] The favorable crystal growth properties along with crystal isotropy and a significant thermal conductivity, κ= 3.6-4.4 W/mK, [2] made of Yb:CNGG a firm candidate for developing ultrashort pulsed laser devices, but CNGG melts congruently only for off-stoichiometry compositions, $Ca_3Nb_{1.5+1.5x}Ga_{3.5-2.5x}\square_xO_{12}$, where x=0.11 to 0.14 stands for the cationic vacancy composition . [3] The Nb/Ga occupancy factor ratios for the two (16*a* and 24*d*) sites are sensitive to the starting melt composition, Ga evaporation from the melt, as well as to the incorporation of other cations used as crystal modifiers (for instance Li^+). To fully understand the Yb^{3+} spectroscopy in CNGG and maximize the fluorescence bandwidth a crystallographic model in terms of charge compensation and occupation sites is required.

In this work we study the occupation sites in the CNGG lattice of several foreign cations with charge ranging from I to IV and ionic radius similar to Nb^{5+} and Ga^{3+}, namely Li^+, Mg^{2+}, Ti^{4+} and Ge^{4+}. Several experimental techniques including X-ray absorption spectroscopy, X-ray and neutron diffraction single crystal refinements and nuclear magnetic resonance are used to determine the sites of the foreign cations incorporated upon Czochralski growth of CNGG single crystals. It is shown that the incorporation of cations with increasing electric charge in the tetrahedral sites of the garnet lattice displaces the $^2F_{5/2}(0')\leftrightarrow{}^2F_{7/2}(0)$ Yb^{3+} transition to larger energy.

Acknowledgements. This work was supported by grants PID2021-128090OB-C21 and PDC2022-133326-I00 funded by MICIN/AEI/10.13039/501100011033 and by "ERDF A way of making Europe" under "The European Union Next GenerationEU/PRTR" program. Beam time awarded at LUCIA-SOLEIL under proposal number 20210943 is acknowledged.

References:

[1] Z. Lin et al., Kerr-lens mode-locking of an Yb:CLNGG laser, *Opt. Express* 31, **2023**, 8575.
[2] M.D. Serrano et al., Design of Yb^{3+} optical bandwidths by crystallographic modification of disordered calcium niobium gallium laser garnets, *J. Mat. Chem. C* 5, **2017**, 11481.
[3] K. Shimamura et al., Growth and characterization of calcium niobium gallium garnet (CNGG) single crystals for laser applications, *J. Cryst. Growth* 128, **1993**, 1021.

The use of Er^{3+} ions as sensitizers in upconverting nanoparticles: from synthesis to biological applications

Tomasz GRZYB, [a] Natalia JURGA, [a] Dominika PRZYBYLSKA, [a] Sylwia RYSZCZYŃSKA, [a] Inocencio Rafael MARTÍN, [b]

[a] Department of Rare Earths, Adam Mickiewicz University, Poznań, Uniwersytetu Poznańskiego 8, Poznań, 61-614, Poland
[b] Departamento de Física, Universidad de La Laguna, Apdo. 456. E-38200 San Cristóbal de La Laguna, Santa Cruz de Tenerife, Spain
tgrzyb@amu.edu.pl

Upconversion (UC) is one of the most studied phenomena in materials science—converting the near-infrared (NIR) wavelength to visible or ultraviolet results in many advanced applications. Upconverting nanoparticles (UCNPs) can be used in nanomedicine to detect and treat cancer, in analytical applications such as luminescent labels, temperature sensors, or anti-counterfeiting.

Typically, Yb^{3+} ions act as NIR sensitizers in UCNPs which results from the properties of the Yb^{3+} ion, i.e., its simple electronic structure and high absorption of radiation at 975 nm wavelength. Excitation with different wavelengths can also result in intense UC [1]. Er^{3+} ions absorb effectively at about 1480-1550 nm, giving emission in the visible range up to NIR [1]. In addition, UCNPs heavily doped with Er^{3+} ions can undergo self-sensitization, which improves the emission intensity. In core@shell UCNPs, the emission can be as effective as in the case of Yb^{3+}-doped systems. However, due to excitation at a wavelength of around 1535 nm, Er^{3+}-doped UCNPs offer more emission bands in the first biological window, which is crucial for biomedical applications. These bands can be utilized for ratiometric temperature sensors [2]. Moreover, the laser radiation with wavelength at around 1535 nm is less scattered in blood than 975 nm used in most of the studied UCNPs, making such UCNPs promising for medical applications. Additionally, by co-doping with various lanthanide ions, such as Tm^{3+} or Ho^{3+} ions, it is possible to improve the spectroscopic properties of UCNPs based on the absorption of Er^{3+}. Moreover, security labels based on the Er^{3+} technology are promising in anti-counterfeit applications, an alternative to the best-known solutions [3].

References:

[1] Grzyb, T.; Kamiński, P.; Przybylska, D.; Tymiński, A.; Sanz-Rodríguez, F.; Haro Gonzalez, P.; Manipulation of up-conversion emission in $NaYF_4$ core@shell nanoparticles doped by Er^{3+}, Tm^{3+}, or Yb^{3+} ions by excitation wavelength—three ions—plenty of possibilities, *Nanoscale,* 13, **2021**, 7322–7333.

[2] Ryszczyńska, S.; Trejgis, K.; Marciniak, Ł.; Grzyb, T.; Upconverting SrF_2:Er^{3+} Nanoparticles for Optical Temperature Sensors, *ACS Appl. Nano Mater.*, 4, **2021**, 10438–10448.

[3] Grzyb, T.; Przybylska, D.; Szczeszak, A.; Śmiechowicz, E.; Kulpiński, P.; Martín, I. R. Multifunctional Cellulose Fibers: Intense Red Upconversion under 1532 Nm Excitation and Temperature-Sensing Properties, *Carbohydr. Polym.*, 294, **2022**, 19782.

Thin film deposition of organic-inorganic quinoline-tin dioxide pn-junction for optoelectronic devices

Lucas P. FONSECA,[a)] Natália C. OLIVEIRA [a,b)], Lucas M. MARTINS,[b)] Luis V A SCALVI [a)]

[a)] *São Paulo State University, Lab of Electro-Optical Experiments on Materials - Physics Dept-FC, Bauru, SP, Brazil* [b)] *São Paulo State University, Chemistry Dept-FC, Bauru, SP, Brazil* luis.scalvi@unesp.br

Quinolinic derivatives have been applied in organic optoelectronics, generating efficient layers concerning electron transport. The quinolinic nucleus has in its central structure an aromatic azaheterocycle with a benzene ring fused at positions 2 and 3 of a pyridine ring, which gives them a strong electron-acceptor characteristic. On the other hand, SnO_2 is an oxide semiconductor used as transparent electrodes in many optoelectronic systems [1]. The n-type electrical conductivity of SnO_2 is linked to interstitial tin ions and oxygen vacancies, which act as donors in the matrix. Layers of SnO_2 and quinoline derivatives combined as a hybrid structure leads to the formation of an optically excitable p-n junction. One of the great challenges is the deposition of quinolines in the form of films, with high homogeneity of the quinoline layer on SnO_2. Thus, the performance of systems deposited by electrodeposition and drop-casting are compared. The quinoline was synthesized according to the literature [2], with N,N-diethyl-p-phenylenediamine and 4-formylbenzoic acid forming a Schiff base, which reacts with phenylacetylene to give the quinoline derivative. The reaction occurs under stirring and reflux, over 4 days, with a hydrochloric acid 0.5 M solution as a catalyst. The quinoline is extracted and recrystallized. For electrical characterization of hybrid structures, devices are built with metallic contacts of Sn or In, deposited by resistive evaporation, allowing evaluation both parallel and perpendicular to the direction of deposition. Cyclic voltammetry for quinolline electrodeposition (fig. 1) shows a reduction peak that decreases for each cycle, which probably means protonation of quinoline ring and indicates film deposition, confirmed by the SEM (inset fig 1). When deposited by drop casting, with annealing after each layer at 50°C for 10 min on a hot plate, and 20 min in the oven, the best solvent is acetone, adhering effectively to fluorine-doped tin dioxide (FTO) and also to silica. They present characteristic peaks of optical absorption [3]. Previous heating of the substrate (70°C) leads to increased transparency.

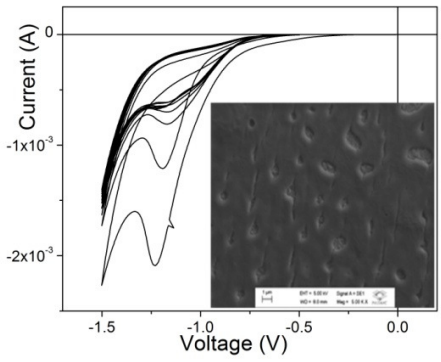

Acknowledgements: FAPESP (Proc. 2018/09235-4, 2022/08483-0 and 2022/12998-5)

References:

[1] Y. Liu, Y.; S. Wei,s.; G. Wang, G.;J. Tong, J.; J. Li, J.; D. Pan D.;, Quantum-sized SnO_2 nanoparticles with upshifted conduction band: a promising electron transportation material for quantum dot light-emitting diodes *Langmuir* vol 36, **2020**, 6605-6609,

[2] Martins, L. M.; Moreno, V. F.; Rosario, I. S.; Graeff, C. F. O.; Silva-Filho, L. C. Bronsted Acid Mediated Facile Greener Multicomponent Synthesis of 2,4-Diaryl-quinoline Derivatives in Water*Orbital* vol. 14, **2021**, 1-9

[3] Santos, G.C.; Andrade Bartolomeu, A.; Ximenes, V.F.; Silva-Filho, L.C., Facile Synthesis and Photophysical Characterization of New Quinoline Dyes *J. Fluorescence* vol. 27, **2017**, 271-280

HYPHa project - A voyage of developing a low-cost integrated photonic platform

Muhammad Ali BUTT,[a)] Krzysztof ROLA,[b)] Malgorzata GUZIK,[b, c)], Alicja BACHMATIUK,[b)] Cuma TYSZKIEWICZ,[d)] Pawel KARASIŃSKI,[d)] Tadeusz MARTYNKIEN,[e)] Jacek OLSZEWSKI,[e)] Andrzej KAŹMIERCZAK,[a)] Ryszard PIRAMIDOWICZ,[a)]

[a)] Warsaw University of Technology, Institute of Microelectronics and Optoelectronics, ul. Koszykowa 75, 00-662 Warszawa, Poland
[b)] Lukasiewicz Research Network-PORT Polish Center for Technology Development, ul. Stablowicka 147, 54-066, Wroclaw, Poland
[c)] University of Wroclaw, Faculty of Chemistry, ul. F. Joliot-Curie 14, 50-383 Wroclaw, Poland
[d)] Silesian University of Technology, Department of Optoelectronics, ul. B. Krzywoustego 2, 44-110 Gliwice, Poland
[e)] Wroclaw University of Science and Technology, Department of Optics and Photonics, Wybrzeze Wyspianskiego 27, 50-370 Wroclaw, Poland

ali.butt@pw.edu.pl

HYPHa project is a joint venture to develop a low-cost integrated photonics platform based on silica-titania materials deposited *via* a sol-gel method and a dip-coating procedure. The dip-coating technique is cost-effective and makes it possible to produce a high-quality and low-loss silica-titania thin-films on ~~a~~ glass or buffered silicon substrates [1]. Fabrication techniques such as reactive ion etching (RIE), wet-chemical etching, and nanoimprint lithography (NIL) are being researched to structure silica-titania layers. Currently, the development of the silica-titania platform is realized, and some successful results related to structuration are being demonstrated. Additionally, several photonic components such as ring resonator, subwavelength grating waveguide, 1D-photonic crystal waveguide, reverse rib waveguide, and demultiplexer systems are being numerically investigated [2-4]. We believe that with the success of such a photonic platform, the integrated photonics industry will be revolutionized in terms of performance and fabrication cost.

References:

[1] Butt, M.A.; Tyszkiewicz, C.; Karasinski, P.; Zieba, M.; Kazmierczak, A.; Zdonczyk, M.; Duda, L.; Guzik, M.; Olszewski, J.; Martynkien, T.; Bachmatiuk, A.; Piramidowicz, R., Optical thin films fabrication techniques- Towards a low-cost solution for the integrated photonic platform: A review of the current status. Materials, 15, **2022**, 4591.
[2] Butt, M.A.; Shahbaz, M.; Kozlowski, L.; Kazmierczak, A.; Piramidowicz, R., Silica-titania integrated photonics platform-based 1x2 demultiplexer utilizing two serially cascaded racetrack microrings for 1310 nm and 1550 nm telecommunication wavelengths. Photonics, 10, **2023**, 208.
[3] Butt, M.A.; Kozlowski, L.; Piramidowicz, R., Numerical scrutiny of a silica-titania-based reverse rib waveguide with vertical and rounded sidewalls. Applied Optics, 62, **2023**, 1296-1302.
[4] Butt, M.A.; Tyszkiewicz, C.; Karasinski, P.; Zieba, M.; Hlushchenko, D.; Baraniecki, T.; Kazmierczak, A.; Piramidowicz, R.; Guzik, M.; Bachmatiuk, A., Development of a low-cost silica-titania optical platform for integrated photonics applications. Optics Express, 30, **2022**, 23678-23694.

Demonstration of Dose Rate Monitoring System with Garnet-Type Scintillators

Daisuke Matsukura[a), b)], **Shunsuke Kurosawa**[b), c), d)], **Akihiro Yamaji**[b), c)], **Yuji Ohashi**[b), c)], **Yuui Yokota**[b)], **Kei Kamada**[b), c), e)], **Hiroki Sato**[b), c)], **Masao Yoshino**[b), c)], **Takashi Hanada**[b)],**Rikito Murakami**[b)], **Takahiko Horiai**[b), c)], **Akira Yoshikawa**[b), c), e)], **Takushi Takata**[f)], **Hiroki Tanaka**[f)]

[a)] *Tohoku University, Graduate School of Engineering,*
[b)] *Institute for Materials Research, Tohoku University, Japan,*
[c)] *New Industry Creation Hatchery Center, Tohoku University, Japan,*
[d)] *Institute of Laser Engineering, Osaka University, Japan,*
[e)] *C&A Corporation, Japan,*
[f)] *Institute for Integrated Radiation and Nuclear Science, Kyoto University, Japan,*
daisuke.matsukura.p5@dc.tohoku.ac.jp

For the decommissioning of Fukushima Daiichi Nuclear Plants, the real-time dose-rate monitor under the high dose-rate situation is required to remove the debris remaining inside the plants. To realize such monitoring system, we have proposed a dose monitor consisting of a scintillator, optical fiber and CCD spectrometer (Fig. 1), and scintillation photons are read with the CCD spectrometer under the lower dose condition [1]. Since optical fiber is planned to use with a length of over 100 m, suppression of the photon loss through the fiber is necessary. Also, some noises originating from the optical fiber such as luminescence and Cherenkov photons with dominant emission bands of less than 550 nm must be separated from the scintillator light [2, 3]. Therefore, longer emission wavelength (goal: 650-1000 nm) and higher light output compared to that of conventinal material (Cr-doped α-Al_2O_3) are required for the scintillator.

We focused on Nd-doped $Y_3Al_5O_{12}$ (Nd:YAG) crytals, which is known as a laser material with infra-red emission. The Nd:YAG single crystals doped with different Nd concentrations were grown by the micro-pulling down method[4], and the optical properties of the crystals were investigated. Each sample showed an emission wavelength of approxemately 880 nm originating from 4f-4f transition ($^4F_{3/2}$ to $^4I_{9/2}$) of Nd^{3+} by X-ray excitation.

We succeeded in showing a dynamic range (approxemately 1-700 Gy/h) for the monitoring system coupled with a 20 m-long optical fiber under high dose rate conditions. Figure 2 shows the calibration curve for signal intensity of emission spectra as a function of dose rate. After the irradiation, we checked the afterglow, and 1%-level of the maximum of intensity during the irradiation was observed after approximately 18 sec of irradiation off including the movinng time for the source return (~25 sec). This results shows afterglow was neglisible, and Nd:YAG was found to have good properties for the system.

In this paper, we show the detail results of optical and scintillation properties of Nd:YAG and discuss the feasibility to use this system in the Plants.

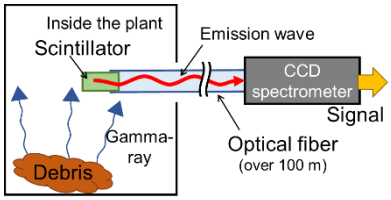

Fig. 1 Schematic view of the radiation dose monitoring system

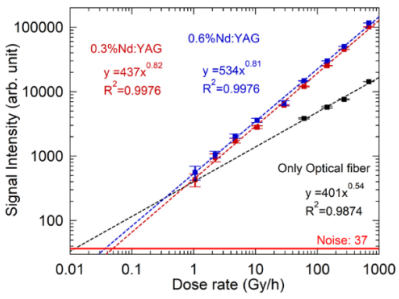

Fig. 2 Calibration curve for signal intensity of emission spectra (integration range: 800-980 nm) as a function of dose rate

[1] Fukushima Nuclear Accident Archive, Topics Fukushima (No.70), (2015)
[2] H. Liu *et al*., Rev. Sci. Inst., vol. 89 (2018).
[3] Fosco Connect, optical fiber loss and attenuation, https://www.fiberoptics4sale.com/blogs/archive-posts/95048006-optical-fiber-loss-and-attenuation
[4] A. Yoshikawa et al., Optical Materials, 30 (2007) 6-10

Chemosensing of low molecular weight biothiols via surface-enhanced Raman spectroscopy (SERS)

Mariacristina TURINO, [a, b] Luca GUERRINI, [a]

[a] Universitat Rovira i Virgili (Tarragona Spain), [b] ICMAB (Barcelona, Spain);
Email: luca.guerrini@urv.cat

Low molecular weight thiols (biothiols) are highly active compounds extensively involved in human physiology and whose abnormal levels have been associated with multiple diseases.[1] To overcome the intrinsic limitations of conventional analytical approaches, major efforts have been devoted in recent years to developing new nanosensing methods for the low cost and fast quantification of this class of analytes in minimally pre-treated samples.

To this end, we designed a novel strategy for engineering a highly efficient surface-enhanced Raman scattering (SERS) platform for the dynamic sensing of biothiols.[2] SERS combines Raman spectroscopy with nanotechnology into an ultrasensitive and highly specific analytical tool.[3] Colloidally stable silver nanoparticles clusters equipped with a specifically designed azobenzene derivative (AzoProbe) were generated as highly SERS active substrates.[2] These aggregates were further encapsulated by thiol-containing polyethylene glycol (PEG-SH) to afford high colloidal stability in complex biological media. In the presence of small biothiols (e.g., glutathione: GSH), breakage of the AzoProbe diazo bond causes drastic spectral changes that can be quantitatively correlated with the biothiol content, with a limit of detection of ca. 5 nM for GSH. An identical response was observed for other low molecular weight thiols, while larger macromolecules with free thiol groups (e.g., bovine serum albumin) do not produce distinguishable spectral alterations.[2] This indicates the suitability of the SERS sensing platform for the selective quantification of small biothiols in biofluids.

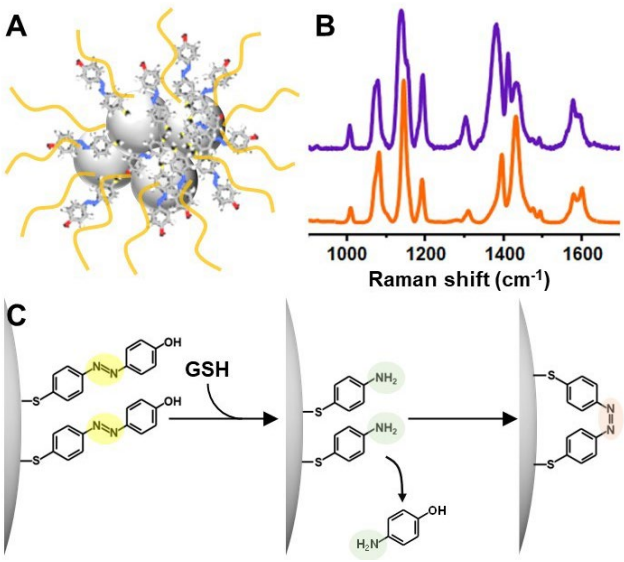

Figure 1. (A) Schematic of a colloidally stable silver nanoparticle cluster modified with the AzoProbe molecular sensor and PEG-SH. (B) SERS spectra of clusters before (purple) and after (orange) mixing with GSH. (C) Outline of the proposed molecular mechanism for detection.

References:

[1] Estrela, J.M.; Ortega, A.; Obrador, E., Glutathione in cancer biology and therapy. *Crit. Rev. Clin. Lab. Sci.*, 43, **2006**, 143-181.

[2] Turino, M.; Alvarez-Puebla, R.A.; Guerrini, L. Plasmonic Azobenzene Chemoreporter for Surface-Enhanced Raman Scattering Detection of Biothiols. *Biosensors*, 12, **2022**, 267.

[3] Schlücker, S., Surface-Enhanced Raman Spectroscopy: Concepts and Chemical Applications. *Angew. Chem., Int. Ed.*, 53, **2014**, 4756-4795.

Recent developments of composite scintillators and LED converters based on the epitaxial structures of oxide compounds

Yuriy Zorenko[a], Vitalii Gorbenko[a], Anton MarkovskiyY[a], Yurii Syrotych[a], Sandra Witkiewich-Łukaszek[a], Tetiana Zorenko[a], Jiri A. Mares[b], Martin Nikl[b], Oleg Sidletskiy[c,d], Sergii Nizankovskiy[e], Kei Kamada[f], Akira Yoshikawa[f]

[a)] Institute of Physics, UKW in Bydgoszcz, 85-090 Bydgoszcz, Poland;
[b)] Institute of Physics, Czech Acad.Sci., 16200 Prague, Czech Republic
[c)] Institute for Scintillation Materials, NAS of Ukraine, 61072 Kharkiv, Ukraine
[d)] Centre of Excellence ENSEMBLE3 Sp. z o.o., 01-919, Warsaw, Poland
[e)] Institute for Single Crystals, NAS of Ukraine, Ukraine, 61001 Kharkiv, Ukraine
[f)] Institute for Materials Research, Tohoku University, Sendai 980-8577, Japan
Presenting authors email: zorenko@ukw.edu.pl

This report presents the review of our latest achievements in the development of multilayered composite luminescent materials based on the single crystalline films (SCFs) and single crystals (SCs) of garnet, perovskite and orthosilicate compounds using the liquid-phase epitaxy (LPE) growth method for application in the environmental radiation monitoring, microimaging techniques and industrial lighting.

We created **multilayered composite scintillators** of phoswich-type (phosphor sandwich) based on SCFs and SCs of different compounds for simultaneous registration of different types of ionizing radiations in mixed high energy photon and particle fluxes [1]. Such composite scintillators consist from *three-layer epitaxial structures* containing two SCF scintillators grown „step-by-step" using the LPE method onto substrates from SC scintillators. Films and crystal parts of composite scintillators were fabricated from efficient scintillation materials with differing scintillation decay achieved by different types of dopants and various host compositions [1].

We show results of fabrication of new types composite scintillators, based on the film and crystals of Ce^{3+} doped $R_3B_5O_{12}$ (R=Lu, Y, Gd, Tb; B= Al, Ga) garnets, Ce^{3+} and Pr^{3+} doped $(Lu,Y,Gd)AlO_3$ perovskites and Ce^{3+} and Bi^{3+} doped $(Lu,Y,Gd)_2SiO_5$ orthosilicates using LPE method as well as their luminescent and scintillation properties. The application-minded tests of these prototypes of three layered composite scintillators for simultaneous registration of α- and β-particles and γ-quanta were performed, and further analyzed to optimize their scintillation figure-of merit.

The report presents also the brief review of developments of **multilayered composite** converters for WLED based on the SCFs of $(Gd, Lu,Tb)_3 Al_5O_{12}$:Ce garnets, grown by the LPE method onto undoped and Ce^{3+} doped YAG and LuAG SC substrates [2]. The results of their luminescent and photo-conversion properties (color coordinates, color rendering index, luminous efficacy) are also presented.

References:

[1] S. Witkiewicz-Lukaszek, V. Gorbenko, T. Zorenko, Y. Syrotych, J.A. Mares, M. Nikl, O. Sidletskiy, P. Bilski, A. Yoshikawa, Yu. Zorenko. Composite detectors based on single crystalline films and single crystals of garnet compounds. Materials, *15*(3), **2022**, 1249.

[2] A. Markovskyi, V. Gorbenko, T. Zorenko, S. Witkiewicz-Lukaszek, O. Sidletskiy, A. Fedorov, Yu. Zorenko, Development of Three-Layered Composite Color Converters for White LEDs Based on the Epitaxial Structures of YAG:Ce, TbAG:Ce and LuAG:Ce Garnets. Materials *16*(5), 2023, 1848.

Scintillation Properties of Tl-doped $Cs_3(Cu, Li)_2I_5$ Crystals for Cosmic Dark Matter Search

[a,c] Yusuke Urano, [b] Shunsuke Kurosawa, [a] Akihiro Yamaji, [b] Akira Yoshikawa, [C] Kenichi Fushimi, [C] Reiko Orito

[a] Institute for Materials Research (IMR), Tohoku University,
[b] New Industry Creation Hatchery Center (NICHe), Tohoku University,
[c] Graduate School of Sciences and Technology for Innovation, Tokushima University,
urano.yusuke.s1@dc.tohoku.ac.jp

Abstract

The search for cosmic dark matter (DM) is an important issue in modern physics. Weakly interacting massive particles (WIMPs) are considered to be the most promising candidate for DM [1], and WIMPs only interact via gravity and weak interaction. WIMPs are expected to detect via the low energy nuclear recoil associated with rare scattering of WIMP on target nuclei, while the mass of WIMPs is predicted to have the order of GeV~TeV, roughly. The scintillation materials used in DM search must have high light output, high energy resolution, and chemical stability. Moreover, large Stokes shift samples have the advantage to maintain the light output when we use large-size scintillation crystals to suppress self-absorption. Since NaI(Tl) scintillators have a high light output of 40,000 photons/MeV) [2], this scintillator is used as conventional material for WIMPs search. However, NaI(Tl) is hard to handle due to hygroscopicity.

We focused on the halide scintillator $Cs_3Cu_2I_5$ (CCI). In previous studies, CCI crystals were reported to have high light output (98,200 photons/MeV) and energy resolution (3.3 % at 662 keV) [3,4]. In addition, CCI is a chemically stable crystal with low hygroscopicity. Although the mass of DM is unidentified, doping $Cs_3Cu_2I_5$ with Li is expected to improve sensitivity to the DM with various masses of Li, Cs, Cu, and I. Thus, $Cs_3(Cu, Li)_2I_5$ crystals were grown by the Bridgeman method, and scintillation properties were evaluated.

Scintillation decay of $Cs_3(Cu, Li)_2I_5$ was evaluated to be 758 ± 7 ns with a photomultiplier tube, and its energy resolution was estimated to be ~ 6.9 % (FWHM, 662 keV). The non-proportional response (NPR) value for $Cs_3(Cu, Li)_2I_5$ showed in Fig. 2. Compared to Li-free CCI, the emission wavelength was not changed by doping Li, while the excitation wavelength was blue-shifted from 360 to 334 nm. Thus, the Stokes shift was confirmed to be broadening.

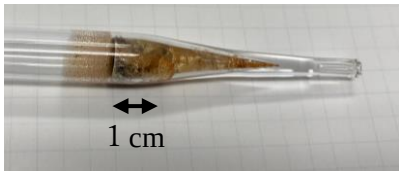

Fig.1 Grown $Cs_3(Cu, Li)_2I_5$ crystal in the ampoule

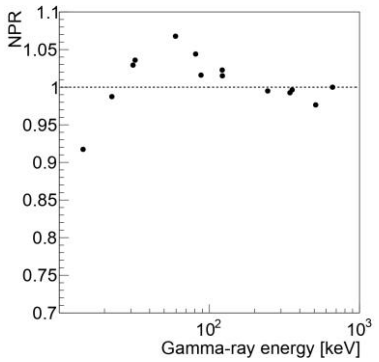

Fig.2 NPR behavior as a function of gamma-ray energy

References:

[1] K. Fushimi *et al*., "PICOLON dark matter search project", J Phys Conf Ser, 2156 012045 (2022).
[2] M.A. Oliván *et al*., "Light yield determination in large sodium iodide detectors applied in the search for dark matter", Astropart. Phys. 93 86 (2017)
[3] T. Jun *et al*., "Lead-free highly efficient blue-emitting $Cs_3Cu_2I_5$ with 0D electronic structure", Adv. Mater., 30 1804547 (2018).
[4] L. Stand *et al*., "Crystal growth and scintillation properties of pure and Tl-doped $Cs_3Cu_2I_5$", Nucl. Instrum. Methods Phys. Res. A, 991 164963 (2021).

Acentric Barium chalcogenides for nonlinear optics in the mid-IR

Valentin PETROV [a)]

[a)] *Max Born Institute for Nonlinear Optics and Ultrafast Spectroscopy, Max-Born-Str. 2a, 12489 Berlin, Germany; e-mail: petrov@mbi-berlin.de*

The number of non-oxide nonlinear crystals for frequency conversion in the mid-IR (3–30 μm) part of the spectrum is limited and only few of them are commercially available [1]. In the last decade there have been substantial efforts and progress in the development of new Ba chalcogenide compounds with improved properties compared to the classical I-III-VI_2 chalcopyrites $AgGaS_2$ (AGS) and $AgGaSe_2$ (AGSe) with tetragonal $\bar{4}2m$ symmetry which represent the benchmarks for frequency down-conversion of solid-state laser systems operating near 1 μm (Nd- or Yb-lasers) and near 1.5 μm (Er-lasers).

In this presentation I will review the main properties, including transmission, dispersion, birefringence, nonlinear coefficients, thermo-optic coefficients, etc., of five such non-centrosymmetric Ba crystals that have been characterized recently using large size single crystalline samples of high optical quality. These chalcogenide crystals have been grown by the vertical Bridgman-Stockbarger method. They include the orthorhombic (*mm*2) $BaGa_4S_7$ (BGS), the monoclinic (*m*) $BaGa_4Se_7$ (BGSe), the trigonal (3) $BaGa_2GeS_6$ (BGGS) and $BaGa_2GeSe_6$ (BGGSe), and the hexagonal (6*mm*) $Ba_2Ga_8GeS_{16}$ (B2GGS). In almost all their characteristics, including thermo-mechanical properties such as expansion, conductivity and hardness, as well as their anisotropy, these new nonlinear materials seem to be superior compared to the corresponding sulphide (AGS) and selenide (AGSe) chalcopyrites. Based on the larger bandgaps, the same is expected for their damage resistivity in different temporal regimes. In addition, these new materials do not require post-growth annealing procedures and the polished surface is chemically stable. The main difficulties so far have originated from the low-symmetry of the trigonal and monoclinic compounds, which complicates the characterization and the orientation of elements for nonlinear frequency conversion.

All of the Ba chalcogenide crystals possess the phase-matching capability to cover parts of the mid-IR spectral range by down-conversion of 1.064 μm laser radiation, show clear transparency and are free of two-photon absorption (TPA) at this pump wavelength. The selenides transmit up to ~18 μm, with clear transparency at 10.6 μm. The main applications of these nonlinear crystals will be in frequency down-conversion of advanced all-solid-state laser sources operating in the near-IR between 1 and 3 μm [1] but also for harmonics generation of CO_2 gas lasers (selenides only). The sulphides might prove unique for pumping near 1 μm while for pump wavelengths near 2 μm and beyond, the selenides possess a much longer mid-IR cut-off limit compared to the widely used II-IV-V_2 chalcopyrite $ZnGeP_2$ [1].

References:

[1] Petrov, V., Frequency down-conversion of solid-state laser sources to the mid-infrared spectral range using non-oxide nonlinear crystals. *Prog. Quantum Electron.,* Vol. 42**, 2015**, 1-106.

Correlation between Sc concentration and $Lu_3(Al,Sc,Ga)_5O_{12}$:Pr single crystal lattice distortion, atom distribution, Raman, luminescence, and scintillation properties

Karol Bartosiewicz[a)], Wioletta Dewo[b)], Takahiko Horiai[c)], Damian Szymanski[d)], Akihiro Yamaji[c)], Shunsuke Kurosawa[c),e),f),g)], Jan Pejchal[h)], Vladimir Babin[h)], Tomasz Runka[b)], Vitali Nagirnyi[i)], Marco Kirm[i)], Akira Yoshikawa[c),e)] Martin Nikl[h)]

[a)]Faculty of Physics, Kazimierz Wielki University, Powstancow Wielkopolskich 2, 85-090, Bydgoszcz, Poland; [b)]Faculty of Materials Engineering and Technical Physics, Poznan University of Technology, Piotrowo 3, 60-965 Poznań, Poland; [c)]New Industry Creation Hatchery Center, Tohoku University, 2-1-1 Katahira Aoba-ku, Sendai, Miyagi 980-8577, Japan; [d)]Institute of Low Temperature and Structure Research, Polish Academy of Sciences, Okolna 2, Wrocław, 50-422, Poland; [e)]Institute for Materials Research, Tohoku University, 2-1-1 Katahira Aoba-ku, Sendai, Miyagi 980-8577, Japan; [f)]Institute of Laser Engineering, Osaka University, 2-6 Yamadaoka, Suita, Osaka 565-0871, Japan; [g)]Faculty of Science, Yamagata University,1-4-12, Kojirakawa-machi, Yamagata 990-8560, Japan; [h)]Institute of Physics, Academy of Sciences of the Czech Republic, Na Slovance 1999/2, 182 00 Praha, Czechia, [i)]Institute of Physics, University of Tartu, W. Ostwald Str. 1, 50411, Tartu, Estonia; karol@ukw.edu.pl

Pr^{3+} doped $Lu_3Al_5O_{12}$ (LuAG:Pr) single crystal belongs to the family of high performance complex oxides scintillators. Pr^{3+} centers offer high quantum efficiency and fast response (~20 ns decay time) in the 310 nm emission band [1]. However, the LuAG host lattice contains electron traps related to antisite defects and oxygen vacancies, which significantly reduce the yield of scintillation light and slow down the kinetics of scintillation decay. The balanced substitution of Al for Ga atoms in LuAG:Pr crystals successfully deactivates trapping processes associated with trapping centers, consequently accelerating the scintillation response, but a slight decrease of the light yield is observed as well. The admixing with Sc^{3+} ions can improve scintillation characteristics due to spectral overlap of the Sc-related emission (Sc-trapped exciton) centered around 275 nm with the $4f \rightarrow 5d_1$ absorption band of Pr^{3+} ions [2]. However, the incorporation of large Sc atoms into the $Lu_3Al_{2.5}Ga_{2.5}O_{12}$:Pr crystal lattice can lead to lattice distortion and trigger the global structural rearrangements.
This research discusses in details the response of the $Lu_3Al_{2.5}Ga_{2.5}O_{12}$:Pr crystal lattice to the incorporation of a large Sc substitute and the consequences on the crystal growth process, the host lattice perturbation, atom segregation, Raman, optical, luminescence, and scintillation properties. The EDS elemental mapping revealed an apparent change in the radial distribution of atoms. Raman spectroscopy verified the correlation between the concentration of Sc atoms and the degree of distortion of the crystal lattice. The distortion of the crystal structures was also reflected in the high-resolution photoluminescence (PL) emission spectra and PL mapping. The scintillation properties gradually deteriorated with increasing concentration of Sc atoms.

Acknowledgments: This work was supported by the National Science Centre Poland (NCN) No.: 2020/39/D/ST3/0271,

References:

[1] J. Pejchal, et al., J. Phys. D: Appl. Phys. 42 (2009) 055117
[2] P. Prusa, et al., J. Cryst. Growth 318 (2011) 545-548

Investigations on the electric-dipole allowed $4f^2$ 5d → $4f^3$ broadband emission of Nd^{3+}-doped $20Al(PO_3)_3$-80LiF glass for potential VUV scintillator of neutron detection

Melvin Empizo[a)], Kohei Yamanoi [a)], Nobuhiko Sarukura [a)], Akira Yoshikawa [b)], Malgorzata Guzik [c)], Yannick Guyot [d)], Georges Boulon [d)]

a) Institute of Laser Engineering, Osaka University, 2-6 Yamadaoka, Suita, Osaka 565-0871, Japan
b) Institute for Materials Research, Tohoku University, 2-1-1 Katahira, Aoba-ku, Sendai 980-8577, Japan
c) Faculty of Chemistry, University of Wroclaw, u. Joliot-Curie 14, Wroclaw 50-383, Poland
d) Institute Light Matter, Univ Lyon, Claude Bernard/Lyon 1 University, CNRS, Villeurbanne 69622, France
presenting author e-mail : georges.boulon@univ-lyon1.fr

Research efforts are geared towards the design and development of potential scintillator materials. Large-area and high-quality crystals that are required for most radiation detection applications are difficult to produce because of the restrictions by their crystal growth technologies including high production costs and slow growth processes. The complex fluorophosphate glass, $20Al(PO_3)_3$-80LiF (APLF) which is more stable to moisture than other metaphosphates and easier to synthesize than a crystal has been developped by the Institute of Laser Engineering, Osaka University. APLF glass has a high lithium (Li) content of 31.6 mmol cm^{-3} essential in enhancing the detector sensitivity to low-energy (270 keV) fast neutrons.

Among rare earth ion dopants, neodymium (Nd^{3+}) is a well-known optical activator of laser materials for which the Nd^{3+} transitions are largely analyzed in the $4f^3$ configuration, but rarely in the $4f^2$5d configuration, which lies in the VUV region. The most important property of these glasses is that they exhibit electric-dipole allowed interconfigurational $4f^2$5d → $4f^3$ ($^4I_{9/2}$) broadband emissions with a maximum at 187 nm (VUV) and a decay time of ~5.0 ns, faster than Pr^{3+} or Ce^{3+}-doped APLF glasses [1-2]. Consequently, the Nd^{3+}-doped APLF glass can be ranked as one of the advanced potential scintillator materials in time-of-flight (TOF) detectors for high-counting-rate fast neutron detection [3].

References

[1] M. Empizo & al, Journal of Luminescence, 193 (2018) 13
[2] Y. Minami & al, Journal of Non-Crystalline Solids, Volume 521, 119495 (2019)
[3] M. Empizo & al, Journal of Alloys and Compounds, 856 (2021) 158096

Transmission measurements of GaAsP layers grown from the vapour phase by heteroepitaxy

Li WANG[a)], Shivashankar VANGALA[b)], Vladimir TASSEV[b)], Valentin PETROV[a)]

[a)] Max Born Institute for Nonlinear Optics and Ultrafast Spectroscopy, Max-Born-Str. 2a, 12489 Berlin, Germany, [b)] Air Force Research Laboratory, Wright-Patterson AFB, OH 45433, USA; e-mail: petrov@mbi-berlin.de

The acentric cubic semiconductors GaAs and GaP are attractive materials for nonlinear frequency conversion in the mid-IR due to their high second-order nonlinearity, thermal conductivity, and optical quality when grown from the vapour phase. Fabricated by epitaxy on orientation-patterned (OP) templates, they can be quasi-phase matched for efficient three-wave interactions without spatial walk-off. Tailoring of their properties by growing mixed ternary compounds by heteroepitaxy will enable pumping of nonlinear frequency down converters by Er-fiber laser systems at 1.56 µm and idler wavelengths beyond the mid-IR limit of GaP. The chosen substrates are GaAs wafers due to their much lower price and higher quality compared to GaP. The fabrication, crystalline structure, quality and homogeneity of ternary $GaAs_{1-x}P_x$ layers have been widely studied by various techniques [1], however, optical properties have not been well assessed from transmission measurements. Millimeter-thick samples of $GaAs_{1-x}P_x$ with sufficient aperture do not exist. Here we present transmission measurements with 167-322 µm thick layers of GaAsP with different composition [1].

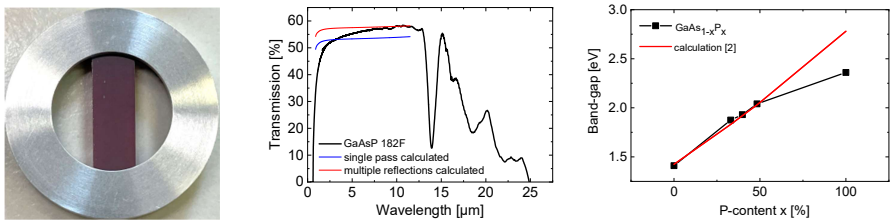

Fig. 1. 295-µm thick $GaAs_{0.517}P_{0.483}$ (left), the measured/calculated transmission (middle), and estimated band-gap for the five compositions of $GaAs_{1-x}P_x$ (symbols) with calculated dependence of the direct band-gap following [2] (right).

Unpatterned layers with x=0%, 33%, 39.8%, 48.3%, and 100% were grown, separated from the substrate and chemically polished to a roughness of 0.8 nm. Their actual thickness was derived from observed interference fringes. Figure 1 shows the transmission for x=48.3%. At 10 µm it amounts to 58% which coincides with the value calculated accounting for multiple reflections. This sample presents the worst case of increasing residual losses towards the band-gap. The estimated band-gaps are shown in Fig. 1 together with the empirical relation $1.424 + 1.172x + 0.186x^2$ for the direct band-gap compiled in [2], where 1.424 eV stand for the GaAs. Note that GaP with a direct band-gap at 2.78 eV, has an indirect band-gap at 2.23 eV. A strong absorption band is seen around 13.3 µm in GaP and at 19.1 µm in GaAs. The band at 13.3 µm is present in all samples except pure GaAs. The parasitic absorption band in the 2-4 µm range known for pure GaP, is absent in the ternary compounds.

References:

[1] Tassev, V.; Vangala, S.; Brinegar, D.; Parker, M.; Barlow, T., Thick heteroepitaxy of binary and ternary semiconductor materials for nonlinear frequency conversion in the mid and longwave infrared region, *Phys. Stat. Sol. A* 218, **2021**, 2000443.

[2] Swaminathan, V.; Macrander, A. T., *Materials aspects of GaAs and InP based structures*, Prentice-Hall, Englewood Cliffs, NJ, 1991.

Lead halide perovskite nanocomposites for fast timing detectors

Eva MIHÓKOVÁ, [a), b)] **Jan KRÁL,** [a), b)] **Fiammetta PAGANO,** [c), d)] **Nicolaus KRATOCHWIL,** [c)] **Václav ČUBA,** [b)] **Kateřina DĚCKÁ,** [a), b)] **Etiennette AUFFRAY** [c)]

[a)] Institute of Physics of the Czech Academy of Sciences, Prague, 162 00, Czech Republic [b)] FNSPE, Czech Technical University in Prague, 115 19, Czech Republic [c)] European Organization for Nuclear Research (CERN), Meyrin, 1211, Switzerland [d)] Department of Physics, University of Milano-Bicocca, Milano, 20 126, Italy; mihokova@fzu.cz

Lead halide perovskite nanocrystals of the formula $CsPbX_3$ (X=Cl,Br,I) have recently attracted attention as potential time taggers in scintillating heterostructures [1] intended for new generation of detectors requiring fast timing [2]. Such detectors are desirable in the time-of-flight (TOF) techniques in medical imaging as well as high energy physics. Cesium lead halide nanoparticles feature favourable properties, in particular, ultrafast scintillation decays [3] thanks to quantum confinement effect. However, they suffer from poor chemical stability and low stopping power for ionizing radiation. The first drawback can be overcome by incorporation of nanocrystals in the polymer matrix. The second can be helped by combination of such nanocomposite with the standard bulk scintillator in resulting heterostructure.

In this work we study synthesis, structural and optical characteristics including the timing performance of $CsPbBr_3$ and $CsPb(Br/Cl)_3$ nanocrystals embedded in polystyrene matrix. We focus on nanocomposites with high nanocrystal loading. Favourable luminescent properties of nanocrystals can be compromised by agglomeration of nanoparticles in the process of nanocomposite preparation. To limit this effect we use advanced polymerization techniques and copolymerizable ligands. We measure scintillation characteristics of prepared nanocomposites, especially scintillation decays. Their time resolution is also assessed using a novel setup [4] with low energy pulsed X-ray excitation where the signal is detected by the analog silicon photomultiplier. Prepared nanocomposites feature more than twofold better time resolution with respect to the LYSO:Ce crystal currently used in the TOF positron emission tomography.

References:

[1] Turtos, R. M.; Gundacker, S.; Omelkov, S.; Mahler, B., Khan, A. H.; et al.,On the use of cdSe scintillating nanoplatelets as time taggers for high-energy gamma detection. *Npj 2D Mater. Appl.,* 3, **2019,** 37(1-10).

[2] Konstantinou, G.; Lecoq, P.; Benlloch, J. M.; Gonzalez, A. J., Metascintillators for ultrafast gamma detectors: A review of current state and future perspectives. *IEEE Trans. Radiat. Plasma Med. Sci.,* 6, **2021,** 510-516.

[3] Děcká, K.; Král, J.; Hájek, F.; Průša, P.; Babin, V., Mihóková, E.; Čuba, V., Scintillation response enhancement in nanocrystalline lead halide perovskite thin films on scintillating wafers. Nanomaterials, 12, **2021**, 14 (1-11).

[4] Pagano, F.; Kratochwil, N.; Salomoni, M.; Frank, I.; Gundacker, S.; Pizzichemi, M.; Paganoni, M.; Auffray, E., A new method to characterize low stopping power and ultra-fast scintillators using pulsed X-rays. *Front. Phys.,* 10, **2022,** 1-11.

New strategies for efficient optical pressure & temperature sensors

Víctor LAVÍN,[a)] Marcin RUNOWSKI,[a),b)] Akira YOSHIKAWA,[c),d),e)]
Kei KAMADA,[c),d)] Przemysław WOŹNY,[e)] Teng ZHENG,[f)]
Ulises R. RODRÍGUEZ-MENDOZA, [a)] Inocencio R. MARTÍN [a)]

[a)] Departamento de Física, MALTA-Consolider Team & IUdEA, Universidad de La Laguna, Apartado de Correos 456, E-38200 San Cristóbal de La Laguna, Santa Cruz de Tenerife, Spain
[b)] Faculty of Chemistry, Adam Mickiewicz University, ul. Uniwersytetu Poznańskiego 8, 61-614 Poznań, Poland
[c)] New Industry Creation Hatchery Center (NICHe), Tohoku University, 6-6-10 Aoba, Aramaki, Sendai 980-8579, Japan
[d)] C&A Corporation, Sendai 980-8579, Japan
[e)] Institute for Materials Research, Tohoku University, 2-1-1 Katahira, Sendai 980-8577, Japan
[f)] School of Information and Electrical Engineering, Zhejiang University City College, Hangzhou, Zhejiang, China

vlavin@ull.edu.es

The control of extreme conditions of pressure (P) and/or temperature (T) is the subject of multidisciplinary studies involving physics, chemistry, materials science, biology or geology, as well as of enormous interest in many industrial processes. High P conditions can be induced in a solid with the help of a diamond anvil cell, whereas low/high T only needs a more conventional cryostat or furnace, respectively. P-T determination is a key issue requiring calibrated standards, and indirect, in situ pressure and/or temperature calibrations can be performed by taking advantage of the high sensitivity to P and/or T changes of some rare earth emission lines. In this work, we present different rare earth ions in materials and nanomaterials that have been successfully tested as optical P- and/or T- sensors.

References:

[1] Holzapfel, W. B.; Isaacs, N. S., High-pressure Techniques in Chemistry and Physics, Oxford University Press (**1997**).
[2] Tröster, Th., in Handbook on the Physics and Chemistry of Rare Earths, K. A. Gschneidner Jr, L. Eyring, eds., Amsterdam: Elsevier Science B.V., Vol. 33, **2003**, Ch. 217, 515-589.
[3] Runowski, M., Pressure and temperature optical sensors: luminescence of lanthanide-doped nanomaterials for contactless nanomanometry and nanothermometry, in Handbook of Nanomaterials in Analytical Chemistry: Modern Trends in Analysis, C.M. Hussein (ed), (**2020**) 227-273. DOI: 10.1016/B978-0-12-816699-4.00010-4

[2] Brown, J.; Black, A., Title of Book section. In *Book Title*, Green, B.; White, C., Eds. Publisher: City, Vol., **2010**, 13-15.
[3] Brown, J.; Green, B., *Title of the book*. Publisher: City, 15, **2010**, 565.

Tuning the optical properties of gold nanostars

Nicolas Pazos-Perez, [a)]

[a)] *Department of Physical and Inorganic Chemistry, Universitat Rovira i Virgili, Spain.*
nicolas.pazos@urv.cat

During the last years, the controlled synthesis of Au nanoparticles (NPs) has attracted the interest of many research groups. Thus, a remarkable success in the development of Au NPs has been achieved. Nowadays, it is possible to prepare quite homogeneous with a la carte dimensions structures like spheres, cubes, rods, decahedra or octahedra and therefore, controlling their optical properties. Among all possible morphologies, spiked NPs are one of the most efficient plasmonic structures for a wide variety of applications ranging from sensing and imaging to photothermal treatments. However, despite all the advances made in the synthesis of plasmonic nanostructures, there is still a lack of tunability in the optical properties of spiked NPs. Therefore, the ability to concentrate large electromagnetic fields at the apexes of the NSt tips upon illumination was till now restricted to concrete wavelengths and so were also, their possible applications.

In the presented work we demonstrate the possibility of tuning the concentration of the electromagnetic fields at the apexes of the NSt tips by an optimized bottom-up approach that allows the preparation of highly homogeneous plasmonic nanostars (NSt) with a la carte optical properties. Produced Au NSt as shown in Figure 1, exhibit absorbance maximums that can be tuned from the visible to the infrared. [1]

Furthermore, the effect of the plasmon tunability on the optical enhancing properties of the synthesized structures was effectively tested for sensing using surface-enhanced Raman scattering spectroscopy (SERS) with visible and NIR lasers.

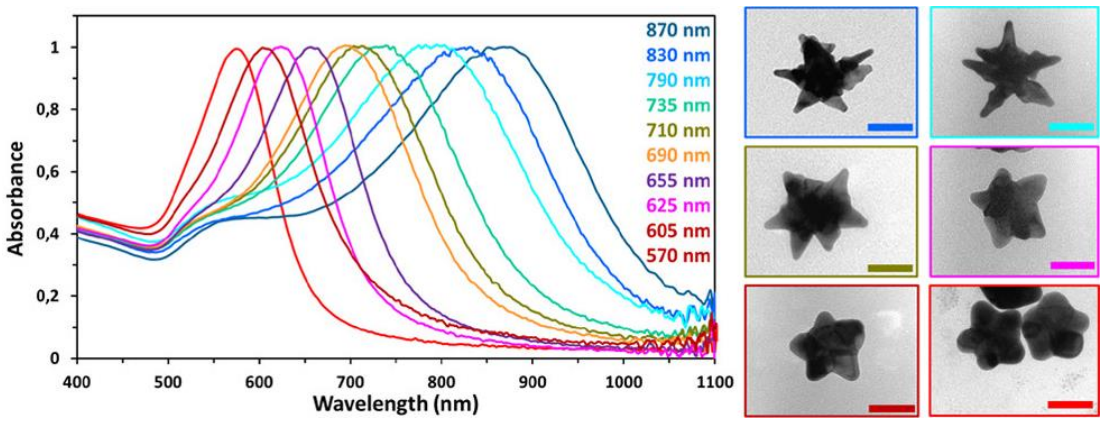

Figure 1. Normalized UV–vis spectra of different Au NSt solutions with plasmon resonances ranging from the visible to the infrared (left). TEM images of Au NSt corresponding to selected UV-vis spectra (rigth).

References:

[1] Pazos-Perez, N.; Guerrini, L.; Alvarez-Puebla, R., Plasmon Tunability of Gold Nanostars at the Tip Apexes. *ACS Omega* ***2018****, 3, 12, 17173–17179*.

Anisotropic thermo-mechanical properties of $BaGa_2GeS(e)_6$ crystals

Michael SUSNER[a)], Joel MURRAY[a)], Ginka EXNER[b)], Benjamin CONNER[a)], Alexandar GRIGOROV[b)], Ryan SIEBENALLER[a)], Elizabeth IVANOVA[b)], Emmanuel ROWE[a)], Michael McLEOD[a)], Shekhar GUHA[a)], Valentin PETROV [c)]

[a)] *Air Force Research Laboratory, Wright-Patterson AFB, OH 45433, USA*
[b)] *Department of Physics, Faculty of Physics and Technology, Plovdiv University Paisii Hilendarski, 4000 Plovdiv, Bulgaria*
[c)] *Max Born Institute for Nonlinear Optics and Ultrafast Spectroscopy, Max-Born-Str. 2a, 12489 Berlin, Germany; e-mail: shekhar.guha@us.af.mil*

The quaternary chalcogenides $BaGa_2GeS_6$ (BGGS) and $BaGa_2GeSe_6$ (BGGSe) (point group 3) are viable alternatives to the well-established chalcopyrite (point group $\bar{4}2m$) mid-IR nonlinear optical crystals $AgGaS_2$ (AGS) and $AgGaSe_2$ (AGSe) [1]. Most of their optical properties are now well documented [1]. Here we study the anisotropic thermal expansion, thermal conductivity, hardness and Young's modulus of BGGS and BGGSe.

The thermal expansion was evaluated using powdered samples and X-ray diffraction in the 200-430 K temperature range. The temperature T dependence for the two lattice constants a and c was fitted with a quadratic law and the relative thermal expansion coefficient α was obtained as a linear fit $A + B \cdot T$. The coefficients A and B and the room temperature (RT) values of α are summarized in Table 1. The anisotropy of the thermal expansion defined as α_a - α_c is roughly 2-3 times smaller compared to AGS and AGSe, respectively, with both coefficients α being positive without the anomalous behaviour typical for AGS and AGSe.

The thermal diffusivity (κ) and specific heat capacity (c_p) of BGGS and BGGSe were measured in a contactless way over a temperature range from 184 to 473 K by the flash analysis technique. For both crystals the anisotropy of the calculated thermal conductivity k (Table 1) is rather low (< 20%). Compared with RT values known from the literature on AGS and AGSe, BGGS and BGGSe show roughly 30% lower thermal conductivity, respectively.

Table 1. Thermal expansion, thermal conductivity, hardness and Young's modulus of BGGS and BGGSe.

	BGGS		BGGSe	
	a	*c*	*a*	*c*
A [ppm/K]	16.7	8.38	20.4	8.43
B [ppm/K^2]	-0.0153	-0.00481	-0.0273	-0.0153
α at RT [ppm/K]	12.1 ± 1	6.93 ± 0.4	12.2 ± 1	3.84 ± 0.4
c_p at RT [J/gK]	0.40 ± 0.01		0.27 ± 0.008	
k at RT [W/mK]	0.91 ± 0.03	1.10 ± 0.03	0.63 ± 0.02	0.76 ± 0.02
Hardness H_{IT} [GPa]	4.99 ± 0.08	4.66 ± 0.05	4.10 ± 0.04	4.25 ± 0.07
Hardness VHN [kg/mm^2]	463	432	380	394
Young's modulus E_{IT} [GPa]	65.1 ± 0.5	71.3 ± 0.5	53.5 ± 0.1	61.1 ± 0.5

The hardness and Young's modulus were obtained from nanondentation tests using a Berkovich tip. The averaged (over 10 runs) RT results for the a-cut and c-cut plates are summarized in Table 1. The hardness of BGGS is ~40% higher than AGS and that of BGGSe ~70% higher than AGSe, comparing with microhardness results from the literature.

References:

[1] Petrov, V.; Badikov, V. V.; Badikov, D. V.; Kato, K.; Shevyrdyaeva, G. S.; Miyata, K.; Mero, M.; Wang, L.; Heiner, Z.; Panyutin, V. L., Barium nonlinear optical crystals for the mid-IR: characterization and some applications, *J. Opt. Soc. Am. B*, Vol. 38, **2021**, B46-B58.

New nanoprobe designs for bioimaging and contactless luminescence thermometry

Carlos ALARCÓN-FERNÁNDEZ,[a] Carlos ZALDO,[a] Manuel BAÑOBRE-LÓPEZ,[b] Pedro RAMOS-CABRER,[c] Concepción CASCALES[a]

[a]Instituto de Ciencia de Materiales de Madrid, CSIC, c/ Sor Juana Inés de la Cruz 3, 28049 Madrid, Spain. [b]Advanced (Magnetic) Theranostic Nanostructures Lab, International Iberian Nanotechnology Laboratory - INL, Av. Mestre José Veiga s/n, 4715-330 Braga, Portugal. [c] Center for Cooperative Research in Biomaterials (CIC biomaGUNE), Ps. Miramón 182, 20014 Donostia-San Sebastián, Spain; cezaldo@icmm.csic.es, ccascales@icmm.csic.es

A new direction in bioimaging utilizes hierarchically built exogenous nanoprobes enabling two or even more imaging modalities. The combination of photoluminescence (PL) and magnetic resonance (MR) imaging in a single nanoprobe provides simultaneously high sensitivity and spatial resolution, compensating the individual weaknesses of both imaging modalities. To address the challenge of proposing new nanoprobes for dual NIR-excited PL and MR imaging modalities, this work evaluates a series of trivalent lanthanide (Ln)-doped nanoparticles and core-shell nanostructures based on the scheelite-like $NaGd(WO_4)_2$ host. This host doped with Er^{3+} demonstrated excellent ratiometric thermal sensitivity in the temperature range of interest for biomedical applications (≈ 42 ºC), [1, 2] but the used Er^{3+} green emissions are strongly scattered by human tissues, thus these emissions fall outside of the biomedical transparency windows (BW).

In currently studied nanoprobes, T_1- and T_2-MRI contrasts are delivered by Gd^{3+} (at 1.5 T) and Ho^{3+} (from 3 to 11.7 T), respectively, which are properly distributed in the core-shell nanostructure to avoid interactions between them. Dual contrast T_2/T_1 is possible at magnetic fields from 3 to 7 T. Besides, efficient Tm^{3+} and Ho^{3+} emissions for imaging under Yb^{3+} (≈ 980 nm) NIR-excitation or Nd^{3+} in a surface Yb^{3+}-Nd^{3+} codoped layer for efficient NIR-excitation at ≈ 803 nm allow for simultaneous deep tissue imaging and thermometry within I-II- III- and IV-BWs. Details of the synthesis procedure to obtain well-individualized and monodisperse-sized nanoparticles and core-shell nanostructures, as well as results of their PL properties, MR contrast imaging, ratiometric thermal sensitivity and cytotoxicity are presented.

Acknowledgments

This work has been supported by Spanish grants PID2021-128090OB-C21 and PDC2022-133326-I00 funded by MICIN/AEI/10.13039/501100011033, by 'ERDF A way of making Europe' and the 'European Union NextGenerationEU/PRTR'. C. A-F additionally acknowledges its Ph. D. MICINN grant PRE2019-090446.

References

[1] C. Zaldo et al., Efficient up-conversion in Yb:Er:$NaT(XO_4)_2$ thermal nanoprobes. Imaging of their distribution in a perfused mouse. *PLoS ONE* 12, **2017**, e0177596.

[2] C. Cascales et al., Ultrasmall, water dispersible, TWEEN80 modified Yb:Er:$NaGd(WO_4)_2$ nanoparticles with record upconversion ratiometric thermal sensitivity and their internalization by mesenchymal stem cells. *Nanotechnology*, 28, **2017**,185101.

Proccesing of rare-earth-doped nanostructured glass-ceramics for enhanced photoluminiscence

M.Sedano[1], A. Durán[1], J. Fernández[2], R. Balda[3,4], M. J. Pascual[1*]

*[1]Instituto de Cerámica y Vidrio (ICV-CSIC), 28049, Madrid, Spain [2]Donostia International Physics Center DIPC, 20018 San Sebastian, Spain [3]Dept. Física Aplicada, Escuela Superior de Ingeniería, Universidad del País Vasco (UPV-EHU), 48013 Bilbao, Spain [4]Centro de Física de Materiales, (UPV/EHU-CSIC), 20018 San Sebastian, Spain ; *presenting author: mpascual@icv.csic.es*

The growing field of photonics demands the design of new rare-earth (RE)-based optical materials for their use in efficient optical telecommunications, solid-state lasers and other applications. Transparent oxyfluoride glass-ceramics (GCs) combine the transparency and both mechanical and chemical resistance of aluminosilicate glasses with the low phonon energy and facile incorporation of RE ions in the fluoride crystals. The incorporation of RE ions in the crystalline phases enhances the optical emission intensity, a major property of these materials [1]. Moreover, the additional presence of metallic nanoparticles (Ag, Au, Pt) in the RE-doped glass-ceramics can further enhance the luminescent response.

By the other hand, transparent GC materials have also been obtained by spark plasma sintering (SPS) [2]. This approach combines thermal action with simultaneous compression of the material to reach full densification and high homogeneity in a short time [3]. The structural, mechanical, and optical properties have been characterized and compared with GCs of the same composition prepared by melt-quenching followed by conventional heat treatment. The results confirm the suitability of the SPS processing for the preparation of highly dense and transparent oxyfluoride glass-ceramics containing nanocrystals.

These materials are suitable for the preparation of preforms as precursors for the drawing of optical fibers and as substrates for waveguides written using laser radiation and some examples of the materials preparation and its possible applications will be provided in this presentation.

Keywords: oxyfluoride glass-ceramics; transparent; rare earths, metallic nanoparticles, spark plasma sintering

Acknowledgment
This work was supported by MICINN under Project PID2020-115419GB-C-21/C-22/AEI/10.13039/501100011033.

References
[1] Pablos-Martín, A. De; Durán, A.: Pascual, M.J. Nanocrystallisation in oxyfluoride systems: Mechanisms of crystallisation and photonic properties, Int. Mater. Rev. 57 (2012) 165–186. https://doi.org/10.1179/1743280411Y.0000000004
[2 Babu, S.; Galusek, D.; Durán, A., Pascual, M.J. Glass-ceramics processed by spark plasma sintering (SPS) for optical applications, Appl. Sci. 10 (2020) 1–21. https://doi.org/10.3390/APP10082791.
[3] Babu, S.; Balda, R.; Fernández, J.; Sedano, M.; Gorni , G.; Cabral, A.A.; Galusek, D.; Durán, A.; Pascual, M.J. $KLaF_4$: Nd^{3+} doped transparent glass-ceramics processed by spark plasma sintering. Journal of Non-Crystalline Solids 578, 121289 (2022). https://doi.org/10.1016/j.jnoncrysol.2021.121289.

Localized-enhancement of 1L MoS_2 photoluminescence on ferroelectric domain walls

J. J. RONQUILLO,[a] J. FERNÁNDEZ-MARTÍNEZ,[a] Daniel GALLEGO-FUENTE,[b] H.P. van der MEULEN,[a,c] G. LÓPEZ-POLÍN,[a] P. ARES,[b,c] J. GÓMEZ-HERRERO,[b,c] M.O RAMÍREZ,[a,c] and L. E. BAUSÁ[a,c]

[a] Dept. Física de Materiales, Universidad Autónoma de Madrid, 28049 Madrid, Spain
[b] Dept. Física de la Materia Condensada, Universidad Autónoma de Madrid, 28049 Madrid, Spain
[c] Condensed Matter Physics Center (IFIMAC), Universidad Autónoma de Madrid, 28049 Madrid, Spain
presenting author e-mail: joan.ronquillo@estudiante.uam.es

Two-dimensional (2D) Transition Metal Dichalcogenides (TMDs) are an interesting class of materials with promising properties for the next generation of optoelectronic devices. Their atomic thickness nature offers a unique opportunity to engineer their properties by means of the surrounding environment. In this context, ferroelectric crystals as substrates for TMDs provide a means for electrostatic doping due to the remnant polarization, avoiding complex doping strategies that hinder fabrication processes of devices.

In this work we analyze the effects of integrating a (1L) monolayer MoS_2 on $LiNbO_3$ (LN), one of the most versatile and attractive current platforms for integrated photonics. We demonstrate, ferroelectric-induced electrostatic doping in monolayer 1L MoS_2 when deposited on a LN crystal with hexagonal domains of alternating polarity. The MoS_2 doping is optically probed by spatially resolved scanning micro-photoluminescence (μ-PL) at low and room temperature. The results show the presence of p- and n-doped regions in MoS_2 depending on the polarization of the ferroelectric domain, as revealed by the different contributions of exciton and trion quasiparticles to the PL spectrum. Additionally, the μ-PL of 1L MoS_2 is analyzed on the vicinities of the ferroelectric domain walls, where the lateral MoS_2 p-n homojunctions are located. A significant enhancement of the MoS_2 exciton PL is systematically observed on alternating domain walls. This result can be explained by the exciton dissociation at the depletion region on a first wall (p-n homojunction), which induces a long-term local carrier accumulation and electron-hole recombination in an adjacent p-n homojunction, resulting in the MoS_2 PL enhancement.

These results open new avenues for the optical control ultra-thin p-n-lateral homojunctions in 2D materials integrated on relevant optoelectronic platforms.

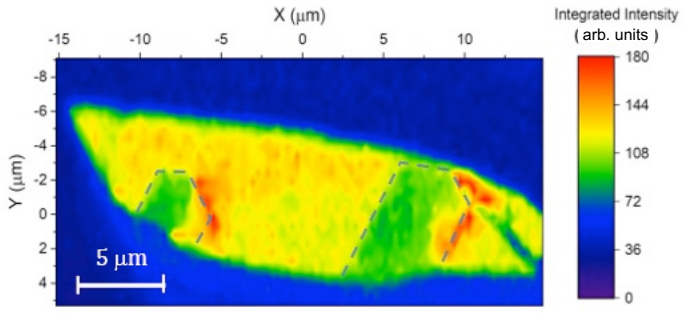

Figure 1. Image of the spatial variation of the 1L MoS_2 PL showing the exciton-dominant region (p type in yellow) and the trion-dominant region (n type in green). The emission enhancement (red) is observed on the vicinities of alternating ferroelectric domain walls.

High pressure annealing effects on optical and scintillation properties for $Gd_3(Ga,Al)_5O_{12}$:Ce scintillator single crystal

Yuui YOKOTA,[a,b] Takahiko HORIAI,[b] Masao YOSHINO,[b] Akira YOSHIKAWA,[a,b]

[a] Institute for Materials Research, Tohoku University
[b] New Industry Creation Hatchery Center, Tohoku University
yui.yokota.a5@tohoku.ac.jp

Garnet-type scintillator single crystals have been developed for various radiation detectors in various devices for medical, environmental and physics measurement fields. $Gd_3(Ga,Al)_5O_{12}$:Ce [GGAG:Ce] scintillator single crystals indicate relatively high light yield, great energy resolution and fast decay time under γ-ray irradiation[1]. However, GGAG:Ce single crystal has oxygen defects in the as-grown single crystal because oxygen defect can generate during the crystal growth under inert or reduction atmosphere [2]. In the previous report [3], crystal growth under oxygen atmosphere by the Floating Zone method affected the scintillation properties of GGAG:Ce scintillator single crystals and their improvement could be observed[3]. In this study, as-grown GGAG:Ce single crystal under inert atmosphere was annealed at high pressure under oxygen atmosphere using the hot isostatic pressing (HIP) equipment to compensate the oxygen defects and the scintillation properties were investigated.

A plate-shaped specimen was prepared from the GGAG:Ce bulk single crystal grown by the Czochralski method under inert atmosphere and it was annealed at 1500°C and 200 MPa for 30 hours under Ar+20%O_2 atmosphere. Optical and scintillation properties of the GGAG:Ce single crystal before and after the HIP annealing were evaluated. Transmittance and photoluminescence spectra, pulse-height spectra and decay curves under γ-ray irradiation were measured.

Emission spectra of GGAG:Ce single crystal under 445 nm excitation before and after the HIP annealing are shown in Fig. 1. An emission peak originated from 5d-4f transition of Ce^{3+} ion was observed around 550 nm for both spectra. On the other hand, the emission peak shifted toward longer wavelength by the HIP annealing from 535 to 550 nm, suggesting that the crystal field around Ce^{3+} ion was changed by the HIP annealing. Details of other optical and scintillation properties will be reported.

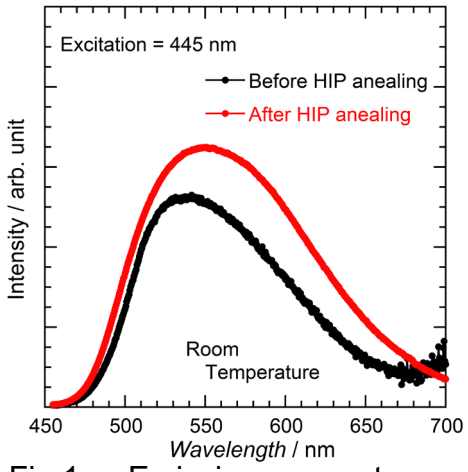

Fig.1 Emission spectra of GGAG:Ce before and after the HIP annealing.

References:

[1] Kamada, K., et al., Composition Engineering in Cerium-Doped $(Lu,Gd)_3(Ga,Al)_5O_{12}$ Single-Crystal Scintillators. *Cryst. Growth Des.* Vol.11, **2011**, 4484-4490.

[2] Park, C.; et al., Investigation of Optical Properties of Ceramic Ce:GAGG by High Temperature Annealing. *J. Korean Phys. Soc.* Vol.75, **2019**, 962−967.

[3] Wu, T.; et al., Fast $(Ce,Gd)_3Ga_2Al_3O_{12}$ Scintillators Grown by the Optical Floating Zone Method. *Cryst. Growth Des.* Vol.22, **2022**, 180-190.

Nanoporous scintillators for radioactive gas detection

R.Marie-Luce,[1] P.Mai,[2], F.Lerouge,[1] Y.Cheref,[1,2] S.Pierre,[3] B.Sabot,[3] F.Chaput,[1] and C. Dujardin[2,*]

[1] *Laboratoire de Chimie Lyon, Ecole Normale Supérieure de Lyon, Université Claude Bernard Lyon1, CNRS UMR 5182, France*
[2] *Institut Lumière Matière , Université Claude Bernard Lyon1 CNRS UMR 5306, France*
[3] *Université Paris-Saclay, CEA LIST, Laboratoire National Henry Becquerel, Palaiseau, France*

**E-mail: christophe.dujardin@univ-lyon1.fr*

The measurement of pure beta emitting radioactive elements such as ^{3}H and ^{85}Kr, is a major and a mandatory measurement for nuclear safety authorities issue for the monitoring of the territory, in particular for the monitoring of the expending nuclear activities for the carbon-free production of electricity. The short penetration length of these electrons in the air makes their detection very challenging. It requires mixing the radioactive gas with the sensitive element which is done with ionization chamber (gas-gas mixture) or liquid scintillation (gas-liquid mixture for ^{3}H only). However, these two methods do not meet all the needs since neither of them combines sensitivity to both gases, real-time analysis, and ease of wide deployment on the territory. Here we demonstrate that the new approach, based on the gas-solid mixture, allows to combine all the criteria allowing the efficient and real time detection of tritium and ^{85}Kr, and more generally of pure beta radioactive elements. We show that by synthesizing a transparent and scintillating nanoporous material, here a highly porous aerogel based on doped inorganic scintillators, we detect in real time with an efficiency of 95% and 20% the ^{85}Kr and the ^{3}H (illustrative results are presented Figure 1). We achieve sub-Bq.cm^{-3} in 100 s of accumulation, which is the best performance obtained so-far in real time. In this contribution, the latest results in terms of new materials characteristics including time-resolved luminescence, and detection performances will be presented.

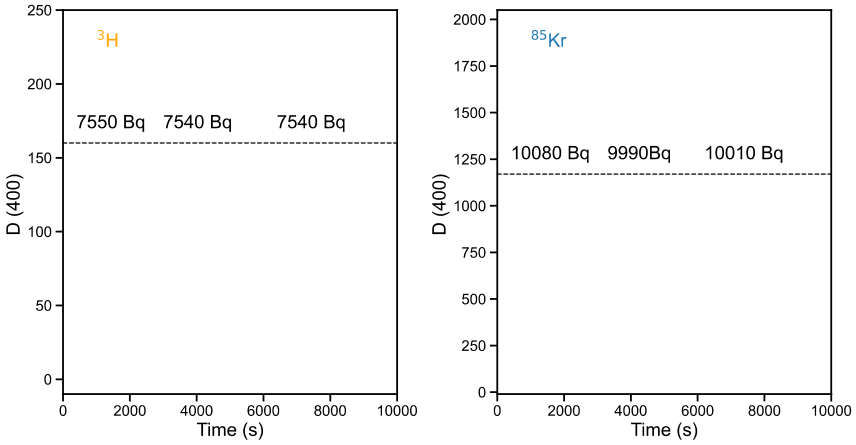

Figure 1: Typical measurements and their reproducibility for ^{3}H and ^{85}Kr detection. D(400) corresponds to the number of double coincidences measured in 400ns.

Acknowledgement: The authors acknowledge support from the European Community through the grant n° 899293, HORIZON 2020 – SPARTE.

Controlling the spatial coherence and subwavelength waveguiding of rare earth quantum emitters by plasmonic nanostructures

J. FERNÁNDEZ-MARTÍNEZ,[a)] M. O RAMÍREZ,[a,b)] S. CARRETERO-PALACIOS,[a)] P. MOLINA,[a)] J. BRAVO-ABAD,[b,c)] N.J. VAN HOOF,[d)] J. GÓMEZ-RIVAS,[d)] and L. E BAUSÁ[a,b)]

[a)] *Dept. Física de Materiales, Universidad Autónoma de Madrid, 28049 Madrid, Spain*
[b)] *Condensed Matter Physics Center (IFIMAC), Universidad Autónoma de Madrid, Spain*
[c)] *Dept. de Física Teórica de la Materia Condensada, Universidad Autónoma de Madrid, Spain*
[d)] *Dutch Institute for Fundamental Energy Research, DIFFER, and Eindhoven University of Technology, 5612 AE Eindhoven, The Netherlands, presenting author e-mail: luisa.bausa@uam.es*

Controlling the properties of rare earth emitters (RE) in solid-state platforms in the absence of an optical cavity is highly desirable for quantum light-matter interfaces and photonic networks. A promising approach is to combine plasmonic nanostructures with RE doped crystals, which can provide robust solid-state platforms with emergent functionalities at subwavelength scales.

Here, we show the capability of inducing directionality and spatial coherence in the emission of Nd^{3+} ions distributed into a solid-state platform in the absence of photonic cavity [1]. To that end, we have used a plasmonic chain formed by closely-spaced Ag nanoparticles, which transforms the incoherent emission from Nd^{3+} ions into spatially coherent light. In addition, we demonstrate the possibility of ultra-long-range waveguiding Nd^{3+} fluorescence by means of the plasmonic chain. Namely, sub-diffraction fluorescence waveguiding is demonstrated over several tens of microns in the technologically relevant NIR spectral range of 900–1100 nm. The spatial coherence and the long-range energy transport originate from the coherent near-field coupling of the Nd^{3+} emitters with the plasmon mode of the chain and the low dissipative losses displayed by this mode.

The work provides fundamental insights for controlling the coherence properties of quantum emitters offering new avenues for the design of integrated photonic circuits, as well as imaging, quantum technologies or sensing devices on solid-state platforms.

References

[1] J. Fernández-Martínez, et al. *Opt. Express* **29**, 16 (2021).
[2] J. Fernández-Martínez, et al. *Nanomaterials* **12**, 4296 (2022).

Core@shell structure with highly doped Nd^{3+} sensitizing ions for temperature sensing and bioimaging

Dominika Przybylska, [a] Natalia STOPIKOWSKA, [a] Anna EKNER-GRZYB, [b] Bartosz F. GRZEŚKOWIAK, [c] Tomasz GRZYB [a]

a) Department of Rare Earths, Faculty of Chemistry, Adam Mickiewicz University in Poznań, Uniwersytetu Poznańskiego 8, Poznań 61-614, Poland, [b]Faculty of Biology, Adam Mickiewicz University in Poznań, Uniwersytetu Poznańskiego 6, Poznań, 61-614, Poland, [c]NanoBioMedical Centre, Adam Mickiewicz University in Poznań, Wszechnicy Piastowskiej 3, Poznań 61-614, Poland
dominika.przybylska@amu.edu.pl

In recent years there has been a notable rise in interest in multifunctional materials, especially those at the nanoscale [1-3]. In this area, upconverting nanoparticles (UCNPs), capable of converting radiation from the infrared (lower energy) to visible or ultraviolet light (higher energy), are particularly promising. Those materials have some crucial advantages, especially significant for biomedical applications, like negligible autofluorescence, large anti-Stokes shift, deep penetration into tissue, reduced photodamage of the cells and the possibility to use inexpensive continuous lasers [4-5]. The upconversion phenomenon has been observed for various metal ions and organic compounds, among which it is most often described for rare earth ions (RE). However, to achieve efficient emission, UCNPs should be adequately designed, e.g., choosing a matrix characterized by low phonon energy, appropriate sensitizer and activator and their concentration, and using core@shell structure, which is helpful, especially for a higher concentration of activator and sensitizer ions [6]. In the presented study, core@shell structures with a high concentration of Nd^{3+} in a shell to achieve effective emission under 808 nm excitation wavelength were synthesized. The morphology, optical properties and thermal sensitivity were investigated. The obtained results are very promising and make the presented UCNPs pioneering in multifunctional materials for bioimaging and temperature sensing.

References:

[1] D. Ju, X. Gao, S. Zhang, Y. Li, W. Cui, Y. Yang, M. Luo, S. Liu, Temperature-dependent upconversion luminescence multicolor tuning and temperature sensing of multifunctional β-$NaYF_4$:Yb/Er@β-$NaYF_4$:Yb/Tm microcrystals, *CrystEngComm.*, 23, **2021,** 3892–3900.

[2] J. Li, S. Xu, Y. Yu, K. Liu, Y. Gao, B. Chen, 808 nm triggered multifunctional UCNPs@PDA nanocomposites for temperature sensing and photothermal conversion, *J. Mater. Sci. Mater. Electron*, 33, **2022,** 6563–6575.

[3] X. Yan, T. Li, L. Guo, H. Li, P. Chen, M. Liu, Multifunctional BiF_3:Ln^{3+} (Ln = Ho, Er, Tm)/Yb^{3+} nanoparticles: An investigation on the emission color tuning, thermosensitivity, and bioimaging, *RSC Adv.*, 9, **2019**, 10889–10896.

[4] J. Yao, C. Huang, C. Liu, M. Yang, Upconversion luminescence nanomaterials: A versatile platform for imaging, sensing, and therapy, *Talanta*, 208, **2020,** 120157.

[5] F. Auzel, Upconversion and Anti-Stokes Processes with f and d Ions in Solids, *Chem. Rev.* 104, **2004,** 139–173.

[6] J. Zhou, Q. Liu, W. Feng, Y. Sun, F. Li, Upconversion luminescent materials: Advances and applications, *Chem. Rev.* 115, **2015,** 395–465.

Scintillation properties of composite scintillators based on doped orthosilicate compounds

Sandra WITKIEWICZ-LUKASZEK[a*], Vitaly GORBENKO[a], Tetiana ZORENKO[a], Jiri A. MARES[b], Romana KUCERKOVA[b], Martin NIKL[b], Oleg SIDLETSKIY[c], Yuriy ZORENKO[a]

[a]*Institute of Physics, Kazimierz Wielki University, Bydgoszcz, 85090, Poland*
[b]*Institute of Physics, AS Czech Republic, Prague, 6253, Czech Republic*
[c]*Institute for Scintillation Materials, NAS of Ukraine, 61001 Kharkiv, Ukraine*
**e-mail: s-witkiewicz@wp.pl*

The single crystals (SC) of Ce^{3+} doped A_2SiO_5 (A = Lu, Y) orthosilicates have been developed as promising scintillators for positron emission tomography (PET) due to their desirable properties such as high density, fast decay time and high light output [1]. Meanwhile, apart from their applications in crystal form, these orthosilicates also attract attention regarding the development of single crystalline film (SCF) scintillating screens for microtomography using the liquid phase epitaxy (LPE) method [2].

Recently, we developed various types of the doubly- and three-layered composite scintillators (CS), based on the SCFs of Ce^{3+} and Pr^{3+} doped (Y, Lu)AG simple garnets and Ce^{3+} doped $(Y,Lu,Tb,Gd)_3(Al,Ga)_5O_{12}$ mixed garnets, grown using the LPE method onto heavy LuAG:R (R=Pr,Ce,Sc) and GAGG:Ce substrates [3, 4]. The results of our current researches show that the epitaxial structures of orthosilicates can be also considered as promising composite scintillators for simultaneous detection of α-, β-particles and γ-rays.

In this work, two different sets of CSs based on the YSO:Ce SCF/LYSO:Ce SC and $(Y_{0.75}Lu_{0.25})$SO:Bi SCF/LYSO:Ce SC epitaxial structures were grown by the LPE method. For the characterization of the luminescent and scintillation properties of SCF and bulk crystal parts of composite scintillators, the absorption and CL spectra as well as pulse heigth spectra scintillation decay kinetics under α– and β- particle and γ- quantum excitation were applied. Futhermore, we show the possibility of the simultaneous registration of these types of ionization radiation by the way of separation of the scintillation decay kinetics of SCF and SC parts of composite scintillators (Fig.1a). Namely, the $(Y_{0.75}Lu_{0.25})$SO:Bi SCF/ LYSO:Ce SC type of composite scintillator are characterised by high LY of their film and bulk crystal parts and suitable Figure of Merit (FOM) ratios $FOM_{\alpha\beta} = t_\alpha - t_\beta / t_\alpha + t_\beta$, $FOM_{\alpha\gamma} = t_\alpha - t_\gamma / t_\alpha + t_\gamma$ and $FOM_{\beta\gamma} = t_\beta - t_\gamma / t_\beta + t_\gamma$ under simultaneous registration of mentioned types of radiation (Fig.1b).

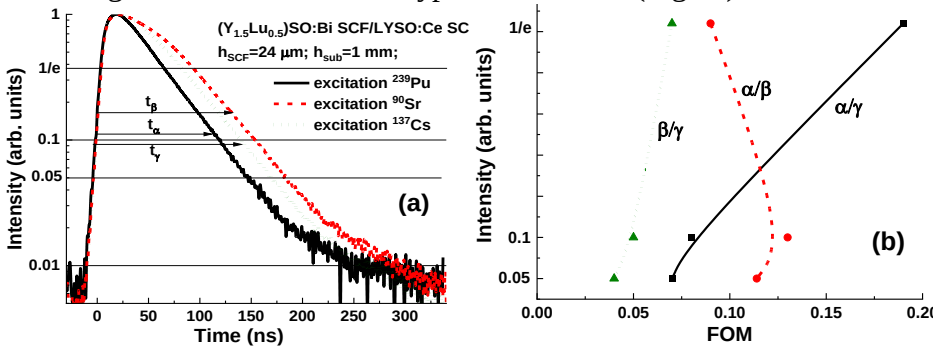

Fig.1. (a) - separation of the scintillation decay curves of $(Y_{1.5}Lu_{0.5})$SO:Bi SCF/LYSO:Ce SC composite scintillators under excitation by α- (^{241}Am) and β- (^{90}Sr) particles and γ-quanta (^{123}Cs). (b) –scintillation intensity decay and FOM values of this composite under registration of the mentioned types of radiation.

References:

[1] W. Chewpraditkul, e.a. *Optical Materials* **35**, 1679-1684 (2013).
[2] T. Martin, T., P.-A. Douissard, M. Couchaud, A. Cecilia, e. a. IEEE Trans. Nucl. Sci., 56, 1412-1418 (2009).
[3] J.A. Mares, S. Witkiewicz-Lukaszek, e. a. *Optical Materials* **96**, 109268 (2019).
[4] S. Witkiewicz-Lukaszek, e. a. *CrystEngComm* **22**, 3713-3724 (2020).6

Second harmonic microscopy of femtosecond laser micro-modifications in BBO crystal

Nuria SEVILLA-SIERRA, Javier R. VÁZQUEZ DE ALDANA, Ignacio LOPEZ-QUINTAS

Grupo de Investigación en Aplicaciones del Láser y Fotónica, Universidad de Salamanca, Pl. La Merced SN. 37008 Salamanca, Spain; nsevillasierra@usal.es

Second harmonic generation microscopy (SHGM) is a microscopy technique based on the non-linear interaction of an intense fundamental beam (i.e., a femtosecond laser) with a sample. As a result, a signal with double the frequency of the incident beam is generated and registered while the sample is scanned. The so-generated images provide information with high spatial resolution about the second-order susceptibility of the sample, thus allowing to gain insight into its microscopic structure. It has been successfully applied to the analysis of biological samples [1], being also very useful in materials science [2].

On the other hand, femtosecond lasers have consolidated as excellent tools with unique properties for 3D micro-structuring of transparent dielectrics, enabling the direct writing (DW) of photonic devices in almost any optical material: the focused laser inside the target produces a localized damage track modifying the refractive index. This mechanism allows the fabrication of miniaturized efficient photonic devices [3].

In this work, we analyze by SHGM the damage tracks created inside a β-BaB_2O_4 (BBO) crystal. BBO is one of the most widely used nonlinear crystals for SHG with ultrashort pulses due to its high optical nonlinearity, wide range of transparency and physical robustness. In addition, it possesses *3m* structure and has the possibility to phase-match the SHG process in a large spectral window, ensuring efficient conversion. We present a detailed study of the damage tracks inscribed with different irradiation conditions and geometries, demonstrating that, under certain conditions, the SHG process in the damage tracks may exhibit a local enhancement. This effect is obs27erved both in phase-matching as in anti-phase-matching conditions, suggesting that the effective non-linear coefficient is enhanced by the high-intensity laser modification.

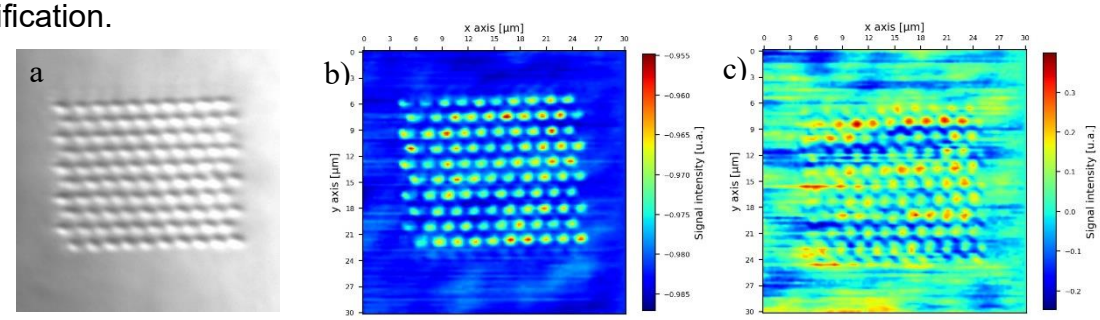

Figure 1: a) Optical image of an array processed with fs laser pulses inside a BBO crystal. b) SHGM image in phase-matching conditions. c) SHGM image in anti-phase-matching conditions.

References:

[1] Freund, I., and Deutsch, M.; Second harmonic microscopy of biological tissue. *Optics Letters*, 11, **1986**, 94.

[2] Yokota, H. et al.; Optical second harmonic microscopy as a tool of material diagnosis. *Physics Research International*, 2012, **2012**, 704634.

[3] Chen F.; Vázquez de Aldana J.R.; *Direct femtosecond laser writing of optical waveguides in dielectrics* in *Laser micro-nano-manufacturing and 3D microprinting,* A. Hu ed. Springer: Switzerland, **2020.**

Designing photon upconversion nanoparticles showing luminescence in whole human blood

Natalia JURGA, Sylwia RYSZCZYŃSKA, Tomasz GRZYB

Department of Rare Earths, Faculty of Chemistry, Adam Mickiewicz University in Poznań, Uniwersytetu Poznańskiego 8, Poznań 61-614, Poland; natalia.jurga@amu.edu.pl

Finding the highly luminescent nanoparticles which can be excited in the range of first, second, or third biological windows is very important [1]. The near-infrared excitation provides low photodamage of biological materials, autofluorescence reduction, and deeper light penetration depth than in the case of UV and visible light [2]. Therefore, much attention has been paid to obtain up-converting nanoparticles (UCNPs) doped with lanthanide ions, which show intense luminescence even in biological fluids [3]. Nowadays, many blood experiments are carried on to determine, e.g., light penetration depth and the presence of analytes which are the markers for some diseases [4].

The main goal of our research was to determine the whole human blood penetration depth based on the luminescence of multi-mode NIR laser-excited UCNPs. The high-quality core/shell materials with hexagonal phases were obtained using precipitation in high-boiling-point solvents and then transferred to the water by acid treatment [5]. The different rare earth ions were used as light sensitizers: Yb^{3+} ions for 975 nm, Er^{3+} for 808, 975, and 1532 nm, or Tm^{3+} for 1208 nm covering the optical transparency windows, important for medicine. We registered the emissions of ligand-free UCNPs in the water and whole human blood at different sample depths. The effect of light absorption and scattering of blood components was observed. The research allowed us to estimate the depth to which the excitation radiation penetrates the sample and how thick a layer of blood allows to observe the emission. The presented results are important for developing UCNPs' applications in biomedicine.

References:

[1] Grzyb, T.; Kamiński, P.; Przybylska, D.; Sanz-Rodríguez, F.; Haro Gonzalez, P., Manipulation of up-conversion emission in $NaYF_4$ core@shell nanoparticles doped by Er^{3+}, Tm^{3+}, or Yb^{3+} ions by excitation wavelength—three ions—plenty of possibilities. *Nanoscale,* 13, **2021,** 7322-7333.

[2] Xu, J.; Gulzar, A.; Yang, P.; Bi, H.; Yang, D.; Gai, S.; He, F.; Lin, J.; Xing, B.; Jin, D., Recent advances in near-infrared emitting lanthanide-doped nanoconstructs: Mechanism, design and application for bioimaging. *Coordination Chemistry Rewievs*, 381, **2019**, 104-134.

[3] Peng, J.; Sun, Y.; Zhao, L.; Wu, Y.; Feng, W.; Gao, Y.; Li, F., Polyphosphoric acid capping radioactive/upconverting $NaLuF_4$:Yb,Tm,^{153}Sm nanoparticles for blood pool imaging in vivo. *Biomaterials*, 34, **2013**, 9535-9544.

[4] Brandmeier, J.C.; Jurga, N.; Grzyb, T.; Hlaváček, A.; Obořilová, R.; Skládal, P.; Farka, Z.; Gorris, H.H., Digital and Analog Detection of SARS-CoV-2 Nucleocapsid Protein via an Upconversion-Linked Immunosorbent Assay. *Analytical Chemistry,* 95, **2023,** 4753–4759.

[6] N. Jurga, D. Przybylska, P. Kamiński, T. Grzyb, Improvement of ligand-free modification strategy to obtain water-stable up-converting nanoparticles with bright emission and high reaction yield. *Scientific Reports*, 11, **2021**.

Surface waveguides with modal shaping in Nd:YAG crystal for sensing applications: design and fabrication with femtosecond laser pulses

Víctor ARROYO[a)], Carolina ROMERO[a)], Javier R. VÁZQUEZ DE ALDANA[a)].

[a)] *Aplicaciones del Láser y Fotónica, Universidad de Salamanca, Pl. La Merced SN. 37008 Salamanca*

Contact e-mail: varroyo@usal.es

The use of femtosecond lasers for the fabrication of photonic devices integrated in transparent dielectric materials has proven to be a very useful and effective technique as it provides some important advantages over other methods commonly used. Among these advantages, we can name two, the fact that it is a one-step process, and the ability to realize three-dimensional structures inside the material with arbitrary geometry [1]. The fabrication process consists in focusing the ultrashort laser pulses inside the material in such a way as to induce a controlled modification of the refractive index in the irradiated zone, following a desired geometry. The development of this technique has allowed the fabrication of complex photonic circuits, which can be used in different scientific fields, such as biomedicine or optical sensing.

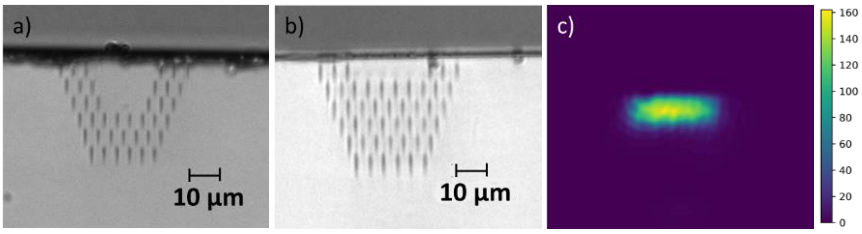

Figure 1: In a) and b), optical microscopy images of the entrance and exit sections, respectively, of a straight waveguide integrated in crystalline Nd:YAG. In panel c) image of the mode of a He-Ne laser (633 nm) coupled in the waveguide.

In this work, we present the design, fabrication and characterization of surface waveguides in Nd:YAG by femtosecond laser pulses. The waveguides, based on "depressed-index cladding" type structures [2], present an optimized design that allows "modal shaping", which permits to progressively increase the contact area of the guided mode with the top surface of the sample. Nd:YAG has been chosen as the paradigmatic crystal, for being one of the active medium in the fabrication of solid-state lasers and active devices, which in turn presents high stability, isotropy and high transparency in the near-infrared optical range.

These types of structures present a great potential for its integration into high efficiency active optical sensors [3] as we expect a considerable increase in the sensing area, while maintaining a controlled single-mode profile. Although the technique has been demonstrated in Nd:YAG, it could be extended to any other transparent crystal.

References:

[1] Osellame, R.; Maselli, V.; Vazquez, R. M.; Ramponi, R.; Cerullo, G., Integration of optical waveguides and microfluidic channels both fabricated by femtosecond laser irradiation. *Applied physics letters*, 90(23), 231118, **2007**.

[2] Okhrimchuk, A., Mezentsev, V., Shestakov, A., & Bennion, I. (2012). Low loss depressed cladding waveguide inscribed in YAG: Nd single crystal by femtosecond laser pulses. *Optics express*, *20*(4), 3832-3843, **2012**.

[3] Li. G.; et al. Intracavity biosensor based on the Nd:YAG waveguide laser: tumor cells and dextrose solutions. *Photonics research* 5, 728, **2017**.

Toward white light emission from Bi and V codoped borosilicate glasses upon UV excitation

Giulio GORNI, [a] Cristina PÉREZ, [a] Isabel MUÑOZ-OCHANDO, Irene LLORENTE,[c] Rosalia SERNA,[a] José GONZALO [a]

[a] Laser Processing Group, Instituto de Óptica (IO), Consejo Superior de Investigaciones Científicas (CSIC), Madrid, 28006;
[b] Centro Nacional de Investigaciones Metalúrgicas (CENIM), Consejo Superior de Investigaciones Científicas (CSIC), 28040 Madrid;
[c] Instituto de Ciencia y Tecnología de Polímeros (ICTP), Consejo Superior de Investigaciones Científicas (CSIC), 28006, Madrid, Spain;
g.gorni@csic.es

Developing low-cost phosphors for application in white light emitted diodes (LEDs) is one of the main challenges of current research activity [1]. The use of rare-earth ions (RE) in combination with a suitable host is one of the most used strategies to produce white light emission. However, the weak absorption cross section of RE ions together with their sharp emission bands make quite difficult obtaining intense white emission. In this study we explore a different approach based on Bi and V codoped borosilicate glasses. Borosilicate glasses are cheap materials with excellent mechanical and chemical properties and they possess a good transparency in the visible spectrum [2]. The blue emission of Bi^{3+} combines with the intense yellow-orange emission from V^{5+} ions to produce broad and intense white light emission upon near UV excitation. A detailed analysis by means of Raman, FTIR, XPS and PL spectroscopy will be shown to correlate the structure and composition of these glasses with their emission properties.

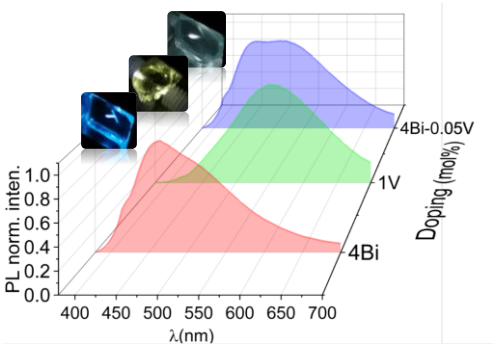

Figure 1: Photoluminescence emission of borosilicate glasses doped with Bi and V. The insets show images of the glasses under 355 nm excitation.

References:

[1] Huang, X.; Liang, J.; Rtimi, S.; Devakumar, B.; Zhang, Z., Ultra-high color rendering warm-white light-emitting diodes based on an efficient green-emitting garnet phosphor for solid-state lighting. *Chem. Eng. J.*, 405, **2021**, 126950.

[2] Liu, X. Y.; Guo, H.; Liu, Y.; Ye, S.; Peng, M. Y.; Zhang, Q. Y., Thermal quenching and energy transfer in novel Bi^{3+}/Mn^{2+} co-doped white-emitting borosilicate glasses for UV LEDs. *J. Mater. Chem. C,* 4, **2016,** 2506-2512.

Local structures of Tm ions in $Ca_2Al_2SiO_7$:Eu,Tm long persistent phosphorescence phosphor studied by X-ray fluorescence holography and positron annihilation lifetime spectroscopy

M. Kitaura,[a)*] H. Masai,[b)] S. Watanabe,[c)] Y. Yamamoto,[d)] T. Kato,[e,f)] K. Kimura,[e)] N. Happo,[g)] K. Hayashi,[e,h)] S. Kodama,[i)] H. Takeda,[i)] T. Nakanishi,[j)]

[a)]***Yamagata Univ.***, [b)]***AIST***, [c)]***Tokyo Inst. Tech.***, [d)]***NAIST***, [e)]***Nagoya Inst. Tech.***, [f)]***Univ. Grenoble Alpes***, [g)]***Hiroshima City Univ.***, [h)]***JASRI/SPring-8***, [i)]***Saitama Univ.***, [j)]***NIMS***

[*)]**kitaura@sci.kj.yamagata-u.ac.jp**

$Ca_2Al_2SiO_7$:Eu,Tm is newly found long persistent phosphorescence (LPP) phosphor [1]. It has been believed that Eu and Tm ions occupy the Ca site in $Ca_2Al_2SiO_7$, because the ionic radii of them are larger than those of Al and Si ions. However, the Tm ion has a trivalent state, different from a divalent state of the Ca ion. This situation makes it difficult for Tm ions to occupy Ca sites simply. The existence of Tm ions at Ca sites will require an additional charge compensation to resolve the charge inconsistency between Tm and Ca ions. Since Tm ions play an important role as an electron trap to cause LPP, it is significant to clarify the local structure and charge compensation mechanism around Tm ions. In the present study, we have investigated local structures of Tm ions in $Ca_2Al_2SiO_7$:Eu,Tm crystals by X-ray fluorescence holography (XFH) and positron annihilation lifetime spectroscopy (PALS). The former and latter have been successfully applied to the local structure analyses of impurities [2] and vacancy-type defects [3]. Figure 1 shows an atomic image around Tm ions on the (001) plane at z=0 Å, reconstructed from Tm Lα-XFH holograms. The reconstructed atomic image was drawn with grey. Open circles indicate the atomic arrangement around the Ca site, determined by the XRD analysis. The reconstructed atomic image could be seen within open circles, indicating that Tm ions occupy the Ca site. The intensity of the atomic image was weakened remarkably, and comparable to that of artifacts outside open circles. This fact implies that positional fluctuation and lattice deformation are introduced around Tm ions.

This work was partially supported by JSPS Grants-in-Aid for Transformative Research Areas (A) “Hyper-Ordered Structures Sciences” via Grant Nos. 20H05878, 20H05881, 21H05546.

References:

[1] *Zhao, L. et al., A new yellow long persistent luminescence phosphor $Ca_2Al_2SiO_7:Eu^{2+},Tm^{3+}$ found by co-doping Ln^{3+} (Ln = Ce, Pr, Nd, Sm, Gd, Tb, Dy, Ho, Er, Tm, Yb, Lu) with Eu in $Ca_2Al_2SiO_7$ host, J. Lumin. Vol. 206, **2019**, 6-10.*

[2] *Hayashi, K. et al., X-ray fluorescence holography, J. Phys: Condens. Matter Vol. 24, **2012**, 093201.*

[3] *Kitaura, M. et al.; Characterization of imperfections in scintillator crystals using gamma-ray induced positron annihilation lifetime spectroscopy: Opt. Mater: X, City, Vol. 14, **2022**, 100156.*

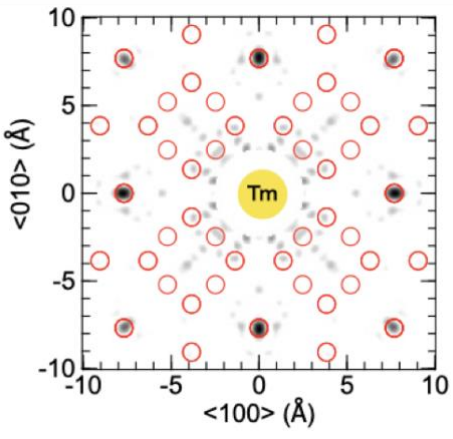

Fig. 1. Atomic image around Tm ions on the (001) plane at z=0 Å, reconstructed from Tm Lα-XFH holograms.

Luminescence and scintillation properties of Tb,Ce co-doped $(Gd,La)_2Si_2O_7$ for radiation imaging

Rikito MURAKAMI, [a] **Shunsuke KUROSAWA,** [c),d)] **Masao YOSHINO,** [c)]

Takahiko HORIAI, [c)] **Akihiro YAMAJI,** [c)] **Yasuhiro SHOJI,** [b)] **Kei Kamada,** [b),c)]

Yuui YOKOTA, [a)] **Akira YOSHIKAWA,** [a),b),c)]

[a)] Institute for Materials Research, Tohoku Univ [b)] C&A Corp. [c)] New Industry Creation Hatchery Center, Tohoku Univ. [d)] Institute of Laser Engineering, Osaka University; rikito.murakami.d4@tohoku.ac.jp

Radiation imaging is an important application for scintillators, including medical imaging and alpha particle detection. Brighter scintillators is required to have higher sensitivity.. Ce:$(La,Gd)_2Si_2O_7$ (Ce:La-GPS) has a relatively high effective atomic number (Z_{eff} = 54) and is known as one of the highest light-yielding materials among silicate scintillators. Ce:La-GPS shows the light output and energy resolution of 42,000 photons/MeV and 5 % (662 keV, FWHM), respectively [1]. However, the emission wavelength of Ce:La-GPS is around 390 nm, resulting in low wavelength sensitivity for CCD or CMOS sensors.

Previously, higher optical output and quantum yields can be obtained by co-doping with energy transfer, such as Gd^{3+} to Ce^{3+} and Ce^{3+} to Tb^{3+} [2]. To enhance the wavelength sensitivity in photodetectors, optical properties of Tb^{3+} was co-doped with Ce:La-GPS was investigated, because green emission derived from the 4f-4f transition of Tb^{3+}. We have previously reported Tb:La-GPS with an emission wavelength of 550 nm, which is suitable for X-ray imaging and fluorescent materials[3]. In addition, we have previously reported that the quantum yield of La-GPS is enhanced by the co-doping of Ce and Tb. However, the imaging performance of the co-doped crystals has not been reported. In this study, we report the luminescence and scintillation properties as well as the radiation imaging properties of Tb,Ce:La-GPS.

Compositional screening for Tb and Ce concentration was performed with sintered compacts, and a single crystal of the composition with a high photoluminescence quantum yield was grown by the micro-pulling-down (μ-PD) method. Photoluminescence properties were measured with an integrating sphere. Transmittance spectra, excitation and emission spectra were obtained for grown crystals at room temperature. In addition, scintillation properties for gamma and alpha radiation were measured using ^{137}Cs and ^{241}Am souces, respectively. Radiation imaging using an ^{241}Am source was also taken using the high-resolution alpha-ray imaging system with an optical microscope [4]. The grown $(Tb_{0.015},Gd_{0.735},Ce_{0.015},La_{0.235})_2Si_2O_7$ single crystal showed a transmittance of over 80%, and position resolution was about 3 times higher than that of conventional Ce:La-GPS. Details of the luminescence and scintillation properties are discussed in the poster presentation.

References:

[1] A. Suzuki, A. Yoshikawa et al., Appl. Phys. Exp. 5, (2012) 102601.
[2] Y. Zorenko et al., Rad. Mes., 56, (2013) 415-419.
[3] S. Kurosawa, R. Murakami, et al., Opt. Mater. (2015) 80-83.
[4] S. Kurosawa, et al., Radiat. Meas. 106 (2017) 187–191.

Tailoring the optical and photometric properties of light sources based on dual-layer ceramics

Anna KOZŁOWSKA, [a] Oskar BOGUCKI, [a] Helena WĘGLARZ, [a] Agnieszka SZYSIAK, [a] Marcin KACZKAN, [b] Bartosz FETLIŃSKI, [b] Bartosz JANASZEK, [b] Marcin KIELISZCZYK, [b] Romain TRIHAN, [c] Fabrice ROSSIGNOL, [c] Anne AIMABLE, [c] Martin IHLE, [d] Steffen ZIESCHE, [d] Piotr GIEMZA, [e]

[a] Łukasiewicz Research Network – Institute of Microelectronics and Photonics, Warsaw, Poland, [b] Warsaw Univ. of Technology, WEITI, Institute of Micro- and Optoelectronics, Warsaw, Poland, [c] Univ. Limoges, CNRS, IRCER, Limoges, France, [d] Fraunhofer Institute for Ceramic Technologies and Systems (IKTS), Dresden, Germany, [e] Teknosystem sp. z o.o, Warsaw, Poland; anna.kozlowska@imif.lukasiewicz.gov.pl

Light sources based on ceramics activated with electroluminescent or laser diodes gained considerable interest during last years. Research presented in this work is focused on dual-layer ceramics with various combinations of rare-earth doping of yttrium aluminium garnet ($Y_3Al_5O_{12}:RE^{3+}$, $YAG:RE^{3+}$). Freeze granulation process and granulate pressing was used to obtain two-layer green-bodies sintered into transparent ceramics in the solid-state process. Desired layer thickness was obtained by precise grinding and polishing of the structures.

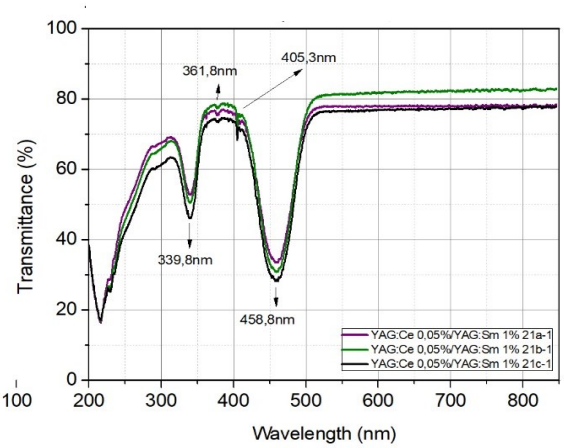

Fig. 1 Transmittance of exemplary dual-layer ceramic samples

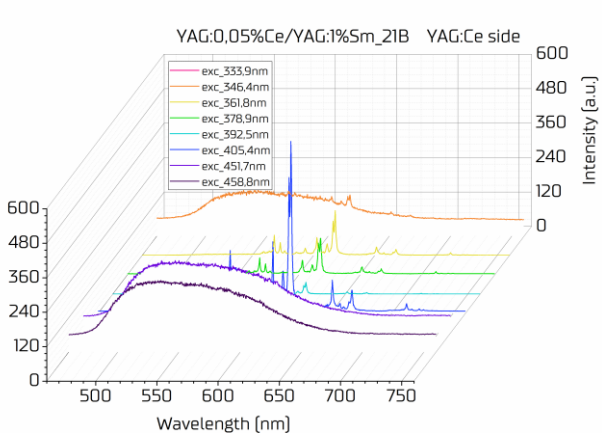

Fig. 2. Emission spectra for YAG:Ce 0,05%/YAG:Sm 1% ceramics for different excitation wavelengths.

Results of transmittance of exemplary dual-layer samples YAG:Ce0,05%/ YAG:Sm1%, with different layer thicknesses, are shown in Fig. 1. High transmittance in the range 500-850 nm indicates a good quality of ceramics. Evolution of emission spectra for different excitation wavelengths is shown in Fig. 2. Proper adjustment of dopant concentration, layer thickness and microstructure of each layer allows to tailor optical properties (absorption, emission, scattering) and photometric (e.g. chromatic coordinates, luminous efficiency) of resulting light source.

Acknowledgements: this work is performed within M-Era.Net call 2019 project entitled „New versatile platform for illumination and sensing”. Research conducted in Poland was financed by NCBR under the grant No: M-ERA.NET2/2019/8/2021.

Ce^{3+} centers in scintillating lithium fluorophosphate glasses

Melvin John F. EMPIZO, [a,b] Keito SHINOHARA, [a] Mayrene A. UY, [a,c] Angelo P. RILLERA, [a,c] Hitoshi ABE, [c,d,e] Nobuhiko SARUKURA, [a,f] Akihiro YAMAJI, [f] Akira YOSHIKAWA, [f] Takahiro MURATA, [g] Malgorzata GUZIK, [h] Yannick GUYOT, [i] Georges BOULON, [i] and Christophe DUJARDIN [i]

[a] University of the Philippines Diliman [b] Osaka University [c] The Graduate University for Advanced Studies (SOKENDAI) [d] High Energy Accelerator Research Organization (KEK) [e] Ibaraki University [f] Tohoku University [g] Kumamoto University [h] University of Wroclaw [i] Université Claude Bernard Lyon 1; mempizo@nip.upd.edu.ph

Lithium fluorophosphate glasses in the form of $20Al(PO_3)_3$-80LiF have been considered as potential scintillator host materials for laser fusion experiments [1]. These glasses have a lithium (Li) content of 31.6 mmol cm^{-3} [2] which is essential in enhancing the detector sensitivity to 270 keV, down-scattered neutrons. The detection of these low-energy neutrons is necessary in analyzing the imploded plasma areal density and in understanding the fusion plasma dynamics. As a comprehensive follow-up of our earlier report [3], we then present the spectroscopic characterization, luminescence properties, and scintillation mechanisms of the Ce^{3+}-doped lithium fluorophosphate glasses. The fluorophosphate glasses are prepared by melt-quenching method with a chemical composition of $20Al(PO_3)_3$-80LiF-$x$$CeF_3$ where x ranges from 0.5 to 3.0 mol%. The existence of stable Ce^{3+} centers in these glasses is confirmed by x-ray absorption spectroscopy along the higher Ce K-edge energy (40443.0 eV) which allows a more direct measurement of the oxidation states than the commonly accessed Ce L-edge energies (5723.4 to 6548.8 eV). Through the characterization of thinner (~ 2.0 mm) samples, the Ce^{3+}-doped APLF glasses have been shown to exhibit absorption and excitation edges as well as intense emission peaks which correspond to the interconfigurational Ce^{3+} 5d → 4f transitions. When the doping concentration increases, the self-absorption also increases, and the emission band appears shifted. Moreover, the strong UV emission have fast average lifetimes of less than 30 ns, a quantum yield of ~ 80 % measured under UV excitation, and a scintillation light yield of up to 620 photons/n of a 1.0 MeV neutron (^{252}Cf) source. The understanding of the properties and mechanisms of the Ce^{3+} centers in these lithium fluorophosphate glasses will likewise pave the way for their development as neutron scintillator materials for laser fusion experiments.

References:

[1] Arikawa, Y.; Yamanoi, K.; Nagai, T.; et al., Note: light output enhanced fast response and low afterglow ^6Li glass scintillator as potential down-scattered neutron diagnostics for inertial confinement fusion. *Rev. Sci. Instrum.*, Vol. 81, **2010**, 106105.

[2] Murata, T.; Fujino, S.; Yoshida, H.; et al., Custom-designed fast-response praseodymium-doped lithium 6 fluoro-oxide glass scintillator with enhanced cross-section for scattered neutron originated from inertial confinement fusion. *IEEE Trans. Nucl. Sci.*, Vol. 57, **2010**, 1426 – 1429.

[3] Yamanoi, K.; Murata, T.; Yanagida, T.; et al., Scintillation and optical properties of Ce-doped fluoride glass samples with different Ce concentrations. *Sensors*, Vol. 27, **2015**, 229 – 335.

Modelling of spectral response of electrically biased suspended graphene over variable trench depth

Kamila LEŚNIEWSKA-MATYS, [a] **Anna KOZŁOWSKA**, [a] **Oskar BOGUCKI**,[a]

a) Łukasiewicz – Institute of Microelectronics and Photonics, Al. Lotników 32/46, 02-668 Warsaw, Poland

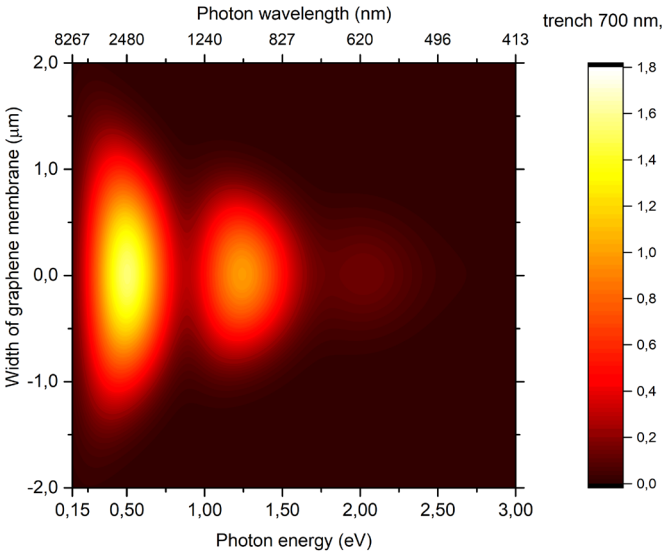

Fig. 1. Simulated intensity of thermal radiation from suspended graphene for 700 nm trench depth.

The light emission from graphene-based light-emitting devices has attracted considerable interest due to its promising applications in optical modulation and optical sensing [1], [2].

In this work, we present the simulation of the multiple thermal light emission peaks and significant spectral modulation based on the interference effects between the light emitted directly from the graphene and the light reflected from the substrate [3].

We consider the influence of temperature (i.e. applied voltage) and variable trench depth below suspended graphene on thermal emission.

In Fig. 1. we present simulated intensity of suspended graphene thermal radiation over the trench 700 nm depth taking into account temperature gradient of the membrane surface.

Acknowledgments

This study was supported by the National Science Centre, Poland, Research Project No UMO-2020/02/Y/ST5/00105, acronim TAGGED.

We would like to thank consortium partners of TAGGED project from Fraunhofer – Institute for Electronic Nano Systems, Freiberg University of Mining and Technology and J. Heyrovsky Institute of Physical Chemistry for helpful discussions and fruitful cooperation.

References:

[1] Junaid M.; Md Khir MH.; Witjaksono G. et al. A Review on Graphene-Based Light Emitting Functional Devices. *Molecules*, Vol. 25, **2020**, 4217.

[2] Kim YD.; Gao Y.; Shiue RJ.; et al. Ultrafast Graphene Light Emitters. *Nano Lett*. Vol, 18, **2018**.

[3] Kim YD.; Kim H.; Cho Y.; et al. Bright visible light emission from graphene. *Nat Nanotechnol*. Vol.10, **2015**, 676-681.

Pr^{3+} ion energy levels and decay times of scintillating fluoride glasses

Keito SHINOHARA, [a)] Melvin John F. EMPIZO, [a,b)] Mayrene A. UY, [a,c)] Angelo P. RILLERA, [a,c)] Hitoshi ABE, [c,d,e)] Kohei YAMANOI, [a)] Toshihiko SHIMIZU, [a)] Nobuhiko SARUKURA, [a,f)] Takahiro MURATA, [g)] Pavlo MAI, [h)] Christophe DUJARDIN, [h)] Malgorzata GUZIK, [i)] and Georges BOULON [h)]

[a)] Osaka University [b)] University of the Philippines Diliman [c)] The Graduate University for Advanced Studies (SOKENDAI) [d)] High Energy Accelerator Research Organization (KEK) [e)] Ibaraki University [f)] Tohoku University [g)] Kumamoto University [h)] Université Claude Bernard Lyon 1 [i)] University of Wroclaw; shinohara-k@ile.osaka-u.ac.jp

Praseodymium (Pr^{3+})-doped fluoride glasses have been considered as potential scintillator materials due their fast decay times as well as higher band gaps, i.e., shorter absorption edges compared to typical oxide materials. In this work, we report our investigations on novel Pr^{3+}-doped scintillating fluoride glasses: namely, $20Al(PO_3)_3$-80LiF-PrF_3 (1.0 mol% Pr^{3+}-doped APLF), $19BaF_2$-$33.25CaF_2$-$42.75AlF_3$-$5YF_3$-PrF_3 (1.0 mol% Pr^{3+}-doped BCAYF), and $19BaF_2$-$33.25CaF_2$-$42.75AlF_3$-$15P_2O_5$-20LiF-PrF_3 (1.0 mol% Pr^{3+}-doped BCAPLF) prepared by conventional melt-quenching method. Through x-ray absorption near-edge structure (XANES) spectroscopy along the Pr LIII edge, it was confirmed that the Pr ions in these complex host glasses exist with 3+ oxidation state. Moreover, the Pr^{3+}-doped glasses exhibit absorption and emission peaks which correspond to the different interconfigurational 4f5d and intraconfigurational $4f^2$ transitions of Pr^{3+} ions. The spectroscopy results also indicate that the Pr^{3+} ions in these fluorides have a 4f5d excited state configuration that overlaps with the $^1S_0$ level of the $4f^2$ ground state configuration but with varying gaps between the lowest 4f5d level and the $^1S_0$ level. Under x-ray excitation, the UV emissions of the Pr^{3+}-doped glasses are primarily dominated by different transitions from the lowest 4f5d level or the $^1S_0$ level resulting in different decay times ranging from 23.83 to 190.81 ns. Our findings show that the gap between the $^1S_0$ level of the 4f configuration and the lowest level of the 4f5d configuration plays a role in achieving faster decay times due to fewer intraconfigurational $4f^2$ transitions in the UV region. Some strategies to obtain fast fluoride glass scintillators (e.g., Pr^{3+}-doped APLF) will likewise be put forward especially for future laser fusion experiments.

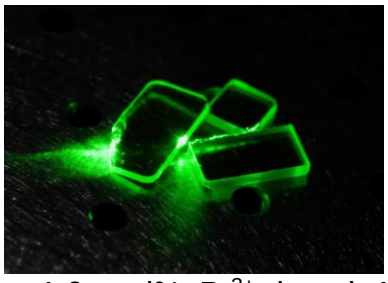

Figure 1. Photograph of the 1.0 mol% Pr^{3+}-doped APLF, BCAYF, and BCAPLF glasses.

Excitonic luminescence in $(Lu,Y)_2SiO_5:Ce^{3+}$ single crystals

Viktorija Pankratova, [a] Kirill Chernenko, [b] Aleksei Kotlov,[c] Anatoli I. Popov, [a] Vladimir Pankratov [a]

[a] Institute of Solid State Physics, University of Latvia, 8 Kengaraga, LV-1063 Riga, Latvia;
[b] MAX IV Laboratory, Lund University, P.O. Box 118, SE-22100 Lund, Sweden;
[c] Photon Science at DESY, Notkestrasse 85, Hamburg, Germany;
presenting author e-mail: vpank@latnet.lv

Although $(Lu,Y)_2SiO_5$ (or LYSO:Ce) has been identified as a possible scintillator material for medical and nuclear applications, there is still a lack of fundamental knowledge about the final stage of energy relaxation processes, which is crucial for the evaluation of scintillator performance in relevant modern applications, such as the new CMS detector in CERN. One of the most crucial factors influencing scintillator performance is the efficiency of energy transfer from the crystal lattice to the luminescence center (Ce^{3+}), which correlates with the intrinsic luminescence of the matrix. One of the possible mechanisms in LYSO is the excitation of Ce^{3+} ions via the relaxation of the self-trapped exciton (STE). The purpose of this study is a detailed study of luminescence properties as well as their temperature dependencies of STE in cerium-doped LYSO single crystals.

The intrinsic luminescence in Ce-doped $(Lu,Y)_2SiO_5$ (or LYSO:Ce) single crystals has been studied by means of excitation luminescence spectroscopy in the vacuum ultraviolet range under synchrotron radiation. Two experimental stations have been applied for the research. The first one is the photoluminescence endstation (Finestlumi) of FinEstBeAMs of MAX IV synchrotron facility (Lund, Sweden) [1-3], while another one is the Superlumi endstation of P66 beamline at PETRA III of DESY (Hamburg, Germany) [4].

A new, previously not reported luminescence band has been discovered at 250 nm. The excitation spectra of this emission, its temperature behavior as well as time-resolved properties (fast decay) allow us to assign this emission to self-trapped exciton in LYSO. Two possible models have been proposed. The first model explains the 250 nm as σ components of the self-trapped exciton, while the second model suggests that it arises from the radiative recombination of the self-trapped exciton in the lutetium sublattice.

References:

[1] R. Pärna, et al., FinEstBeaMS – A wide-range Finnish-Estonian Beamline for Materials Science at the 1.5 GeV storage ring at the MAX IV Laboratory. *Nucl. Inst. Met. Phys. Res. A 859 (2017) 83–89*

[2] V. Pankratov et al., Progress in development of a new luminescence setup at the FinEstBeAMS beamline of the MAX IV laboratory, *Rad. Measur.121 (2019) 91-98*

[3] K. Chernenko et al., Performance and characterization of the FinEstBeAMS beamline at the MAX IV Laboratory, *J. Synchrotron Rad. 28 (2021).1620–1630*

[4] V. Pankratov and A. Kotlov, Luminescence spectroscopy under synchrotron radiation: From SUPERLUMI to FINESTLUMI, *Nucl. Inst. Meth. Phys. Res.B 474 (2020) 35–40*

Influence of swift heavy ions on structural and luminescent properties of several important optical and scintillator materials

Viktorija PANKRATOVA,[a)] Vladimir A. Skuratov, [b)] Anatoli I. POPOV, [a)] Vladimir PANKRATOV [a)]

[a)] Institute of Solid State Physics, University of Latvia, 8 Kengaraga iela, LV-1063 Riga, Latvia
[b)] Joint Institute for Nuclear Research, Joliot-Curie 6, 141980, Dubna, Moscow Region, Russia;
viktorija.pankratova@cfi.lu.lv

Research and development of scintillating materials and novel ionizing radiation detecting devices for particle physics, neutron research, and medical imaging - are on the priority list of many European research centers including CERN.

In the current research radiation damages in the following single crystals relevant for nuclear and high-energy applications have been studied: $Gd_3Ga_2Al_3O_{12}$:Ce,Mg (GGAG:Ce,Mg), $Y_3Al_5O_{12}$ (YAG), $(Lu,Y)_2SiO5$:Ce (LYSO:Ce), $PbWO_4$ and PbF_2. These crystals were irradiated by 156 MeV Xe ions with several different fluences in the range $6.6x10^{10}$-$2x10^{12}$ cm^{-2}.

The induced radiation damages in all samples studied have been characterized by means of optical spectroscopy and VUV luminescence spectroscopy. The dependence of the radiation damage of irradiated crystals on the fluence of incident ions is established. The origin of radiation damage, which has its own characteristics in each specific material, will be discussed.

Photoluminescence and Raman spectroscopy of Ce^{3+} doped $Y_3Al_5O_{12}$ single crystalline films LPE grown onto $Y_3Al_5O_{12}$ and $Lu_3Al_5O_{12}$ substrates

Anton Markovskyi,[a,b] Vitalii Gorbenko,[b] Alexander Fedorov,[c] Piotr Radomski,[d] Tomasz Runka,[d] Yuriy Zorenko [b]

[a] Mechantronic Department, Kazimierz Wielki University in Bydgoszcz, Kopernik, 1, 85-074 Bydgoszcz, Poland;
[b] Institute of Physics, Kazimierz Wielki University, Powstancow Wielkopolskich str., 2, 85-090, Bydgoszcz, Poland.
[c] SSI Institute for Single Crystals, National Academy of Sciences of Ukraine, av. Nauki 60, 61178 Kharkiv, Ukraine
[d] Institute of Materials Research and Quantum Engineering, Faculty of Materials Engineering and Technical Physics, Poznan University of Technology, Piotrowo 3, 60-965, Poznań, Poland
a.mark@ukw.edu.pl

The Ce^{3+} doped $Y_3Al_5O_{12}$ (YAG) and $Lu_3Al_5O_{12}$ (LuAG:Ce) garnets, prepared in different forms: powders, transparent optical ceramics (OC), bulk single crystals (SC) and single crystalline films (SCF), are widely applied nowadays as luminescent converters in white light-emitting diodes, scintillators, cathodoluminescent screens and screens for the visualization of X-ray images, and other optoelectronic devices. The luminescence and scintillation properties of YAG:Ce and LuAG:Ce garnets in different forms depending on the synthesis process, which largely determines the types of intrinsic defects that predominate (vacancies, antisite defects, and their aggregates with impurities), their concentrations and distributions over the main volume and surface of phosphors [1].

Comparative analysis of YAG SCFs doped with Ce^{3+} ions grown onto YAG and LuAG substrates using liquid phase epitaxy (LPE) technique has been studied for the first time in this work by Raman and luminescence spectroscopy using Renishaw InVia Raman microscope. Due to Ce^{3+} doping and intense Ce^{3+} luminescence the Raman spectra had to be measured using the excitation wavelength of 785 nm. The Raman modes recorded for of YAG:Ce/YAG and YAG:Ce/LuAG are overlapped with electronic transitions attributed to rare earth (RE) trace impurities of the samples. Spectroscopic measurements obtained allow a distinction between SCF and the substrate for homoepitaxy-grown YAG:Ce /YAG and quasi-homoepitaxy-grown YAG:Ce /LuAG structures. Such two modes of film growth can result in the different mechano-optical properties of YAG:Ce SCFs related to the presence of mechanical stress on the SCF/substrate interface in the case of quasi-homo-LPE growth due to different YAG and LuAG lattice constants, and the absence of this phenomenon in the case on homo-LPE growth. Furthermore, the identification of a transition layer between YAG:Ce SCF and LuAG substrate, the width of which was about 2 micrometers was performed. The region, where the transformation from the structure of a YAG:Ce film to LuAG single crystal occurs, can be considered as a $Y_{3-x}Lu_xAl_5O_{12}$ solid solution, where x varies from 0 to 1. The measurements of the Ce^{3+} luminescence along the cross-section of epitaxial structures also make it possible to evaluate the transition from the Ce-doped film to the undoped substrate. Such a transition layer in which the luminescence intensity dropped to the minimum level was estimated to be equal to 5 and 9 micrometers for YAG:Ce /YAG and YAG:Ce /LuAG epitaxial structures, respectively.

References:

[1] C.R. Stanek, K.J. McClellan, M.R. Levy, R.W. Grimes, PSS B Basic Res., 243, **2006**, R75–R77.
[2] Z. Xia, A. Meijerink, Chem. Soc. Rev. 46, **2017**,275–299.

Luminescent Properties of Ce-doped Garnet Transparent Ceramics Prepared by the Spark Plasma Sintering Process

Shunsuke KUROSAWA, [a, b, c] **Hiroshi SONE,** [d] **Hiroaki Ujiie,**[d] **Koichi HARADA,** [b] **Akihiro YAMAJI,** [a,b] **Akira YOSHIKAWA** [a,b,c]

[a] *New Industry Creation Hatchery Center, Tohoku University,* [b] *Institute for Materials Research, Tohoku University,* [c] *Industrial Technology Institute, Miyagi Prefectural Government,* [d] *Institute of Laser Engineering, Osaka University; kurosawa@imr.tohoku.ac.jp*

Transparency is required for the material search of optical materials such as laser or scintillator, and we have investigated their optical properties for transparent single-crystals as scintillators or other optical materials grown by the Czochralski growth, micro-pulling down method [1]. Since around 2010, transparent ceramic scintillators have been studied [2] using the Vacuum sintering process or/and Hot Isostatic Pressing (HIP). Spark Plasma Sintering (SPS) Process is a much simpler and shorter sintering time than other methods, and we have investigated the scintillation properties for the transparent ceramics (i.e. Ce:$SrHfO_3$, Nd:Lu_2O_3) prepared by SPS process [3,4]. However, such materials had high-melting temperatures, and the preparation of single crystals (good transparent materials) is hard.

In this study, we prepared $Gd_3(Ga,Al)_5O_{12}$-based materials with a diameter of 20 mm by SPS process as shown in Fig. 1, and compared the optical and scintillation properties for the same material by Czochralski growth and other techniques. Photoluminescence (PL) and radio-luminescence peaks were located at around 550 nm excited by 420-nm photons, X-ray and 5.5-MeV alpha-rays, and this is the same result as the single crystal and ceramics by HIP. Up to now, the SPS sample had a transparency of around 10-20% which is smaller than the HIP sample (~50%) and single crystal (~80%). The light output was around 13,000 photons/MeV, while HIP and single crystals had that of ~ 55,000 photons/MeV. The small light output for the SPS sample might be due to low transparency. Although the SPS sample had light output and transparency, as a material search technique, this process is also effective, especially for high melting temperature samples.

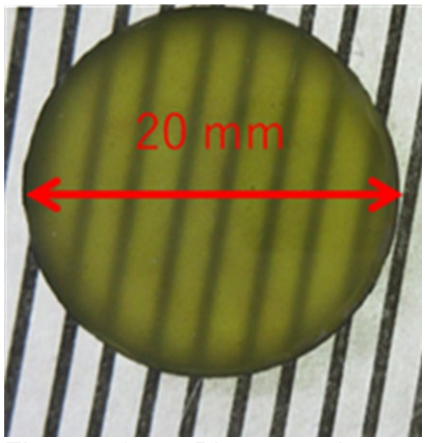

Fig. 1 Phtotograph of $Gd_3(Ga,Al)_5O_{12}$-based scintillator prepared by SPS.

References:

[1] A. Yoshikawa, et al., Journal of Crystal Growth, 270, 427–432 (2004).
[2] N. J. Cherepy et al., SPIE proc. 7805 0I, (2010)
[4] S. Kurosawa, et al., Radiat. Meas., 56, 155–158 (2013)
[3] S. Kurosawa, et al., IEEE Transactions on Nuclear Science, 61(1), 316-319 (2014).

Highly luminescent borogermanate glass with mixed perovskite $CsPb(Br,I)_3$ and $(Cs,Rb)Pb(Br,I)_3$ nanocrystals: properties and applications

Rufina KHARISOVA, Kseniya ZYRYANOVA, Natalia KUZMENKO, Arthur LOSIN, Anastasiia BABKINA

ITMO University; babkinauha@gmail.com

Materials containing perovskite nanocrystals have unique luminescent properties: such as high emission coefficients, narrow bands, and the possibility to obtain radiation in the entire visible range by changing the size of nanocrystals and the ratio of halogens and alkalis [1]. Despite the large number of proposals for the use of perovskite nanocrystals, for example, in solar batteries, LEDs, various detectors, scintillators, etc. [2], many of their properties are unstable while nanocrystals are contacting with air oxygen. To stabilize the properties of perovskite nanocrystals, they are usually placed in a polymer or glass matrix [3].

A series of borogermanate glasses of the system 23.59 B_2O_3 – 38.09 GeO_2 – 6.41 Na_2O – 5.03 ZnO – 1.38 P_2O_5 – 2.85 TiO_2 – 4.99 K_2O – 5.41(1-y) Cs_2O – 5.41y Rb_2O – 2, 26 PbO - 9.98(1-x) Br - 9.98x I mol.%, where x = 0; 0.4; 0.5; 0.6; 0.75; 1; y = 0; 0.25; 0.5; 0.75. Glass was synthesized in an air atmosphere at a temperature of 950°C for 30 min. Perovskite nanocrystals precipitated in the glass matrix upon annealing from 470°C.

In glasses, for which x and y are equal to zero (rubidium and iodine are absent in the composition), mostly $CsPbBr_3$ with admixture of Cs_4PbBr_6 perovskite crystals were nucleated. They have intense luminescence in the region of 500-530 nm, depending on the mean size of the crystals. When iodine ions were added, the luminescence maximum can be tuned in the range 500÷680 nm, depending on the bromine/iodine ratio. The maximum quantum yield was 40% for the composition with x=0.75. With the advent of rubidium, $(Cs,Rb)_4PbBr_6$ (or $(Cs,Rb)PbI_3$) nanocrystals were precipitated. With an increase in the rubidium content, the nanocrystals luminescence maximum shifted to the blue region, the luminescence quantum yield increased up to 51%, and the decay time increased up to 10 ns. Such luminescent properties make it possible to use the materials as scintillators.

References:

[1] Stylianakis, M. M., Maksudov, T., Panagiotopoulos, A., Kakavelakis, G., Petridis, K., Inorganic and hybrid perovskite-based laser devices: a review. *Materials*, Vol. 12, № 6, **2019**, 859.

[2] Li, X., Wu, Y., Zhang, S., Cai, B., Gu, Y., Song, J., Zeng, H., $CsPbX_3$ quantum dots for lighting and displays: room-temperature synthesis, photoluminescence superiorities, underlying origins and white light-emitting diodes. *Advanced Functional Materials*, Vol. 26, № 15, **2016**. 2435-2445.

[3] Yuan, S., Chen, D., Li, X., Zhong, J., Xu, X., In Situ Crystallization Synthesis of $CsPbBr_3$ Perovskite Quantum Dot-Embedded Glasses with Improved Stability for Solid-State Lighting and Random Upconverted Lasing. *ACS Appl. Mater. Interfaces.,* Vol. 10, № 22, **2018**, 18918-18926.

Dual green-red emission of Mn-doped Li_2O-ZnO-GeO2 glass-ceramics

Ekaterina KULPINA, Kseniya ZYRYANOVA, Natalia KUZMENKO, Varvara SHEREMET, Anastasiia BABKINA

ITMO University; babkinauha@gmail.com

Manganese ions as a transition ion are attracted by the fact that under the influence of redox conditions of material synthesis, different coordination, and crystal field strength, they can tune the wavelength of their luminescence maximum from the blue to the red region of the spectrum [1]. On the one hand, commercial red phosphors doped with Mn^{4+} are known [2], which in many respects are not inferior to similar materials with Eu^{2+}. On the other hand, green crystalline phosphors doped with Mn^{2+} with a long lifetime are known [3]. At the same time, in amorphous materials, Mn^{2+} exhibits both yellow-orange and green luminescence with a large half-width and lower intensity [4].

Mn-doped lithium-zinc-germanate glass had the composition of (30-x)Li_2O-xZnO-70GeO_2, where x=5; 7.5; 10; 15; 20; 22.5 mol.%. Glass-ceramics synthesis was carried out via homogeneous crystallization followed by interfacial-controlled growth. Glass-ceramics synthesis at 530–580°C led to nucleation of $Li_2Ge_4O_9$ и Li_2ZnGeO_4 nanocrystals with narrow luminescence of a doublet structure at 667 nm, corresponding to Mn^{4+} ions. In the composition containing 20 mol. % ZnO, the spectrum was dominated by a broad band with a maximum in the region of 540 nm, which was characteristic of Mn^{2+} ions in a tetragonal environment.

Glass-ceramics synthesized at 640°C and more possessed nucleation of $Li_2Ge_4O_9$ и $Li_2Ge_7O_{15}$ and two luminescence bands at 540 and 667 nm simultaneously. At low concentrations of ZnO, the spectrum is dominated by the band at 667 nm, which was characteristic of Mn^{4+} ions. With an increase in the concentration of zinc oxide, the intensity of this band decreased with a simultaneous increase in the intensity of the band at 540 nm, corresponding to Mn^{2+} ions. So, the final intensity ratio of different Mn luminescence bands depended on the Li/Zn ratio in the glass composition.

References:

[1] Félix-Quintero, H., et al., RGB emission of Mn^{2+} doped zinc phosphate glass. *J. Non. Cryst. Solids*, Vol. 466-467, **2017**, 59-63.

[2] Adachi, S., Crystal-field and Racah parameters of Mn^{4+} ion in red and deep red-emitting phosphors: Fluoride versus oxide phosphor. *J. Lumin.*, Vol. 218, **2020**, 116829.

[3] Jin, Y., Hu, Y., Duan, H., Chen, L., Wang, X., The long persistent luminescence properties of phosphors: Li_2ZnGeO_4 and Li_2ZnGeO_4:Mn^{2+}. *RSC Adv.*, Vol. 4, **2014**, 11360–11366.

[4] Peng, Y., Chen, J.,. Li, X., Zhong, J., Huang, H., Chen, D., Tuning Mn^{2+} luminescence in oxyfluoride glasses via Sc^{3+} doping. *J. Alloys Compd*, Vol. 805, **2019**, 483–488.

Structure and luminescence properties of Dy^{3+} doped $Li_3Ba_2Gd_3(WO_4)_8$ tungstate for applications in wLEDs

Sami Slimi[1,*], Abir Douzi[1,2], Eduard Madirov[3], Andrey Turshatov[3], Bryce S. Richards[3], Rosa Maria Solé[1], Magdalena Aguiló[1], Francesc Díaz[1], Ezzedine Ben Salem[2] , Xavier Mateos[1,#]

[1]Universitat Rovira i Virgili (URV), Física i Cristal·lografia de Materials (FiCMA), Marcel·li Domingo 1, 43007, Tarragona, Spain.

[2]I.P.E.I. of Monastir, Unit of Materials and Organic Synthesis, University of Monastir 5019, UR17ES31, Tunisia

[3]Institute of Microstructure Technology, Karlsruhe Institute of Technology, Hermann-von-Helmholtz-Platz 1, 76344 Eggenstein-Leopoldshafen, Germany .

[*]e-mail: sami.slimi@urv.cat, [#]Serra Húnter Fellow

Recently, efforts have continually been made to realize solid-state lighting devices based on white light-emitting diodes (wLEDs). The approach of combining yellow phosphors and blue InGaN diodes is widely used to achieve white light. Among the activator RE^{3+} ions, dysprosium ions (Dy^{3+}) are attractive for achieving yellow emission. The $^4F_{9/2} \rightarrow {}^6H_{13/2}$ and $^4F_{9/2} \rightarrow {}^6H_{15/2}$ transitions of Dy^{3+} fall in the yellow and blue spectral ranges, respectively, of which the $^4F_{9/2} \rightarrow {}^6H_{13/2}$ one is known to be hypersensitive to the crystal field [1]. In this work, yellow emitting tungstate phosphors with composition $Li_3Ba_2Gd_3(WO_4)_8$ doped with different concentrations of Dy^{3+} (from 1 to 10 at.%) were prepared by the solid-state reaction method at 900°C. Their structural (fig.1(a) and (b)), spectroscopic and optical properties were studied systematically in this work.. The identified broad, and strong excitation peak at 450 nm indicates that $Li_3Ba_2Gd_3(WO_4)_8$:Dy phosphors are suitable to be pumped by a blue laser diode (LD). Under excitation at 445 nm, the phosphor showed a stronger yellow emission peak at 575 nm which corresponds to the Dy^{3+}: $^4F_{9/2} \rightarrow {}^6H_{13/2}$ transition, fig.1(c).

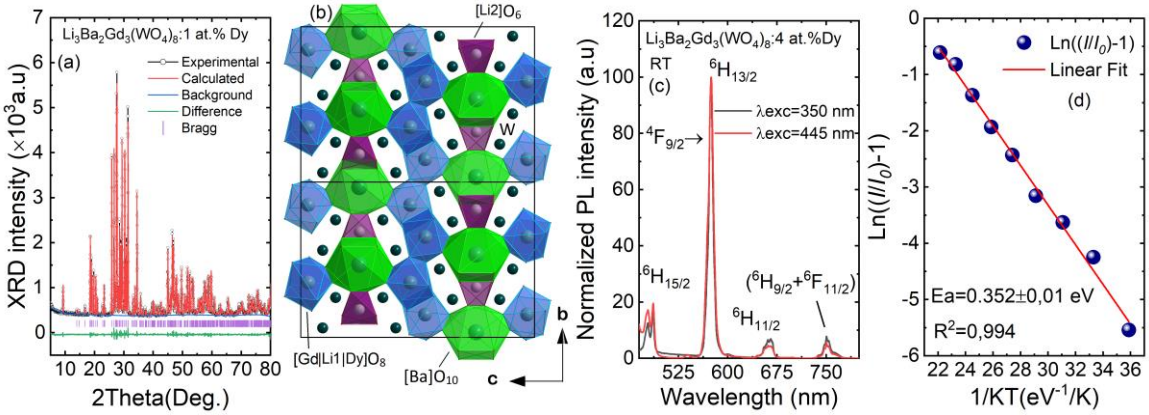

Fig. 1 (a) Rietveld refinement of $Li_3Ba_2Gd_3(WO_4)_8$: 1 at. % Dy; (b) crystal structure of $Li_3Ba_2Gd_3(WO_4)_8$: Dy along b-c crystallographic axis; (c) luminescence spectra of $Li_3Ba_2Gd_3(WO_4)_8$: 4at. % Dy under 350 and 450 nm excitations; (d) activation energy graph for thermal quenching of 4 at.% Dy^{3+} doped quaternary tungstate.

The activation energy of thermal suppression was calculated to be 0.352 ± 0.01 eV, fig.1(d). The measured absolute photoluminescence quantum yield was around 10.5%. The results presented in this work show that $Li_3Ba_2Gd_3(WO_4)_8$: Dy^{3+} phosphors with strong yellow emission can be promising candidates for white-light emitting LED (wLED) applications.

References:

[1] S. Slimi, P. Loiko, K. Bogdanov, A. Volokitina, R.M. Solé, M. Aguiló, F. Díaz, E. Ben Salem, X. Mateos, Structure and luminescent properties of Dy^{3+} activated $NaLa_9(SiO_4)_6O_2$ yellow-emitting phosphors for application in white LEDs, J. Alloys Compd. 896, 2022, 163109.

Optical thermometry properties of a novel quaternary tungstate $Li_3Ba_2Gd_3(WO_4)_8$: Ho, Tm

Abir Douzi[1, 2,*], Sami Slimi[1], Rosa Maria Solé[1], Magdalena Aguiló[1], Francesc Díaz[1], Ezzedine Ben Salem[2], and Xavier Mateos[1,#]

[1]*Universitat Rovira i Virgili (URV), Física i Cristal·lografia de Materials (FiCMA), Marcel·lí Domingo 1, E-43007 Tarragona, Spain.*

[2]*I.P.E.I. of Monastir, Unit of Materials and Organic Synthesis, University of Monastir 5019, UR17ES31, Tunisia.*

[*]*e-mail: abir.douzi1996@gmail.com,* [#]*Serra Húnter Fellow*

In luminescence thermometry, the temperature is determined from the changes in the fluorescence measurement. Indeed, there are several temperature-dependent parameters that can be taken into account, such as the fluorescence intensity ratio (FIR), changes in the emission peak and the fluorescence lifetime. In recent years, temperature detection using upconversion luminescence (UC) of trivalent lanthanide ions (Ln^{3+}), such as thulium ions (Tm^{3+}) and holmium ions (Ho^{3+}), has received much attention. This method is founded on the temperature dependence of the FIR of two thermally coupled energy levels, and thus it allows non-contact temperature sensing [1].

In this work, we succeeded in synthesizing new monoclinic microcrystals of quaternary tungstates $Li_3Ba_2Gd_3(WO_4)_8$: Ho^{3+}, Tm^{3+} using the modified sol-gel method of Pechini. The purity of obtained phase was confirmed by XRD, fig.1(a). The obtained microparticles show an irregular shape with a size of about 0.6 µm. The photoluminescence spectrum in the short-wavelength infrared (SWIR) region of the obtained microcrystals, excited at 808 nm, shows two main bands attributed to electronic transitions: $^3F_4 \rightarrow {}^3H_6$ (1774 nm, P1) of Tm^{3+} and $^5I_7 \rightarrow {}^5I_8$ (2037 nm, P2) of Ho^{3+}, fig.1(b).

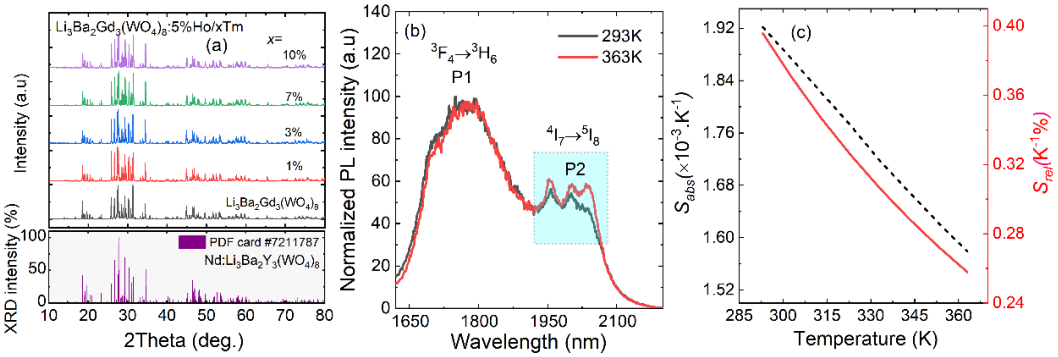

Fig. 1 (a) X-ray diffraction (XRD) patterns of $Li_3Ba_2Gd_3(WO_4)_8$:5 at.%Ho, x at.%Tm with different doping concentration of Tm^{3+} ions (1, 3, 7 and 10); (b) Emission spectra of $Li_3Ba_2Gd_3(WO_4)_8$: 5 at.%Ho, x at.%Tm under excitation at 808 nm at temperatures of 293 and 363 K; (c) Absolute (S_{abs}) and relative (S_{rel}) sensitivities as a function of temperature from 285 to 370 K for $Li_3Ba_2Gd_3(WO_4)_8$: 5 at.%Ho, 10 at.%Tm

The FIR P2/P1 increase with temperature due to thermally coupled levels. The relative S_{rel} and absolute S_{abs} sensitivities were evaluated, fig.(c). S_{rel} was at a maximum of 0.39 $\%.K^{-1}$ at Room temperature of 293K. The repeatability of the measurement was examined by the relative standard deviation and cycle test. The temperature resolution δT parameter is 2.27 at 298K and it's increased to 3.49K at 363K. All these results reveal the potential application of $Li_3Ba_2Gd_3(WO_4)_8$: Ho^{3+}, Tm^{3+} microparticles for optical thermometry.

References:

[1] X. Li, X. Wang, H. Zhong, L. Cheng, S. Xu, J. Sun, J. Zhang, X. Li, L. Tong, B. Chen, Effects of Er^{3+} concentration on down-/up-conversion luminescence and temperature sensing properties in $NaGdTiO_4$: Er^{3+}/Yb^{3+} phosphors, Ceram. Int. 42, 2016, 14710–14715.

Spectral Imaging of cultural assets using newly developed fluoride ultraviolet optics

Nobuhiko SARUKURA, [a,b] Keito SHINOHARA, [a] Toshihiko SHIMIZU, [a] Gyo MIYAHARA, [a] and Jose Eleazar R. BERSALES, [a]

[a] Osaka University [b] Tohoku University;
sarukura.nobuhiko.ile@osaka-u.ac.jp

Spectroscopic techniques are attracting attention as a non-destructive method of analyzing cultural assets. Here, we introduce a new approach to survey cultural assets using imaging spectroscopy. Our study is expected to bring a new perspective on the background of these cultural assets.

Optical and luminescence investigation of barium borate doped with Ce^{3+} under ultraviolet (UV) excitation for scintillating glasses

Benchaphorn Damdee,[a)] Masahiro Yamashita,[b)] Kohei Yamanoi,[b)] Keerati Kirdsiri,[a,c)] Keito Shinohara,[b)] Nobuhiko Sarukura,[b)] Anon Angnanon[c)], J. Kaewkhao[a,c)]

[a)]Physics program, Faculty of Science and Technology, Nakhon Pathom Rajabhat University, Nakhon Pathom, 73000, Thailand
[b)]Institute of Laser Engineering, Osaka University, 2-6 Yamadaoka, Suita, Osaka 565-0871, Japan; yamanoi.kohei.ile@osaka-u.ac.jp
[c)]Center of Excellence in Glass Technology and Materials Science (CEGM), Nakhon Pathom Rajabhat University, Nakhon Pathom, 73000, Thailand; jakrapong@webmail.npru.ac.th

Abstract. The melt quenching approach has been used to create Ce^{3+}-doped barium borate glasses with varying CeF_3 and B_2O_3 concentrations. The CeF_3-doped $10La_2O_3$-20BaO-(70-x) B_2O_3: $xCeF_3$ scintillating glasses are characterized by their physical, structural, optical, and luminescence characteristics, and the best CeF_3 concentration is determined to be 0.0-3.0 %mol. Systematically, the effect of CeF_3 on the performance of glass, including its density, absorption, and luminescence properties under ultraviolet (UV) excitation, was investigated. The findings indicated that an increase in CeF_3 concentrations led to an increase in the density of the glasses while simultaneously leading to a decrease in the molar volume. In the photoluminescence (PL) spectra, a broad emission band was seen to have a maximum peaking of about 385 nm. This band was ascribed to 5d-4f transitions of Ce^{3+} ions, and it was observed that these transitions occurred. The optimal doping concentration of CeF_3 contents is 0.5 mol%. The Ce_{LIII}-edge X-ray absorption near-edge structure analysis shows that the Ce^{3+} increases with increasing CeF_3 concentration, which indicates that the starting material.

Keyword: Borate glass, Ce^{3+}, Optical properties, Photoluminescence.

Terahertz time domain ellipsometry and its application in wide-bandgap semiconductors characterization

Makoto NAKAJIMA, [a] **Verdad C. AGULTO,** [a] **Zixi ZHAO,** [a] **Kosaku Kato,** [a] **Toshiyuki IWAMOTO** [a,b]

[a] *Institute of Laser Engineering, Osaka University* [b] *Nippo Precision Co., Ltd.; nakajima.makoto.ile@osaka-u.ac.jp*

Terahertz ellipsometry is an emerging characterization technique to study the dielectric and conductivity properties of various materials. The terahertz region refers to the frequency band between the millimeter and infrared waves of the electromagnetic spectrum, and in this region many low-energy excitations are present such as phonons, plasmons, magnon and rotational transitions [1-5]. The carrier dynamics that occur at terahertz frequencies also elucidate the optical properties of materials. Hence, terahertz investigations are employed in studying next-generation materials such as wide-bandgap semiconductors and other functional materials [1-3].

In terahertz ellipsometry the material properties are probed by irradiating polarized terahertz pulses and then measuring the change in the polarization state of the reflected waves. Figure 1a shows the schematic diagram of the Tera Evaluator terahertz time-domain ellipsometer (Nippo Precision Co., Ltd.) that is capable of highly precise measurements [1]. Figures 1b and 1c show the real and imaginary parts of the refractive index spectra of wide-bandgap GaN single crystals with different conductivities obtained by terahertz ellipsometry. From the refractive index, the free-carrier properties such as the carrier concentration and mobility are extracted by fitting to the Drude optical conductivity model. We demonstrate that terahertz ellipsometry is a practical tool for materials characterization owing to its non-contact and non-destructive approach. At the presentation, we will show the experimental results for GaN, β-Ga_2O_3, ZnO, and SiC.

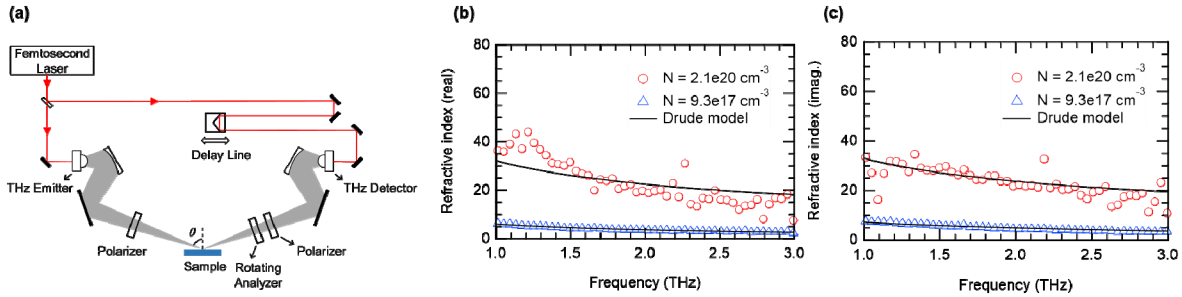

Figure 1. (a) Experimental setup and (b,c) real and imaginary parts of the refractive index spectra of GaN single crystals with different carrier concentrations *N*.

References:

[1] Agulto, V.C., Nakajima, M. et al., Terahertz time-domain ellipsometry with high precision for the evaluation of GaN crystals with carrier densities up to 10^{20} cm^{-3}. *Sci. Rep.,* 11, **2021**, 18129.

[2] Agulto, V.C., Nakajima, M. et al., Anisotropic complex refractive index of β-Ga_2O_3 bulk and epilayer evaluated by terahertz time-domain spectroscopy. *Appl. Phys. Lett.,* 118, **2021**, 042101.

[3] Iwamoto, T., Nakajima, M. et al., Characterization of electrical properties of β-Ga_2O_3 epilayer and bulk GaAs using terahertz time-domain ellipsometry. *Jpn. J. Appl. Phys.,* 62, **2023**, SF1011.

[4] Ota, M., Nakajima, M. et al., Ultrafast visualization of an electric field under the Lorentz transformation. *Nature Physics,* 18, **2022**, 1436-1440.

[5] Fitzky, G., Nakajima, M., et al., Ultrafast Control of Magnetic Anisotropy by Resonant Excitation of 4f Electrons and Phonons in $Sm_{0.7}Er_{0.3}FeO_3$. *Phys. Rev. Lett.*, 127, **2021**, 107401.

Rare earth-diamond hybrid structures for optical quantum technologies

I. G. Balasa[1], M.A. Arranz-Martinez[1], P. Perrin[1], M. Ngandeu Ngambou[2], D. Serrano[1], J. Achard[2], A. Tallaire[1], P. Goldner[1]

[1]Institut de Recherche de Chimie Paris, Chimie ParisTech, PSL University, CNRS, Paris, France
[2]LSPM, CNRS, Université Sorbonne Paris Nord, Villetaneuse, France,
ionut-gabriel.balasa@chimieparistech.psl.eu

The challenge of developing hybrid quantum materials aims to associate distinct optically active centers to achieve new functionalities while preserving the underlying properties of each component. In this work, we combine two optically active materials that have been broadly used for quantum applications and are compatible with scalable fabrication techniques: shallow NV^- color centers in diamond [1] and rare earth (RE) ions in thin films [2]. Here, we present a hybrid structure sketched in Fig. (b) that consists of an Er^{3+} doped Y_2O_3 thin film deposited by direct liquid injection chemical vapor deposition (CVD) on a diamond substrate in which shallow NV^- were implanted. We investigate the crystallinity of the thin film and the optical properties of the embedded Er^{3+} ions, and how the spin and optical properties of the NV^- are affected by the thin film. The photoluminescence spectrum of the $^4I_{13/2}$-$^4I_{15/2}$ Er^{3+} transition measured at 10 K is reported in Fig. (a) and confirms that Er is in the trivalent configuration in the cubic phase of Y_2O_3. The inset of Fig. (a) also presents the decays of the two Er occupational sites in Y_2O_3: C_2 and C_{3i}, measured at 10 K. The obtained decay times are 5.6 ± 0.1 ms and 13.5 ± 0.2 ms respectively and are comparable to bulk crystal references (8.5 ms and 14.6 ms [3]) thus proving that no major non-radiative or quenching effects arise in the nanostructured thin film. Optical and spin properties of the NV^- before and after the thin film deposition are reported in Fig. (c). The top of Fig. (c) presents a wide optically detected magnetic resonance (ODMR) spectrum where the 8 peaks correspond to the degeneracy lift due to 4 distinct projections of the applied magnetic field on the NV axis for two different spin projections (m_s=±1). The bottom part of Fig. (c) is a zoom into one of the spin transitions indicating a constant linewidth around 1.4 MHz, before or after deposition. The spin properties of the NV- at the diamond/film interface have thus not been altered. In conclusion, this is a first proof of the possibility of integrating the rare-earth ions with NV^- centers at the nanoscale level for developing hybrid solid state quantum systems.

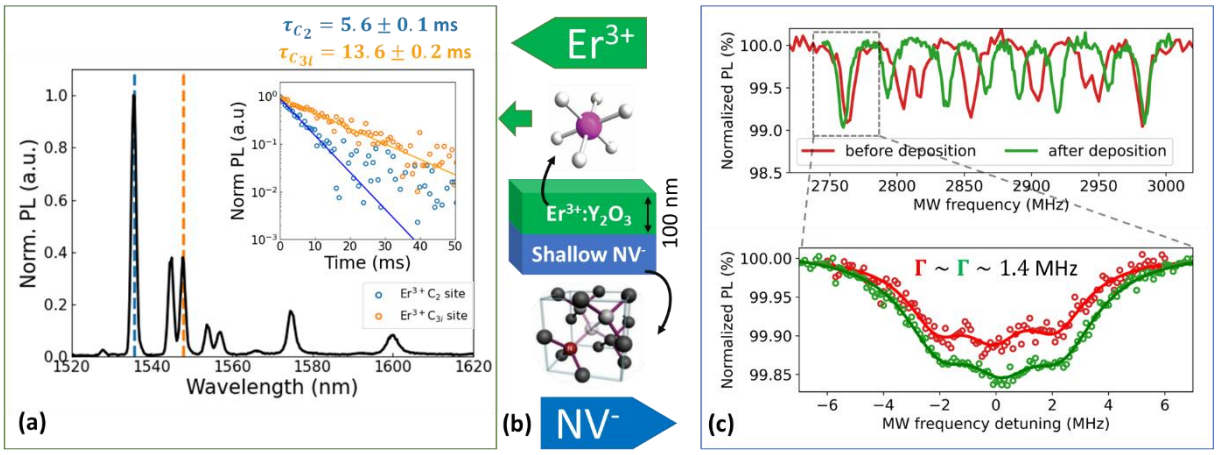

References:

[1] Nao Harada et al., Journal of Applied Physics, 2020, 128, 055304
[2] Midrel Wilfried Ngandeu Ngambou et al 2022 Mater. Quantum. Technol. 2 045001
[3] C. W. Thiel et al., Journal of Luminescence, 2011, 131, 353-361.

Acknowledgments: This project has received funding from the European Union's 2020- European Research Council (ERC) program under grant agreement ID: 101019234 and CNRS 80 Prime Mathyq project.

Inorganic nanoparticles based on rare earth elements for advanced applications

Agata SZCZESZAK,[a] Tomasz GRZYB, [a] Erika PORCEL,[b] Dominika PRZYBYLSKA, [a] Natalia JURGA, [a] Sylwia WASIELEWSKA,[a] Charles BOSSON[b]

[a] Adam Mickiewicz University, Faculty of Chemistry, Department of Rare Earths, Uniwersytetu Poznańskiego 8, 61-614, Poznań, Poland
[b] Universite Paris-Saclay A Institut des Sciences Moléculaires d'Orsay Biophysique et Biophotonique Bâtiment 520 91400 Orsay;

agata_is@amu.edu.pl

The exceptional luminescence properties and specific electronic structure make lanthanide ions (Ln^{3+}) excellent candidates for different applications, e.g., in radiotherapy as sensitizers. Sharp, intense, and well-defined emission bands related to the f-f transitions, the tunable color of the luminescence, and different excitation wavelengths enable the creation and produce materials that can prevent falsifying important documents or identify cancer cell bioimaging [1–3]. Inorganic matrices based on fluorides are ideal for lanthanide ions' doping due to their relatively low phonon energy, which enables them to avoid luminescence quenching. For this reason, nanomaterials based on fluorides doped with Yb^{3+}/Er^{3+}, Tm^{3+}, and Ho^{3+} were used to modify the Lyocell cellulose fibers and paper [4]. It resulted in a different luminescence color, including green, red, or blue emission activated by NIR and UV excitation. Furthermore, this type of modification enables to produce the luminescent markers for documents and goods protection against counterfeiting. Moreover, the core@shell type nanoparticles based on $NaYF_4$ fluoride matrix doped with suitable pairs of Ln^{3+} ions can show bright emission, around 800 nm, under 975 nm excitation, but also under 1532 nm. This type of luminescence highlights the unique and universal properties of Ln^{3+} for designing luminescent nanoparticles for various potential applications, such as confocal microscopy [2].

References:

[1] A. Szczeszak, M. Skwierczyńska, D. Przybylska, M. Runowski, E. Śmiechowicz, A. Erdman, O. Ivashchenko, T. Grzyb, P. Kulpiński, K. Olejnik, Mater. Des. 218 (2022) 110684.
[2] T. Grzyb, P. Kamiński, D. Przybylska, A. Tymiński, F. Sanz-Rodríguez, P. Haro Gonzalez, Nanoscale (2021).
[3] A. Szczeszak, M. Skwierczyńska, D. Przybylska, M. Runowski, E. Śmiechowicz, A. Erdman, O. Ivashchenko, T. Grzyb, S. Lis, P. Kulpiński, K. Olejnik, J. Mater. Chem. C 8 (2020) 11922–11928.
[4] T. Grzyb, D. Przybylska, A. Szczeszak, E. Śmiechowicz, P. Kulpiński, I.R. Martín, Carbohydr. Polym. 294 (2022) 119782.

Optical modulation and humidity sensing performance of Tb:Ce complex inhibited polymeric nanofibres

Pooja, Y. Dwivedi

Department of Physics, National Institute of Technology Kurukshetra, Haryana, 136119,India yashjidwivedi@nitkkr.ac.in

In the present work we carried out systematic study on optical alteration in Tb:Ce$(Sal)_3$Phen, Eu$(DBM)_3$Phen complexes inhibited in polyvinyl alcohol (PVA) polymeric nanofibres, while assembled in stacked formation. We report the feasibility of Tb:Ce$(Sal)_3$Phen and Eu$(DBM)_3$Phen complex dispersed electrospun nanofibres for humidity sensor. Structural, morphological and spectroscopic properties of the synthesized nanofibres were systematically compared using Fourier transform infrared spectroscopy, scanning electron microscopy and Photoluminescence analysis. Synthesized Tb:Ce$(Sal)_3$Phen and Eu$(DBM)_3$Phen complexes inhibited in nanofibres yields characteristic vivid green emission of Tb^{3+} and red emission from Eu^{3+} under UV excitations. The presence of Ce^{3+} ions alongwith the salicylate ligand and Tb^{3+} ion a help to expand the absorption range (290 nm-400 nm) subsequently the emission in blue and green regions. Our analysis revealed the linear enhancement of emission intensity with addition of Ce^{3+} ions. The stacking of different layers of complexes reveal the precise control over the color alteration simply by adding layers, without compromising emission intensity due to interaction between the active ions. Upon exposing the flexible Tb:Ce$(Sal)_3$Phen and Eu$(DBM)_3$Phen complexes dispersed nanofibres mat in different humidity environments, photoluminescence emission intensity shows a linear variation. The prepared nanofibres film shows a good reversibility, small hysteresis, cyclic stability and acceptable response and recovery times i.e. 35 and 45 seconds. The humidity sensing mechanism was proposed on the basis of infrared absorption analysis of dry and humid nanofibres. The detailed colour analysis and photophysics of the observed results will discuss in detail.

Growth, scintillation properties, pulse shape discrimination capability of (Ca,Sr)I_2:Eu scintillator

Masao Yoshino, [a)] **Takashi Iida,** [b)] **Kei Kamada,**[a,d)] **Ryuga Yajima,** [c)] **Takahiko Horiai,** [a)] **Kazuya Omuro,** [c)] **Rei Sasaki,** [c)] **Akira Yoshikawa** [a,c,d)]

[a)] NICHe Tohoku University [b)] Tsukuba University [c)] IMR Tohoku University
[d)] C&A Corporation; E-mail: yoshino.masao@tohoku.ac.jp

Inorganic scintillators are widely used in underground astroparticle physics experiments, such as dark matter searches and neutrino-less double beta decay. In the searches for neutrino-less double beta decay ($0\nu\beta\beta$), scintillators are required to have a high energy resolution in order to distinguish between the mono-energetic electron pairs produced by $0\nu\beta\beta$ and the continuous-energy electron pairs produced by $2\nu\beta\beta$. The main advantage of scintillators containing ^{48}Ca is that ^{48}Ca has the highest Q value (4.3 MeV) of the $0\nu\beta\beta$ candidate isotopes. Good particle identification performance of the scintillator is also very important to discriminate the electron pairs produced by $0\nu\beta\beta$ from the environmental background. We have successfully grown single crystal CaI_2 scintillators and have reported high light yield of 107,000 ph/MeV and excellent pulse shape discrimination (PSD) capability [1, 2]. However, CaI_2 is known to exhibit strong cleavage along the c-plane, which has made it difficult to enlarge the size of the crystal and caused the degradation of energy resolution. In this study, undoped / Eu-doped (Ca,Sr)I_2 with Sr substitution at the Ca site of CaI_2 was grown and evaluated with the aim of reducing the cleavage feature of CaI_2.

Crystal growth was performed using vertical Bridgman-Stockbarger method in quartz ampoules (inner diameter: 6 and 8 mm). Some of the results obtained in this study are shown in Figure 1. The Sr substitution shifted the powder X-ray diffraction (XRD) peaks of the CaI_2 pahse to the low-angle side. Scintillation light yield remained above 95,000 ph/MeV even with 20% Sr substitution. PSD performance will also be reported in this presentation.

References:

[1] T. Iida, K. Kamada, M. Yoshino, K.J. Kim, K. Ichimura, A. Yoshikawa, High-light-yield calcium iodide (CaI_2) scintillator for astroparticle physics, NIM-A. 958 (2020) 162629.

[2] M. Yoshino, et al., Comparative pulse shape discrimination study for Ca(Br, $I)_2$ scintillators using machine learning and conventional methods, NIM-A. 1045 (2023) 167626.

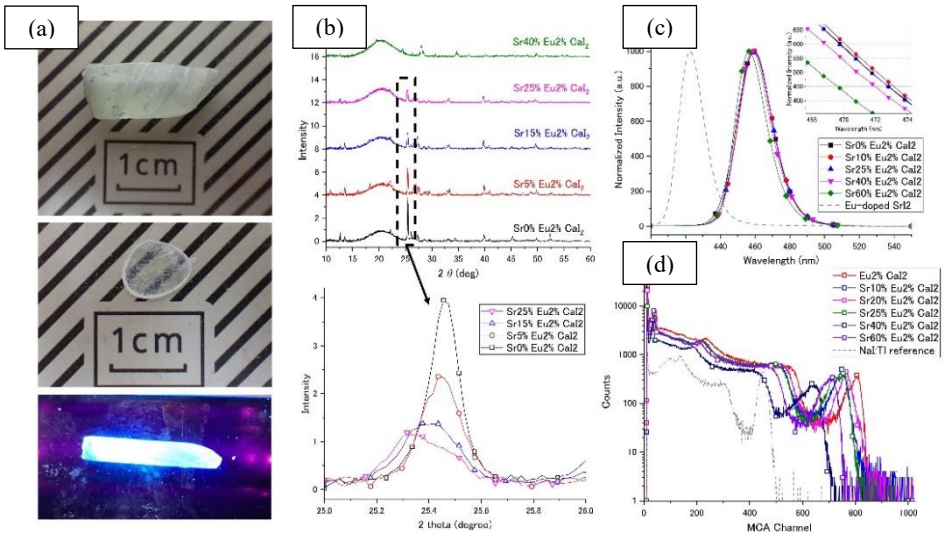

Fig.1 (a) Photographs, (b) powder XRD results, (c) X-ray radioluminescence, and pulse height spectra of ^{137}Cs for the grown (Ca,Sr)I_2:Eu single crystals

Optical and Scintillation Properties of Pr^{3+}-Doped $(La, Y)_2Si_2O_7$ Single Crystals

Yuka ABE, [a, b] Takahiko HORIAI, [b, c] Jan PEJCHAL, [d] Martin NIKL, [d] Yuui YOKOTA, [b, c] Masao YOSHINO, [b, c] Rikito MURAKAMI, [b] Takashi HANADA, [b] Akihiro YAMAJI, [b, c] Hiroki SATO, [b, c] Yuji OHASHI, [b, c] Shunsuke KUROSAWA, [b, c] Kei KAMADA, [b, c] Akira YOSHIKAWA, [b, c]

[a] Graduate School of Engineering, Tohoku University, [b] Institute for Materials Research, Tohoku University, [c] New Industry Creation Hatchery Center, Tohoku University, [d] Institute of Physics of the Czech Academy of Sciences
yuka.abe.p5@dc.tohoku.ac.jp

1. Introduction Pr^{3+}-doped materials are promising candidates for scintillator applications because of their fast $5d_1$-4f emission in wide bandgap host materials with medium- or high-crystal field strength. As for the study of Pr^{3+}-doped scintillators, single crystal growth and optical characterization of scintillators with garnet-structure, e.g. $Y_3Al_5O_{12}$ and $Lu_3Al_5O_{12}$, and pyrochlore-structure, e.g. $Lu_2Si_2O_7$, have been performed [1-3]. These studies have shown that Pr^{3+} $5d_1$-4f emission has faster decay time compared to Ce^{3+} $5d_1$-4f emission, which would be suitable for applications requiring high timing resolution, for example time-of-flight positron emission tomography (TOF-PET). In this study, we focused on Pr^{3+}-doped $(La,Y)_2Si_2O_7$ to develop novel Pr^{3+}-doped scintillators, and carried out single crystal growth and characterization.

2. Materials and Methods The crystal growth was performed using micro-pulling-down (μ-PD) method [4]. As starting materials, we used Y_2O_3, La_2O_3, Pr_2O_3 and SiO_2 powders with a purity of more than 99.99%. The crystal structure of the grown crystals was estimated by the powder X-ray diffraction analysis. In addition, the photoluminescence (PL) excitation and emission spectra and scintillation properties such as the light outputs and decay times were evaluated.

3. Results The crystals grown by μ-PD method are illustrated in Figure 1. We were succeeded in growing transparent $(Pr_x La_{0.600} Y_{0.400-x})_2Si_2O_7$ (x = 0.001-0.020) crystals. After cutting and mirror polishing to 1 mm thickness, the PL excitation and emission spectra were measured. From the PL emission spectra, the typical broad emission due to the Pr^{3+} $5d_1$-4f transitions was observed in the wavelength range of 250-340 nm (Figure 2). These emission peaks were identified as $5d_1$-$^3H_4$, -$^3H_5$, -$^3H_6$, -$^3F_{3,4}$ transitions, respectively, from the short wavelength side. Details of the optical and scintillation properties of Pr^{3+}-doped $(La,Y)_2Si_2O_7$ crystals will be presented.

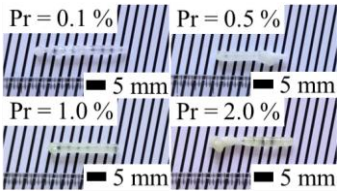

Fig. 1 Photograph of the grown Pr:$(La, Y)_2Si_2O_7$ crystals.

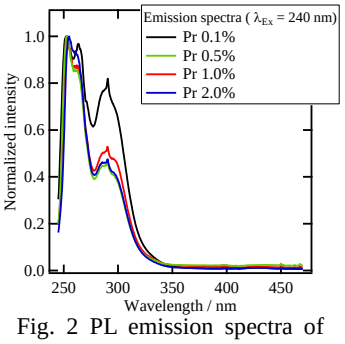

Fig. 2 PL emission spectra of Pr: $(La, Y)_2Si_2O_7$.

References:

[1] Pejchal, J.; Yoshikawa, A. et al., Pr^{3+}-doped complex oxide single crystal scintillators. J. Phys. D, 42., **2009**, 055117.
[2] Ogino, H.; Yoshikawa, A. et al., Scintillation characteristics of Pr-doped $Lu_3Al_5O_{12}$ single crystals. J. Cryst. Growth, 292., **2006**, 239-242.
[3] Nikl, M. et al., Luminescence and scintillation kinetics of the Pr^{3+} doped $Lu_2Si_2O_7$ single crystal. *Chem. Phys. Lett.*, 493, **2010**, 72-75.
[4] Yoshikawa, A. et al., Challenge and study for developing of novel single crystalline optical materials using micro-pulling-down method. Opt. Mater., 30, **2007**, 6-10.

Crystal Growth and Optical Properties of Ce-doped $(Gd, Y, Tb)_3Ga_3Al_2O_{12}$ Scintillators for X-ray Imaging

Kazuya OMURO[a), b)], Masao YOSHINO[b), c)], Kei KAMADA[b), c), d)], Kyoung Jin KIM[b)], Takahiko HORIAI[b), c)], Rikito MURAKAMI[b)], Akihiro YAMAJI[b), c)], Takashi HANADA[b)], Yuui YOKOTA[b)], Shunsuke KUROSAWA[b), c), e)], Yuji OHASHI[b), c)], Hiroki SATO[b), c)], Akira YOSHIKAWA[b), c), d)]

[a)] Tohoku University, Graduate School of Engineering, Japan,
[b)] Institute for Materials Research, Tohoku University, Japan,
[c)] New Industry Creation Hatchery Center, Tohoku University, Japan,
[d)] C&A Corporation, Japan,
[e)] Institute of Laser Engineering, Osaka University, Japan,
kazuya.omuro.r5@dc.tohoku.ac.jp

Introduction Scintillators are widely used in X-ray imaging, which are applied for medical diagnostics and airport security controls. To obtain images with excellent contrast in short exposure times, scintillators are required to have high density and light yield. Recently, it has reported that substituting ternary by quaternary garnet in the matrix material dramatically improves the light yield of Ce- and Tb-doped scintillators. Korzhik et al. estimated a very high light yield of 200,000 ph/MeV for Tb-doped (Gd, Y)$_3$Ga$_3$Al$_2$O$_{12}$ (GYAGG:Tb) ceramics [1]. However, single crystals of GYAGG:Tb has not been reported. In this study, we report on the growth of GYAGG:Ce, Tb single crystals using the micro-pulling-down method and the evaluation of their scintillation properties and imaging performances.

Materials and Methods As starting materials, CeO_2, Tb_4O_7, Gd_2O_3, Y_2O_3, Ga_2O_3 and Al_2O_3 powders with a purity of 99.99% were used and weighed in stoichiometric composition. Ce 0.5% doped GYAGG:Tb crystals were grown by the micro-pulling-down (μ-PD) method [2]. The Tb concentrations were varied at 0.5, 5.0, 10.0, and 15.0 mol%.

Results The crystals grown by μ-PD method are shown in Fig. 1. We were succeeded in growing transparent GYAGG:Ce, Tb crystals. In the photoluminescence (PL) emission spectra (Fig. 2), the typical emission spectra associated with the Ce^{3+} $5d_1$-4f transition and Tb^{3+} 4f-4f transition were simultaneously observed in GYAGG:Ce, Tb crystals. The results of scintillation properties and X-ray imaging tests will be presented.

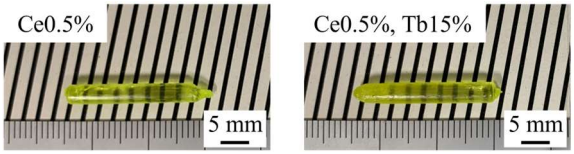

Fig. 1 Photograph of the grown GYAGG:Ce, Tb crystals

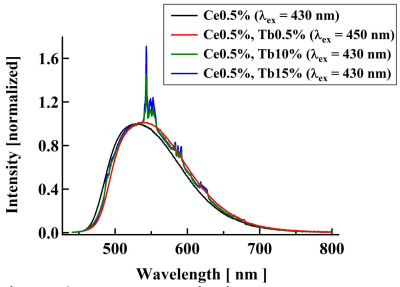

Fig. 2 PL Emission spectra of GYAGG:Ce, Tb crystals

References:

[1] Korzhik, M. et al., J. Lumin., Vol. 234, **2021,** 117933.
[2] Yoshikawa, A. et al., Opt. Mater., Vol. 30, **2007**, 6-10.

Er^{3+}-doped CaF_2 nanocubes: Synthesis and optical characterization

Eugenio CANTELAR, Ginés LIFANTE-PEDROLA, Marta QUINTANILLA, Juan Antonio SANZ-GARCÍA, Fernando CUSSÓ

Departamento de Física de Materiales, C-04, Facultad de Ciencias, Universidad Autónoma de Madrid, 28049, Madrid, Spain; *eugenio.cantelar@uam.es*

Fluoride nanoparticles activated with trivalent lanthanide ions (Ln^{3+}) are arousing great interest in applications that demand efficient luminescent transitions and, therefore, high quantum efficiency values. Additionally, it is also common that the application needs of high emission intensities, only achievable if a large number of optical centers is available [1]. However, it is not easy to simultaneously satisfy both requirements and, in general, a compromise between quantum efficiency and high values of active ion densities must be sought.

The population dynamics in Ln^{3+}-doped nanoparticles (NPs) is in general complex, being strongly dependent on the active ion concentration. In diluted NPs the population dynamics is governed by radiative and non-radiative transitions, while in high concentrated NPs the situation is clearly different: As the active ion concentration increases, the spontaneous transitions start to compete with ion-ion interactions (energy migration and cross relaxation processes). These loss mechanisms, usually known as concentration quenching processes, are usually appreciable under CW and pulsed excitation conditions. Additionally, when lifetime measurements are performed, there is another important aspect that should be under consideration: the possibility of radiation trapping; that is, the reabsorption of the emitted radiation.

In this work, CaF_2:Er^{3+} NPs with variable dopant concentration were synthesized by a direct precipitation method [2]. X-Ray Powder Diffraction, SEM and TEM have been used to analyze the particle crystalline structure and morphology. The basic spectroscopy of Er^{3+} ions has been studied under CW and pulsed excitation as function of the dopant level. The dependence of the emission intensity of the main emission bands reveals the presence of luminescence quenching processes. The dynamics of the emitting manifolds, recorded under pulsed excitation, has confirmed the presence of these processes together with the existence of radiation trapping. A treatment, commonly used in bulk doped materials, has been applied to determine the intrinsic total transition probabilities of the main erbium emitting levels in absence of quenching and radiation trapping. The intrinsic total transition probability of $^4I_{13/2}$ level has been used to perform a modified Judd-Ofelt analysis. Finally, the non-radiative transition probabilities of $^4I_{11/2}$, $^4F_{9/2}$ and $^2H_{11/2}$:$^4S_{3/2}$ levels, calculated from the intrinsic transition probabilities and the radiative ones, has allowed to determine the gap law in the CaF_2:Er^{3+} NPs.

References:

[1] Nsubuga A., Sgarzi M., Zarschler K., Kubeil M., Hübner R., Steudtner R., Graham B., Joshi T., Stephan H., Facile preparation of multifunctionalisable 'stealth' upconverting nanoparticles for biomedical applications, *Dalton Trans.,* 47, **2018**, 8595.

[2] Cantelar E., Sanz-García J.A., Sanz-Martín A., Muñoz Santiuste J.E., Cussó F., Structural, photoluminescent properties and Judd-Ofelt analysis of Eu^{3+}-activated CaF_2 nanocubes, *J. Alloys. Comp., 813, **2020**, 152194.*

Tracer-based sorting with lanthanide-activated phosphors for plastics recycling

Andrey TURSHATOV[a)], Ian A. HOWARD[a,b)], Bryce S. RICHARDS[a,b)]

[a)]Institute of Microstructure Technology, Karlsruhe Institute of Technology, Hermann-von Helmholtz-Platz 1, 76344, Eggenstein-Leopoldshafen, Germany
[b)]Light Technology Institute, Karlsruhe Institute of Technology, Engesserstrasse 13, 76131 Karlsruhe, Germany
andrey.turshatov@kit.edu

In 2018, the EU agreed on ambitious targets: to increase the reuse and recycling of plastic waste to 50% by 2025 and 55% by 2030, compared to 35% in 2020. A new tracer-based sorting (TBS) of plastics is complementary to existing near-infrared sorting and can significantly improve the sorting of bulk end-of-life plastics from industrial and municipal waste. A key element of the TBS technology is different sorting codes based on luminescent tracers with specific excitation/emission spectral lines and high photoluminescence quantum yield. Unique properties of lanthanide (Ln^{3+}) luminescence, such as large Stokes and anti-Stokes shifts, high signal-to-noise ratio, high resistance to photo- and photochemical degradation, availability of cheap NIR laser diodes for excitation, sharp emission lines make them promising as photonic tracers for plastics recycling [1,2].

In our work, we present examples of the Ln^{3+} luminescent tracers used in the TBS process and explain a new way to distinguish between different types of packaging materials (e.g., food grade and non-food grade polyolefin packaging).

References:

[1] Gao G., Turshatov A., Howard IA, Busko D, Joseph R, Hudry D, Richards BS, *Advanced Sustainable Systems*, 1, **2017**, 1600033.

[2] Woidasky J, Sander I, Schau A, Moesslein J, Wendler P, Wacker D, Gao G, Kirchenbauer D, Kumar V, Busko D, Howard IA, Richards BS, Turshatov A, Wiethoff S, Lang-Koetz C, *Resources, Conservation and Recycling*, 161, **2020**, 104976.

Growth and scintillation properties of $LaCl_3$/^{6}LiCl /$SrCl_2$ ternary eutectic for thermal neutron detection

Rei SASAKI,[a),b)] Kei KAMADA,[b),c),d)] Ryuga YAJIMA,[a),b)] Kyoung Jin KIM,[b),c)] Naoko KUTSUZAWA,[d)] Masao YOSHINO,[c),d)] Rikito MURAKAMI,[b),d)] Takahiko HORIAI,[c),d)] Akihiro YAMAJI,[b),c)] Shunsuke KUROSAWA,[b),c)] Yuui YOKOTA,[b),c)] Hiroki SATO,[b),c)] Takashi HANADA,[b)] Vladimir. V. KOCHURIKHIN,[d)] and Akira YOSHIKAWA,[b),c),d)]

[a)] Department of Materials Science, Graduate School of Engineering, Tohoku University,Japan.; rei.sasaki.s8@dc.tohoku.ac.jp[b)] Institute for Materials Research, Tohoku University, Japan[c)] New Industry Creation Hatchery Center, Tohoku University, Japan.
[d)] C&A corporation, Japan.

[Background] Thermal neutron detectors are widely used in a variety of fields, including homeland security, boron neutron capture therapy, and astrophysics. The basic principle of thermal neutron detection is to convert thermal neutrons to low-energy radiation using ^{3}He, ^{6}Li, ^{10}B, and ^{113}Cd [1]. Recently, increasing demand and supply disruptions have limited the use of ^{3}He gas, pointing to the need for the development of inorganic solid scintillators for thermal neutron detection. Indeed, several new single-crystal scintillators for neutron detection have been reported in the past decade. Among them, $LiCaAlF_6$ (LiCAF) is the most promising candidate for $LiCaAlF_6$-based single-crystal scintillators because it contains ^{6}Li in its host lattice and has the ability to discriminate between neutron and gamma-ray pulse shapes [2]. However, being chemical compound, the ^{6}Li content is limited by the chemical formula and cannot be increased. Therefore, ^{6}Li-containing eutectic materials such as LiF/CaF_2, LiF/LaF_3, $LiCl/CeCl_3$, $LiCl/Li_2SrCl_4$, $LiCl/BaCl_2$, $LiBr/CeBr_3$, $LiBr/LaBr_3$, $CeCl_3/LiCl/CaCl_2$[3] etc. have been investigated to achieve higher neutron capture cross sections. In this study, $LaCl_3$/^{6}LiCl /$SrCl_2$ ternary eutectic was investigated as a novel thermal neutron scintillator.

[Results] Ce and Eu doped $LaCl_3$/^{6}LiCl /$SrCl_2$ ternary eutectic were grown by the VB method in a quartz ampoule with 4 mm inner diameter. Figure 1 shows a example photograph of the prepared Ce:$LaCl_3$/^{6}LiCl /$SrCl_2$ ternary eutectic plate cut from the grown eutectic rod. The eutectic plate showed slight transparency. Expected $LaCl_3$, ^{6}LiCl and $SrCl_2$ phases were observed by powder XRD and BEI analysis. The Ce doped eutectic showed 360 nm emission ascribed to Ce^{3+} 4f5d transition. Figure 2 shows the scintillation decay curve of the Ce:$LaCl_3$/^{6}LiCl/$SrCl_2$ ternary eutectic under ^{252}Cf thermal neutron excitation. The decay time was 16.0 ns (87.3%) ,162.7 ns (12.7%). The light yield was 32,000 photons / neutron. The detailed growth method, eutectic structure, scintillator properties and pulse shape discrimination capability will be reported on the presentation.

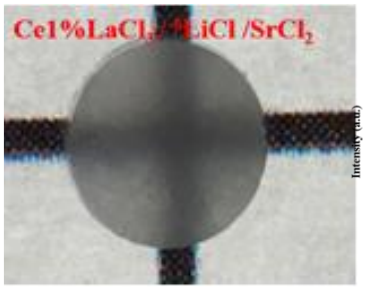

Fig. 1 A photograph of the eutectic plate.

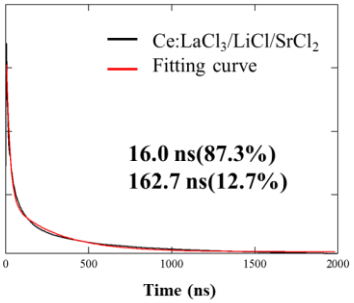

Fig. 2 Scintillation decay curve of the Ce doped eutectic.

References:

[1] C. W. E. Van Eijk, et al., Nucl. Instrum. Methods Phys. Res. A 529 (2004) 260.
[2] A. Yoshikawa, et al., IEEE Trans.Nucl. Sci. 56 (2009) 3796- 3799.
[3] R.Sasaki, et al., Crystals. 12 (2022) 1760.

A novel $CeCl_3$/NaCl/$SrCl_2$ ternary eutectic scintillator for fast and high resolution radiation imaging applications

Kei Kamada,[a,b,c] Rei Sasaki,[b),d)] Kyoung Jin Kim,[a),c)] Naoko Kutsuzawa,[c)] Masao Yoshino,[a),c)] Rikito Murakami,[b),c)] Takahiko Horiai,[a),c)] and Akira Yoshikawa[a),b),c)]

[a)] New Industry Creation Hatchery Center, Tohoku University, Japan; kei.kamada.c6@tohoku.ac.jp [b)] Institute for Materials Research, Tohoku University, Japan.[c)] C&A corporation, Japan. [d)] Department of Materials Science, Graduate School of Engineering, Tohoku University,Japan

[Introduction] Scintillators are used in a wide range of fields such as medicine as medical equipment including X-ray computed tomography and non-destructive testing. In these applications, sintered Tb:Gd_2O_2S powder and Tl:CsI whisker fabricated by vapor deposition are the most common scintillators, and the fineness of the arraigned structure determines the position resolution. To realize high-resolution imaging, we have focused on phase-separated scintillator fibers (PSSFs), such as GAP/α-Al_2O_3 [1] and $BaCl_2$/NaCl/KCl, CsI/CsCl/NaCl [2], have been proposed as new scintillator materials. Such scintillators can be obtained through the unidirectional solidification of the eutectic composition. For PSSFs, the scintillator phase with a high refractive index can be grown as a fiber-like structure in the growth direction. Higher sensitivity can be achieved with PSSFs compared to powdered or needle scintillators by increasing the thickness of the PSSFs. In this research, a novel ternary eutectic scintillator of $CeCl_3$/NaCl/$SrCl_2$ was investigated.

[Results] In the $CeCl_3$/NaCl/$SrCl_2$ eutectic, $CeCl_3$ with the highest refractive index was selected as the scintillator phase ($CeCl_3$:2.2@380nm, NaCl:1.54@nD and $SrCl_2$:1.65@nD). CeCl3 was reported with its excellent scintillation such as high light yield (30,000 photons/MeV); and fast decay time with four components of 4.4 ns (6.6%), 23.2 ns (69.6%), 70 ns (7.5%) and >10 μs (16.3%). The volume ratio of $CeCl_3$: NaCl : $SrCl_2$ is 34.3 : 22.0 : 43.7 and calculated density of the eutectic is 3.17 g/cm^3. Crystal growth was performed by the vertical Bridgman–Stockbarger method in a quartz ampoule with an inner diameter of 4 mm. Expected $CeCl_3$, NaCl and $SrCl_2$ phases were observed by powder XRD analysis. The ample was pulled down at a rate of 0.2 mm/min. The grown eutectic was cut and polished to give optically transparent 1 mm thick samples (Fig. 1). The BEI image of the growth direction is shown in Fig. 2. Each phase appears to be uniformly dispersed and align along the growth direction. 360 nm emission was observed under X-ray irradiation and was ascribed as Ce^{3+} 4f5d emission of $CeCl_3$. Scintillation decay time was as fast as 6 ns (17.5%), 12 ns (29%) and 28ns (53.5%). Eutectic structure, luminescence properties and imaging test results will be shown in my presentation.

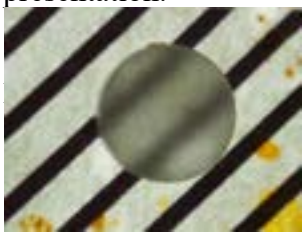

Fig. 1 A photograph of the eutectic plate.

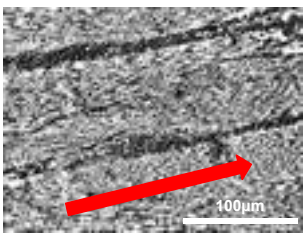

Fig. 2 BEI of the growth direction. (Red arrow indicate growth direction)

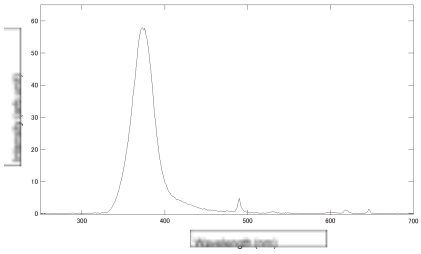

Fig. 3 Radioluminescence spectra of the eutectic under X-ray excitation

References [1] K. Kamada, et al. *Ieee Trans. Nucl. Sci.*, vol. 65, no. 8, pp. 2036–2040, 2018. [2] Y. Takizawa, K. Kamada, et al. *J. Cryst. Growth*, p. 126266, 2021,

Structural and spectroscopic properties studies of perovskite-type cubic Nd^{3+}-doped $M_3Y(PO_4)_3$ (M = Sr^{2+} or Ba^{2+}) solid-solution

Kacper Albin PROKOP,[a),b)] Miłosz SICZEK,[a)] Elżbieta TOMASZEWICZ,[c)] Krzysztof ROLA,[b)] Yannick GUYOT,[d)] Georges BOULON,[d)] Małgorzata GUZIK, [a),b)]

[a)] University of Wrocław, Faculty of Chemistry, Poland [b)] Łukasiewicz Research Network - PORT Polish Center for Technology Development, Poland [c)] West Pomeranian University of Technology in Szczecin, Poland [d)], Institute Light Matter (iLM), University Claude Bernard/Lyon1, e-mail: kacper.prokop@uwr.edu.pl

Considering perovskite-type cubic phosphates of chemical formula $M_3Y(PO_4)_3$ (M = Sr^{2+} or Ba^{2+}) as potential candidates to obtain new optical polycrystalline ceramics with high transparency, two series of eulytite-type Nd^{3+}-doped $Ba_3Y(PO_4)_3$ and $Sr_3Y(PO_4)_3$ solid-solution were obtained. First, the relationship between their structure and spectroscopic properties as well as the effect of the size of divalent Sr^{2+}/Ba^{2+} cation creating a network was investigated in detail. The samples were synthesized *via* the conventional high-temperature solid-state reaction method. All the obtained materials are mono-phase and crystallize in the cubic system (s.g. $I\bar{4}3d$, No. 220). Furthermore, the crystal structure of $Ba_3Y(PO_4)_3$ and $Sr_3Y(PO_4)_3$ was solved based on the small single crystals selected from micro-crystalline powders. In such a cubic structure, the M^{2+}/Y^{3+} cations are randomly disordered on a single crystallographic site with C_3 point symmetry. The Nd^{3+} ions reside at the Y^{3+} symmetry site but partial substitution of Ba^{2+} or Sr^{2+} sites cannot be excluded. Studied phosphates show not only cation disorder but also disorder in the oxygen sublattice, which is reflected in their spectroscopic properties. The multisite character and the inhomogeneous distribution of Nd^{3+} in both types of materials, determined using absorption at 4.2K and laser-excited site-selective spectroscopy at 77K, are also clearly seen in the excited state dynamics of $^4F_{3/2}$ doublet analysis. The samples activated up to 20 mol% demonstrated a weak concentration quenching process and a greater order for the barium host lattice.

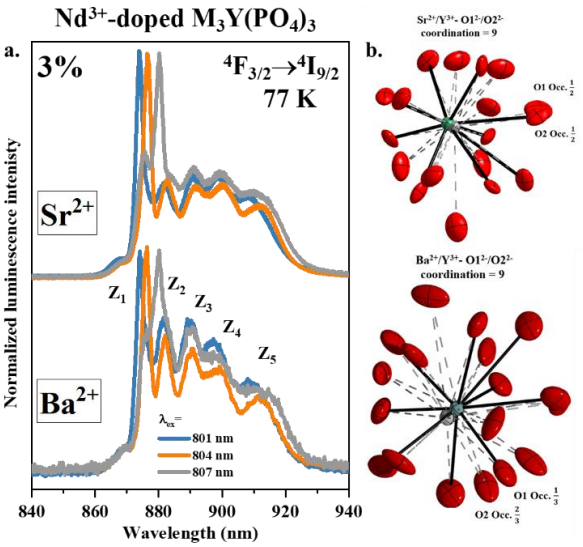

Site selective luminescence specta of 3% Nd^{3+}-doped $M_3Y(PO_4)_3$ (M=Sr^{2+}, Ba^{2+}) at 77 K (a) and coordination of Y^{3+}/Ba^{2+} and Y^{3+}/Sr^{2+} cations by possible O^{2-} anions (b).

Acknowledgments:
The research was financed by ARQUS (European University Alliance) support from UCBLyon1. K.A.P. would like to thank the Ministry of Science and Higher Education in Poland for Grant No. DWD/5/0361/2021 in the framework of the Implementation Doctorate Program.

Fabrication of Mach-Zehnder interferometer structures based on low-cost SiO_2:TiO_2 optical platform for integrated photonics applications

Kacper Albin PROKOP,[a), b)] Łukasz DUDA,[a), b)] Jakub PAWŁÓW, [a), b)] Maria ZDOŃCZYK, [a), b)] Krzysztof ROLA,[b)] Muhammad A. BUTT, [c)] Magdalena ZIĘBA,[d)] Paweł KARASIŃSKI,[d)] Joanna CYBIŃSKA,[a),b)] Małgorzata GUZIK,[a),b)]

[a)]Łukasiewicz Research Network – PORT Polish Center for Technology Development, Poland
[b)]University of Wrocław, Faculty of Chemistry, Poland
[c)]Warsaw University of Technology, Institute of Microelectronics and Optoelectronics, Poland
[d)]Department of Optoelectronics, Silesian University of Technology, Poland
kacper.prokop@uwr.edu.pl

A new construction of Mach-Zehnder interferometer based on a sol-gel SiO_2-TiO_2 (silica-titania) material platform is proposed. According to the current experience on this topic [1,2], the silica-titania waveguide platform proves its advantage due to low cost, low loss, and easy-to-develop integrated optics systems. The integrated photonic circuits studied here were obtained for very attractive optical platforms: Si/SiO_2 and Si/SiO_2/SiO_2:TiO_2. The SiO_2:TiO_2 thin films were deposited *via* a sol-gel dip-coating method. Such systems, modelled in detail are capable of operating from visible to near-IR wavelength ranges. The Mach-Zehnder configurations investigated in this work are attractive for on-chip sensing devices. Fabricating highly effective and economical photonic devices of such is the final purpose of discussed research.

The study is organized into two parts. In the first part, a detailed investigation of photolithography parameters' is presented. The determination of best factors such as UV exposure dose, development time or hard-baking temperature was very important. The search for the best parameters was aimed at obtaining continuous, defect-free, well-separated waveguides (WG) of Mach-Zehnder structures with specific separation between WGs. In the second part, the results of etching silica-titania waveguiding structures, based on optimized lithographic patterns, are presented. The fabrication of Mach-Zehnder WG structures on SiO_2-TiO_2 films was well-controlled by etch rate of the samples by utilizing dry etching technique - inductively coupled plasma reactive-ion etching (ICP-RIE). The first results showed faster and more efficient etching for silica-titania films supported on Si/SiO_2 substrates in comparison to already studied glass substrates.

References:

[1] M. A. Butt, *et al*., Development of a low-cost silica-titania optical platform for integrated photonics applications. Opt. Express, Vol. 30., **2022,** 23678-23694.
[2] M. A. Butt, *et al*., HYPHa project: a low-cost alternative for integrated photonics. Phot. Lett. Pol., Vol. 14., **2022,** 25-27.

Acknowledgments
The research was co-financed by the Foundation for Polish Science from the European Regional Development Fund within the project POIR.04.04.00-00-14D6/18 "Hybrid sensor platforms for integrated photonic systems based on ceramic and polymer materials (HYPHa)" (TEAM-NET program).

Application of hard metal (Al, Cu, Cr) masks for dry etching of sol-gel-derived silica-titania photonic structures

Łukasz DUDA, [a, b] Krzysztof ROLA, [a] Krzysztof CZYŻ, [a] Jakub PAWŁÓW, [a, b] Kacper PROKOP, [a, b] Maria ZDOŃCZYK, [a, b] Muhammad A. BUTT, [c] Magdalena ZIĘBA, [d] Paweł KARASIŃSKI, [d] Małgorzata GUZIK, [a, b] Joanna CYBIŃSKA, [a, b] Alicja BACHMATIUK, [a]

[a] *Łukasiewicz Research Network – PORT Polish Center for Technology Development, Poland*
[b] *University of Wrocław, Faculty of Chemistry, Poland*
[c] *Warsaw University of Technology, Institute of Microelectronics and Optoelectronics, Poland*
[d] *Department of Optoelectronics, Silesian University of Technology, Poland*
lukasz.duda@port.lukasiewicz.gov.pl

Inductively coupled plasma reactive ion etching (ICP-RIE), despite being known for a long time, is still used for etching a variety of different materials to obtain photonic devices. Films based on silica-titania, fabricated using both sol-gel and dip-coating methods are promising materials for this application due to their relatively low optical losses, stability over time and low fabrication costs [1]. However, the main challenge in this field is obtaining high dimensional control and high overall quality (*e.g.* roughness of waveguides' sidewalls) of photonic structures in nanoscale.

In this work we present utilization of ICP-RIE method for fabrication of the optical waveguide structures in the SiO_2-TiO_2 films formed using sol-gel synthesis and dip-coating method on soda-lime glass substrates. Instead of implementation of an organic photoresist mask for ICP-RIE, three different types of metal mask – aluminium (Al), copper (Cu) and chromium (Cr) were used. The technological process is schematically presented in the Figure 1. Quality of the obtained waveguides was compared to structures obtained in similar process but with the photoresist masking layer instead of metal. It was found that application of the hard metal mask could improve the quality of the etching, especially the roughness of waveguides' sidewalls.

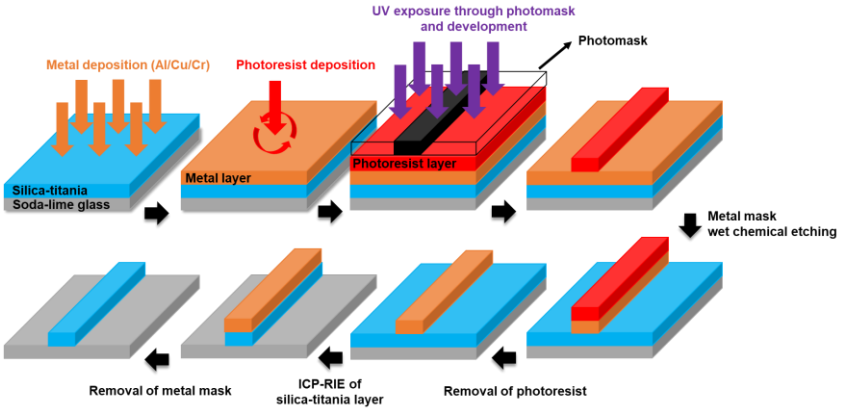

Fig. 1 Process of ICP-RIE etching of silica-titania film using hard metal mask.

References:

[1] Karasiński, P.; Tyszkiewicz, C.; Domanowska, A.; Michalewicz, A.; Mazur, J.; Low loss, long stable sol-gel derived silica-titania waveguide films, *Materials Letters,* 143, **2015**, 5-7.

The research was co-financed by the Foundation for Polish Science from the European Regional Development Fund within the project POIR.04.0400-00-14D6/18 "Hybrid sensor platforms for integrated photonic systems based on ceramic and polymer materials (HYPHa)" (TEAM-NET program).

Fabrication of surface relief gratings (SRGs) in hydrogen bonded polymer-dye complexes and their replication for security features

Łukasz DUDA, [a, b], Krzysztof CZYŻ, [a], Weronika ZAJĄC [a, b], Maciej CZAJKOWSKI, [a] Małgorzata GUZIK, [a, b], Joanna CYBIŃSKA [a, b]

[a] *Łukasiewicz Research Network – PORT Polish Center for Technology Development, Poland*
[b] *University of Wrocław, Faculty of Chemistry, Poland*
lukasz.duda@port.lukasiewicz.gov.pl

Surface relief grating (SRG) structures may be fabricated in hydrogen bond complexes of a polymer with an azo-dye in a holographic setup – utilizing two interfering laser beams (Fig. 1) [1]. Fabricated surface patterns can be transferred into a target film through preparation of a soft elastomeric stamp (PDMS). Replication of the pattern may be performed in *e.g.* thermoplastic polymer films by means of thermal nanoimprint lithography (TNIL) [2].

Tuning of geometry in the holographic setup allows for fabrication of the structures with various spatial periodicity. Differential visual effect of the fabricated patterns is specific and can be used in originality protection features. Finding reliable materials for both fabrication and reproduction of the grating structures seems to be important technological aspect.

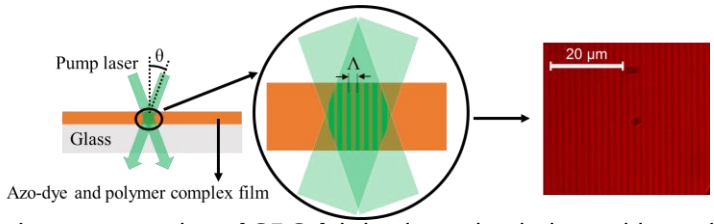

Fig. 1 Schematic representation of SRG fabrication using holographic method and optical microscopy image of a grating fabricated in thin film of azo-dye and polymer complex.

In this work, we present the results of the grating structures fabrication in different polymer films using different methods. Poly(4-vinyl pyridine) (P4VP) films doped with various azo dyes, as well as other azo materials were employed for the laser inscription. In such films, the grating structures were fabricated using two interfering laser beams. Then, using thermal nanoimprint lithography (TNIL), the grating structures were reproduced in thin submicrometric poly(methyl methacrylate) (PMMA) and poly(vinyl alcohol) (PVA) films with various thickness. Diffraction efficiency of the reproduced gratings strongly depends on parameters of the transfer process *e.g.* temperature. It was found, that thickness of the films does not influence the diffraction efficiency of the replicated gratings. Further work is being carried out to accelerate and enhance the process of the inscription of the periodic structures and their transfer to various type of the substrates.

References:

[1] Sobolewska, A. et al., High-Modulation-Depth Surface Relief Gratings Using s–s Polarization Configuration in Supramolecular Polymer–Azobenzene Complexes, The Journal of Physical Chemistry C, 118, **2014**, 23279-23284.

[2] Yabu, H. et al., Thermal nanoimprint lithography of polymer films on non-adhesive substrates by using mussel-inspired adhesive polymer layers, Journal of Materials Chemistry C, 1, **2013**, 1558-1561.

These studies were supported by the National Centre for Research and Development (Poland) within the framework of the 12th edition of the LIDER programme – project contract no. LIDER/39/0203/L-12/20/NCBR/2021

Organic dye-doped systems based on different matrices: properties and potential applications in fluorochromic temperature indicators and photonics

Łukasz DUDA, [a, b] **Maciej CZAJKOWSKI**, [a] **Małgorzata GUZIK**, [a, b]

[a] *Łukasiewicz Research Network – PORT Polish Center for Technology Development, Poland*
[b] *University of Wrocław, Faculty of Chemistry, Poland*
lukasz.duda@port.lukasiewicz.gov.pl

Embedding of organic luminescent dye into some matrices may induce specific interaction between them. This in turn may influence the luminescent properties of the dye due to presence of its different forms *e.g.* separated or aggregated. A variety of organic luminescent dyes and matrices (liquid crystals, polymers) enables for fabrication of different systems with designed properties such as spectral range of emission but also with additional functionalities such as temperature sensitivity [1].

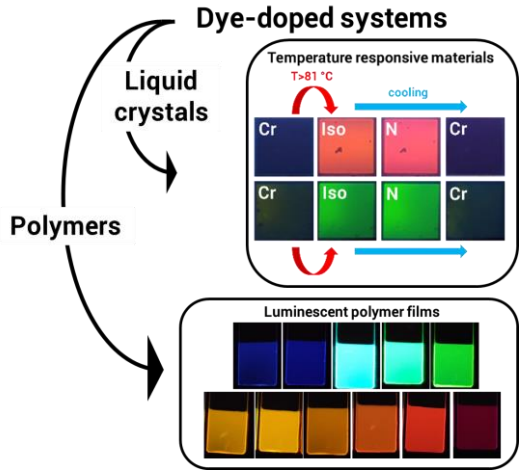

Fig. 1 Photographs of the fabricated dye-doped liquid crystalline and polymer systems for different application.

Here, we describe the systems based on organic luminescent dyes and different matrices (Fig. 1). They may be used for fabrication of thermofluorochromic materials (liquid crystal matrices) or thin films serving as waveguides (polymer matrices). In the selected liquid crystalline matrix a visible change of the luminescent properties upon heating from crystalline (Cr) to nematic (N) or isotropic (Iso) phase was found for selected dyes. This finding served as base for preparation of thermofluorochromic indicators. The studies were performed for the known commercially available dyes but also for the novel dye from diketofurofuran family (DFF). For the latter, detailed studies (*e.g.* determination of solubility and quantum yield of emission) in several crystal and liquid crystal matrices were additionally performed. On the other hand, the properties of the dye-doped polymer films fabricated using the dip-coating method were investigated using profilometry and spectroscopic ellipsometry. Depending on the material, films with different thickness (in the submicrometric range) and refractive index (up to 1.62) were fabricated. The selection of dyes from different families allowed obtaining films emitting in the visible spectral range. Moreover, it was found that the high photoluminescence quantum yield of the dyes could be maintained or drastically decreased in a polymer matrix (compared to the values reported for liquid solutions). The results were dependent on the type of the investigated dye.

References:

[1] Czajkowski M.; et *al*., Novel highly luminescent diketofurofuran dye in liquid crystal matrices for thermal sensors and light amplification, *Journal of Materials Chemistry C*, 11, **2023,** 4426-4438.

The research was supported by the National Science Centre of Poland (NCN) under grant OPUS 16 no. 2018/31/B/ST8/02832. Ł. D. would like to thank the Ministry of Science and Higher Education in Poland for Grant No. DWD/4/64/2020 in the frame of Implementation Doctorate Programme

Structural and spectroscopic properties of nano-crystalline Nd^{3+}-doped $GdPO_4$ obtained by ionic liquid and oleic acid-assisted methods

Jakub PAWŁÓW[a),b)], Maria ZDOŃCZYK[a),b)], Małgorzata GUZIK[a),b)], Georges BOULON[c)], Yannick GUYOT[c)], Magdalena WILK-KOZUBEK[b)], Anja-Verena MUDRING[d)], Joanna CYBIŃSKA[a),b)]

[a)] University of Wrocław, Faculty of Chemistry, Poland
[b)] Łukasiewicz Research Network – PORT Polish Center for Technology Development, Poland
[c)] Institute Light Matter (iLM), Claude Bernard/Lyon1 University, Villeurbanne, France
[d)] Stockholm Univ, Dept Mat & Environm Chem, Sweden
E-mail: jakub.pawlow@port.lukasiewicz.gov.pl

We report the detailed analysis of both structural and spectroscopic investigation of monazite-type Nd^{3+}-doped $GdPO_4$ nano-powders obtained *via* three wet synthesis methods *i.e.* ionic liquid assisted hydrothermal (IL HT) and microwave method (IL MW) as well as oleic acid assisted hydrothermal method (OA HT). Powder X-ray diffraction confirmed that the obtained $GdPO_4$ nano-powders crystallize in a monoclinic system ($P2_{1/n}$) with the average grain size ranging from 40 to 100 nm, the smallest grains are obtained *via* IL MW method, and no other phase has been detected for any of the materials obtained. SEM and TEM were used to demonstrate the differences in the morphology and grain size, which results in the spectroscopic properties of nano-materials. Nine-fold coordinated Gd^{3+} ion in $GdPO_4$ is easily substituted by the Nd^{3+} one with the C_1 symmetry due to their similar ionic radii, so that high-resolution low-temperature absorption and emission spectra do not show any structural distortion. The $^4F_{3/2}$ excited state dynamics studied at 77 K have shown abnormal behavior, similar to that already observed for Nd^{3+} ion embedded in the YPO_4 and $LuPO_4$ tetragonal orthophosphates crystallizing in xenotime-type crystal system [1,2].

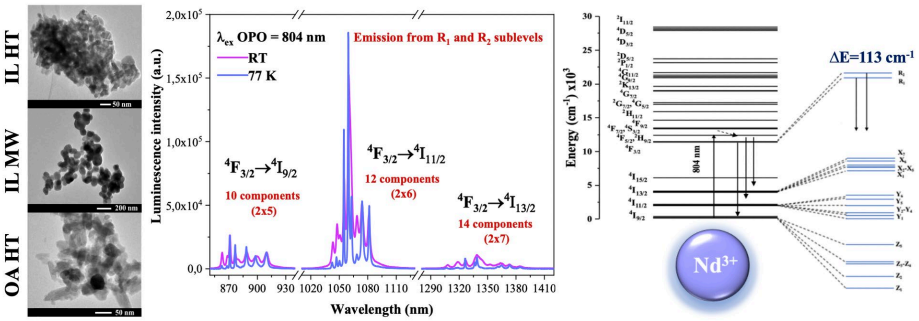

Fig. 1 TEM micrographs, emission spectra and energy level diagram of Nd^{3+}-doped $GdPO_4$ nanoparticles.

References:

[1] J. Pawłów, K.A. Prokop, M. Guzik, Y. Guyot, G. Boulon, J. Cybińska, Nano/micro-powders of Nd^{3+}-doped YPO_4 and $LuPO_4$ under structural and spectroscopic studies. An abnormal temporal behavior of f-f photoluminescence, *J. Lumin.*, 236, 2021, 117997

[2] J. Pawłów, M. Zdończyk, M. Guzik, G. Boulon, Y. Guyot, M. Wilk-Kozubek, A.-V. Mudring, J. Cybińska, Influence of ionic liquid and oleic acid assisted methods on the spectroscopic properties of Nd^{3+}-doped $GdPO_4$ nano-particles, *J. Mat .Chem. C*, accepted 19.04.23.

Acknowledgments:

The research was financed by the NCN Poland Fund within the project HARMONIA 9 UMO-2017/26/M/ST5/00563 and ARQUS (European University Alliance) support from UCBLyon1. J.P. would like to thank the Ministry of Science and Higher Education in Poland for Grant No. DWD/5/0362/2021 in the framework of the Implementation Doctorate Program.

Optimization of photolithography process using negative tone resist towards obtaining high-quality photonic structures

Jakub PAWŁÓW[a),b)], Łukasz DUDA[a),b)], Kacper Albin PROKOP[a),b)], Maria ZDOŃCZYK[a),b)], Krzysztof ROLA[a)], Magdalena ZIĘBA[c)], Paweł KARASIŃSKI[c)], Joanna CYBIŃSKA[a),b)], Małgorzata GUZIK[a),b)]

[a)]Łukasiewicz Research Network – PORT Polish Center for Technology Development, Poland
[b)]University of Wrocław, Faculty of Chemistry, Poland
[c)]Silesian University of Technology, Department of Optoelectronics, Poland
E-mail: jakub.pawlow@port.lukasiewicz.gov.pl

In recent years in the integrated optics field of science scientists were focused on optimizing processes for the mass manufacture of photonic devices [1]. One of the most common methods used to obtain waveguide structures in photonic integrated circuits (PICs) is the photolithography process, which is a remarkably efficient technique for microtechnology. It includes several sub-processes such as applying photoresist, exposing to ultraviolet (UV) light and developing the pattern. Conventional photomasks used in photolithography are rigid, fused quartz plates covered with patterned microstructures of an opaque material such as chrome.

In this work, we have investigated the effects of modifying parameters of the photolithography process carried out on soda-lime glass with a SiO_2-TiO_2 layer using fast, negative tone cross-linking photoresists based on polymers. One of the main goals of our research is to create a silica-titania optical waveguide platform and incorporate optical components using etching methods. Photolithography parameters like UV exposure dose, the development time of the resist, as well as dilution of the developer and post-processing hard-bake, were optimized in order to achieve high-quality structures on the analyzed substrates. We believe that this work will be highly beneficial for the researchers working on the photolithography process.

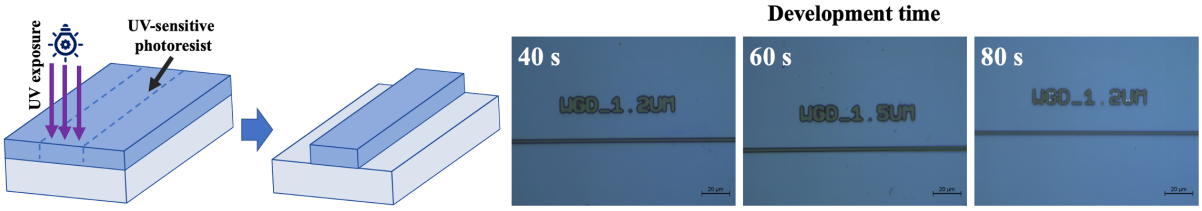

Fig. 1 Scheme of photolithography process and microscope images of obtained structures depending on the development time.

References:

[1] M. A. Butt, C. Tyszkiewicz, P. Karasiński, M. Zięba, A. Kaźmierczak, M. Zdończyk, Ł. Duda, M. Guzik, J. Olszewski, T. Martynkien, A. Bachmatiuk, R. Piramidowicz, Optical Thin Films Fabrication Techniques—Towards a Low-Cost Solution for the Integrated Photonic Platform: A Review of the Current Status, *Materials* 15(13), **2022**, 4591-4616

Acknowledgements:
The research was co-financed by the Foundation for Polish Science from the European Regional Development Fund within the project POIR.04.04.00-00-14D6/18 “Hybrid sensor platforms for integrated photonic systems based on ceramic and polymer materials (HYPHa)" (TEAM-NET program).

Structural and optical properties of dysprosium-doped calcium-oxyapatites $Ca_{10-2x}Dy_xLi_x(PO_4)_6O_2$ $(0 \leq x \leq 1)$

Mohamed MEHNAOUI[a], Rahma NEFZI[a], Yannick GUYOT[b], Gerard PANCZER[b], Riadh TERNANE[a] and Georges BOULON[b]

[a)]*Laboratoire d'Application de la Chimie aux Ressources et Substances Naturelles et à l'Environnement (LACReSNE-LR05ES09), Université de Carthage, Faculté des Sciences de Bizerte, 7021 Zarzouna, Bizerte, Tunisia*

[b)]*Institut Lumière Matière (ILM), UMR-CNRS 5306, Université Lyon1, F-69622 Villeurbanne Cedex, France.*

mehnaouimohamed2005@yahoo.fr

A series of $Ca_{10-2x}Dy_xLi_x(PO_4)_6O_2$ (CDLPO) (x = 0.1, 0.2, 0.3, 0.4 and 1) phosphors was synthesized successfully via a solid-state method at high temperature. The effects of synthesis parameters, Dy^{3+}concentration and charge compensator Li^+ co-doping on the structural and vibrational properties of CDLPO samples were investigated.

The structural and morphological studies of the CDLPO phosphors were carried out by X-ray diffraction (XRD), Infrared spectroscopy, Raman scattering spectroscopyand Scanning Electron Microscopy (SEM). Calcium-oxyapatite system shows a common apatite structure and occurs as a continuous solid solution.

According to the Dy^{3+}emission spectra, two different cation sites have been identified in this apatite structure. Two emission bands of the Dy^{3+} ion are observed, the blue band (460–500 nm) corresponding to the $^4F_{9/2} \rightarrow {}^6H_{15/2}$ transition and the yellow band (550–600 nm) due to the $^4F^{9/2} \rightarrow {}^6H_{13/2}$ transition . The overlap between the emission band of one site and the excitation band of the other site corresponds to an energy transfer phenomenon (Fig. 1). Correlations between the luminescence results and the structural data are discussed.

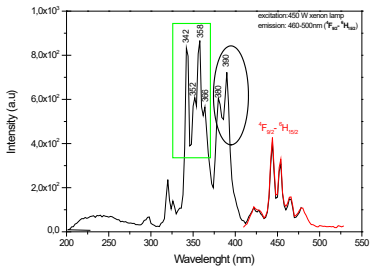

Figure 1. Excitation (black line) and emission (red line) spectra of$Ca_{9.2}Dy_{0.4}Li_{0.4}(PO_4)_6O_2$ sample at room temperature.

New transparent optical ceramics based on isotropic and anisotropic oxide structures - challenges and perspectives

M. GUZIK,[a),b)] K.A. PROKOP [a),b)], J.PAWŁÒW [a),b)], M. WILK,[b)]
E. TOMASZEWICZ,[c)] S. COTTRINO,[d)] V. GARNIER,[d)] G. FANTOZZI,[d)]
S. Le FLOCH [e)], O.BOISRON[e)], Yannick GUYOT,[e)] Georges BOULON[e)]

[a)]Łukasiewicz Research Network - PORT Polish Center for Technology Development, Poland [b)]University of Wrocław, Faculty of Chemistry, Poland
[c)]West Pomeranian University of Technology in Szczecin, Poland
[d)]Univ Lyon, INSA Lyon, UCBL, CNRS, MATEIS, UMR 5510, France
[e)]iLM, UMR 5306 CNRS-University Claude Bernard/Lyon1, France
e-mail: goguzik@poczta.fm

Transparent ceramics with high optical quality are used in various applications, including industrial processing, medicine, aerospace, and high-power laser physics owing to the superior features of ceramics such as enlargement, ease of compositing, uniformity, high concentration of soluble active elements and high mechanical strength. However, so far, only a few compositions of transparent ceramics are well-developed. Transparent polycrystalline ceramics with cubic crystal structures have played important roles in a wide variety of solid-state laser applications, whereas for non-cubic structures, single crystal only has been used. Most transparent ceramics have a cubic crystal structure, and the development of novel ceramics with advanced mid-infrared lasing, magneto-optic properties, scintillation or lighting capability is still being actively pursued.

In general, it is very difficult to achieve high transparency in sintered polycrystalline ceramics due to the various defects that remain after sintering, such as pores, vacancies, secondary phases, impurities, grain boundaries and surface roughness which acts as a light-scattering source.

Here, we present the results of many attempts to obtain sintered polycrystalline ceramics showing transparency from both oxide materials crystallizing in a cubic crystal system as well as in a non-cubic one. For sintering were used nano and micro-powders un-doped and doped with Nd^{3+} ion, which is a very important ion from the potential application point of view *i.e.* as a laser dopant and as a structural probe. The tests were carried out using both a very simple vacuum sintering method as well as a much more advanced Spark Plasma Sintering (SPS) technique. This method is efficient to consolidate ceramics at low temperatures in a short time and made it possible to obtain transparent materials.

Acknowledgments:
The research was financed by NCN Poland in the frame of HARMONIA 8 project No UMO-2016/22/M/ST5/00546, NAWA Poland in the frame of Bekker program PPN/BEK/2020/1/00350/U/00001, NAWA Poland Project N1 PPN/BIL/2018/1/00214/U/00020 and MEAE MESRI France project N1 42883SM, as well as ARQUS (European University Alliance) with support from UCBLyon1. K.A.P. would like to thank the Ministry of Science and Higher Education in Poland for Grant No. DWD/5/0362/2021 in the framework of the Implementation Doctorate Program.

Silicon optomechanical crystal cavities for microwave signal processing and biosensing

Laura MERCADÉ, [a,b] Daniel NAVARRO-URRIOS, [b] Alejandro MARTÍNEZ, [a]

[a] Nanophotonics Technology Center, Universitat Politècnica de València, Camino de Vera s/n, 46022 Valencia, Spain [b] MIND-IN2UB, Departament d'Enginyeria Electrònica i Biomèdica, Facultat de Física, Universitat de Barcelona, Martí i Franquès 1, Barcelona 08028, Spain; laumermo@ntc.upv.es

Optomechanical cavities have become an increasingly important area of research in recent years, with the potential to enable new technologies in fields ranging from quantum computing to sensing and telecommunications [1]. Utilizing a blue-detuned laser to operate an optomechanical cavity can produce fascinating physics and phenomena. One such phenomenon is phonon lasing, which causes the input light to be modulated by a collection of high-purity harmonics that originate from the mechanical resonance of the cavity's fundamental tone [2]. This paper explores how this phenomenon can be utilized to process wireless signals in the optical domain. We demonstrate that by using a silicon optomechanical crystal cavity with a mechanical breathing mode around 4 GHz, we can generate a microwave tone with low phase noise (< -100 dBc/Hz at 100 kHz), making it suitable for practical applications such as satellite communications. We also discuss how the system's stability can be improved by locking two different mechanical modes and bringing them into the phonon lasing states. Moreover, we show that the cavity acts as a nonlinear mixer, making it possible to perform frequency up-conversion on realistic data streams that comply with wireless communication standards [3]. Our findings suggest that ultra-compact optomechanical cavities have the potential for use in the next generation of wireless networks and satellite communications. However, applications in biosensing have also been explored in many optomechanical systems. Specifically, the use of those type of optomechanical crystal cavities as optical and mechanical sensors could be integrated in photonic integrated circuits using cost-effective silicon technology, and providing a better sensing performance that separated photonic and mechanical devices.

References:

[1] Aspelmeyer, M.; Kippenberg, T.J.; Marquardt, F., Cavity Optomechanics. *Reviews of Modern Physics,* Vol., **86,** 1391 (2014).

[2] Mercadé, L.; Martín, L. L.; Griol, .; Navarro-Urrios, D.; Martínez, A., Microwave oscillator and frequency comb in a silicon optomechanical cavity with a full phononic bandgap. *Nanophotonics* Vol. 9, 11 (2020)

[3] Mercadé, L.; Morant, M.; Griol, A.; Llorente, R.; Martínez, A., Photonic Frequency Conversion of OFDM Microwave Signals in a Wavelength-Scale Optomechanical Cavity. *Laser & Photonics Reviews*, 15, 2100175 (2021)

Recent progress on GAGG (Ce,Mg) single crystal growth and their performance for high energy physics.

Kheirreddine Lebbou

Institut Lumière Matière, UMR 5306 Université Lyon1-CNRS, Université de Lyon, Lyon, 69622, Villeurbanne Cedex, France
Kheirreddine.lebbou@univ-lyon1.fr

Abstract

Because of the well-developed crystal growth technology under stationary stable regime, (Ce,Mg)-codoped GAGG single crystal, which has garnet structure are promising candidate for scintillator applications. In addition, (Ce,Mg) ions-doped gadolinium aluminum gallium garnet crystal (Ce^{3+},Mg^{2+}:$Gd_3Al_2Ga_3O_{12}$, Ce^{3+},Mg^{2+}:GAGG) as inorganic oxide material has the advantages of high density, large effective atomic number, high light yield, good energy resolution, fast decay time, and stable physical and chemical properties. With the objective to investigate the feasibility to built a calorimeter based on GAGG assembly single crystal, the effects of the doping concentration (Ce,Mg) and the use of various co-dopant on the light output and the timing properties of GAGG were studied. In the frame of this work, deferent GAGG single crystals were grown (**Figure 1**) as bulk crystal and single crystal fibers by Czochralski and micro-pulling down techniques. They are well characterized to investigate the impact of the composition and the growth parameters on the crystal performance to be used for the next generation of calorimeter for the high energy physics.

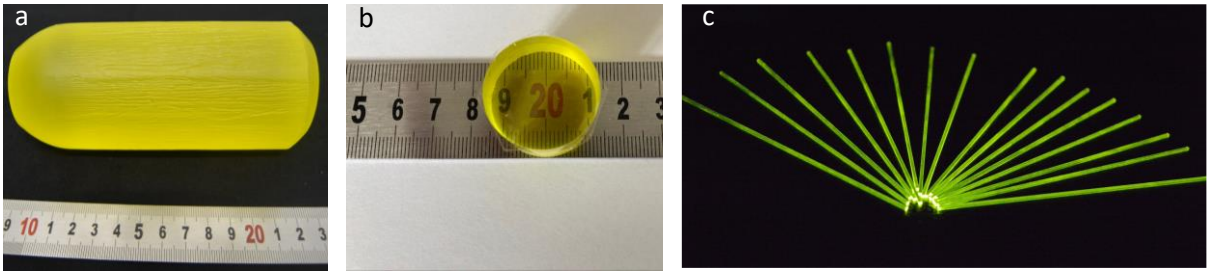

Figure 1 . (a) (Ce,Mg) GAGG crystal grown by Cz, (b) polished (Ce,Mg)GAGG crystals and (c) (Ce,Mg)GAGG single crystal fibers under UV light (263 nm) .

Acknowledgment

This research work is the frame of international collaboration regrouping ILM (Lyon), CERN (Switzerland), ISMA (Ukraine) and SIPAT (China). The work was supported by IRP CNRS research project and TWISMA European project. We are very grateful for their support.

“Chirality at the molecular scale: materials and spectroscopy”

Amina BENSALAH-LEDOUX, [a] Bruno BAGUENARD [a], Hoshang SAHIB [a], Alban GASSENQ [a], Laure GUY[b] and Stéphan GUY [a]

[a] *Institut Lumière Matière, UMR CNRS 5306 ; Université de Lyon, CNRS-Université-Lyon 1, 69622 Villeurbanne Cedex, France*
[b] *Laboratoire de Chimie; Ecole Normale Supérieure de Lyon, 46 Allée d’Italie, 69364 Lyon, France*
amina.bensalah@univ-lyon1.fr

Chirality is a property of symmetry that occurs at all scales. Two objects are chiral if their mirror images do not overlap. In living organisms, chirality has an essential importance, since most of the mechanisms of molecular recognition or biological signal transmission are triggered by this asymmetry. Chirality, at the molecular scale, also plays a fundamental role in the light-matter interaction. We speak of "electromagnetic chirality" for a medium filled with chiral objects, of sub-wavelength size. It is this "electromagnetic chirality" that is at the heart of our research works, through the design, realization and study of chiral materials in the solid state, generally in the form of thin films or powders, but also in solution.

In this context, we develop at ILM within the MNP team, two themes around chirality at the molecular scale: (i) Chiral integrated optics. Here, we want to free planar photonics from the linear polarization diktat, using chiral materials with very high rotational power; (ii) chiral spectroscopies that we have developed in order to study different chiral systems. Our collaboration with colleagues from Strasbourg University provides a nice example of these investigations mixing chiroptical and linear anisotropy properties, applied to soft mechanochemistry.

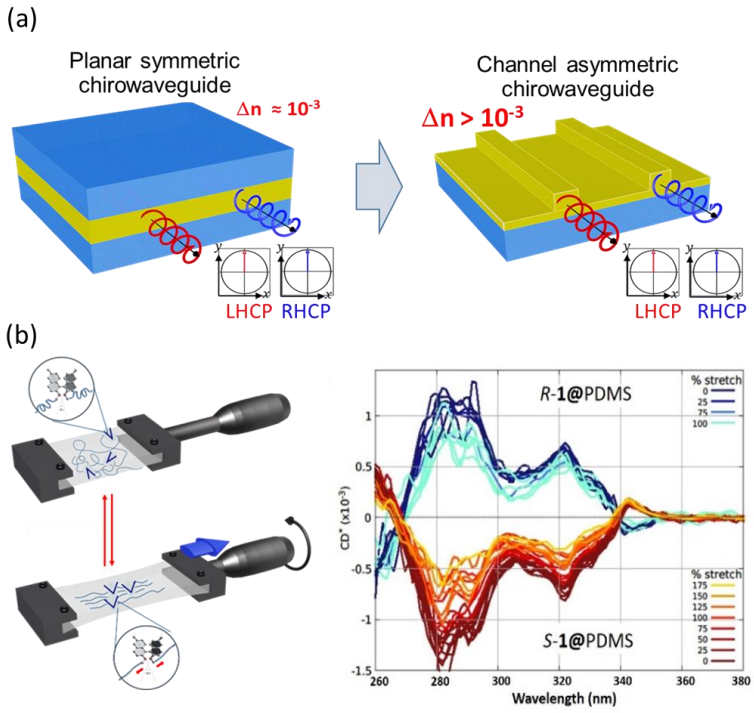

Figure: (a) Planar and Chanal chirowaveguides with circularly polarized eigenmodes, (b) Circular dichroism variation of doubly linked BINOL in PDMS under stretching

Crucible-free bulk crystal growth of oxide single crystals using OCCC method

Akira Yoshikawa[a,b,d], Vladimir V. Kochurikhin[d], Taketoshi Tomida[d], Masao Yoshino[b], Isao Takahashi[b,d], Rikito Murakami[a,d], Takahiko Horiai[b,d], Kei Kamada [b,d], Shunsuke Kurosawa [b], Yuui Yokota[a], Yuji Ohashi[b], Yasuhiro Shoji[d], Akihiro Yamaji[b], Romana Kucerkova [c], Alena Beitlerova[c], Martin Nikl[c]

Institute for Materials Research, Tohoku Univ., Sendai, Japan [a)]
New Industry Creation Hatchery Center, Tohoku University, Sendai, Japan [b)]
Institute of Physics AS CR, Cukrovarnicka 10, 162 53 Prague, Czech Republic [c)]
C&A Corporation, Sendai, Japan [d)]

presenting author e-mail: akira.yoshikawa.d8@tohoku.ac.jp*

Recently it has been found that the Mg^{2+} codoping in Ce doped $Gd_3(Ga,Al)_5O_{12}$ (GAGG:Ce) has increased the light yield and accelerated scintillation decay [1-3]. These effects need further systematic study for full understanding. The detailed discussion is being carried out based on the influence of co-doping, induced host defects, and cerium charge state. So far, the GAGG-based crystals are grown under the Ar or N_2 atmosphere. This enerates large amount of oxygen vacancies and Ga vacancies in the crystal. Such a growth atmosphere is necessary to protect the iridium crucible from oxidation.

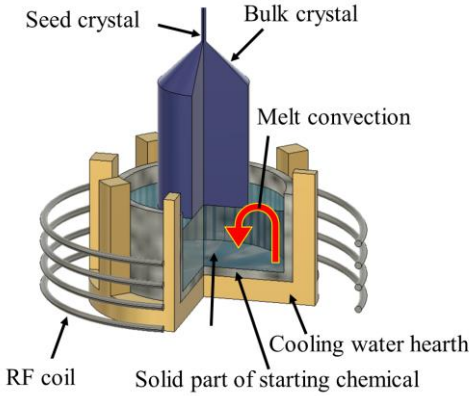

Fig.1 Schematic image of OCCC method.

We report the growth of Ce:GAGG single crystals based on crystal pulling from a melt using a cold container without employing a precious-metal crucible [4-8]. This novel method is described in detail. We have labeled the proposed method, which is a fusion of the skull-melting and CZ methods, the “oxide crystal growth from cold crucible (OCCC)” method. The scintillation properties of the OCCC-grown Ce:GAGG crystals were compared with those of crystals grown by the conventional CZ technique. The best samples from the set are fully comparable in all characteristics with the commercial reference crystal, demonstrating the practical potential of this method. Avoidance of an expensive precious-metal crucible in this method makes crystal growth much more economical [9].

References:

[1] K. Kamada, A. Yoshikawa et al., Cryst. Growth Des., **2011**, 11 (10), 4484–4490.
[2] M.Nikl, A. Yoshikawa Adv. Opt. Mater 3(**2015**)463-481.
[3] P. Sibczynski et al., Nucl. Instrum. Meth. A., vol. 772 (**2015**) 112–117.
[4] Sterling, H. F.; Warren, R. W., Metallurgia **1963**, 67, 301–307.
[5] B. Gayet, J. Holder, G. Kurka: Rev. Haut. Temp. Reftact. **1964**, 1, 153–157 .
[6] Aleksandrov, V. I. et al., *Izvestiya Akademii Nauk SSSR, Neorg. Mater.* **1983**, 19, 104-107
[7] Aleksandrov, V. I. et al., Mayer, *Russ. J. Inorg. Chem*. **1990**, 35, 878–883.
[8] Osiko, V. V.; et al., *Ann. Rev. Mater. Sci.* **1987**, 17, 101–122.
[9] A. Yoshikawa et al., *Cryst. Growth Des.* **2023**, 23, 4, 2048–2054

BiBO: An Effective Nonlinear Crystal for Femtosecond Optical Parametric Oscillators

Masood GHOTBI[a, b], Delnia POURGHOBAD[a], Xavier MATEOS[b]

[a)] University of Kurdistan, Physics Department, Pasdaran St., Sanandaj, Iran
[b)] Universitat Rovira i Virgili (URV), Física i Cristal-lografia de Materials (FiCMA), 43007 Tarragona; massood.ghotbi@urv.cat

Tunable sources of ultrashort laser pulses based on efficient nonlinear materials have a lot of applications in different scientific, medical and industrial applications [1]. BiB_3O_6 (BIBO) is one of the last nonlinear crystals that because of its flexible phase-matching (PM) possibilities, relatively low group velocity mismatches and large effective nonlinear coefficients has proved its strong performance for generating tunable femtosecond pulses in the visible and near-IR spectral ranges [2,3]. Although, the biaxial structure of this crystal makes some complicities for using its full capacity in its different optical planes.

As the first demonstration of a synchronously pumped femtosecond optical parametric oscillator (SPOPO) based on BIBO, we demonstrated a visible femtosecond SPOPO, pumped by the femtosecond blue pulses at 400 nm, produced as the second harmonic of the output of a Kerr-lens mode-locked (KLM) Ti:sapphire laser with 76 MHz repetition rate [3]. In this SPOPO which had a signal output, tunable across the visible spectral range of 500-700 nm, with <150 fs pulses, type I ($e \rightarrow o + o$) PM in the *yz* optical plane of BIBO was applied. The intracavity frequency doubling of this SPOPO resulted in producing tunable femtosecond pulses across the UV spectral range of 250-350 nm [4]. Later a Near-IR SPOPO directly pumped by Ti:sapphire laser at 800 nm inside the *xz* optical plane of BIBO was reported [5].

After the introduction of higher power KLM Yb:KGW laser family, a high power SPOPO using ($o \rightarrow e + e$) PM in the *yz* optical plane and pumped by 515 nm green pulses, producing signal and idler pulses in the spectral ranges of 688-1057 nm and 1150-1900 nm respectively, was reported [6]. Taking advantage of the full capabilities of the green-pumped SPOPO based on BIBO requires the application of the PM inside its *xz* optical plane also, as an important part of the tunability of signal and idler pulses that can be produced by BIBO.

Recently we have presented the application of ($e \rightarrow o + o$) phase matching scheme in a high power SPOPO inside the *xz* optical plane of BIBO. The pump laser was a Yb:KGW that can produce up to 6.8 W of average power with ~100 fs pulses and 76 MHz repetition rate. More than 3.5 W of second harmonic green femtosecond pulses that were generated inside a 1-mm thick BIBO crystal were applied as the pump pulses for our SPOPO. The OPO produces signal and idler pulses in the spectral ranges of 620-695 nm for signal and 1988-3040 nm for idler pulses. The generated signal power range, is from 700 mW at the shortest wavelength of 620 nm (limited by transparency of the corresponding idler pulse) up to 1 W at higher wavelengths. The compressed signal pulses have durations as short as 35 fs.

References:

[1] Vengelis. J, Stasevicius. I, Stankeviciute. K, Jarutis. V, Grigonis. R, Vengris. M, and Sirutkaitis. V, "Characteristics of optical parametric oscillators synchronously pumped by second harmonic of femtosecond Yb:KGW laser," Opt. Commun. 338, **2015,** 277.

[2] Ghotbi. M and Ebrahim-zadeh. M, "Optical second harmonic generation properties of BiB_3O_6," *Opt. Express*, 12, **200**4, 6002-6004.

[3] Ghotbi. M, Esteban Martin, A and Ebrahim-zadeh. M, "Optical second harmonic generation properties of BiB_3O_6," *Opt. Express*, 31, **2006,** 3128-3130.

[4] Ghotbi. M, Esteban Martin, A and Ebrahim-zadeh. M, " Tunable, high-repetition-rate, femtosecond pulse generation in the ultraviolet," Opt. Express, 33, **2008**, 345-347.

[5] Ghotbi. M, Esteban-Martin. A, and Ebrahim-Zadeh. M, Ti:Sapphire-pumped Infrared Femtosecond Optical Parametric Oscillator Based on BiB_3O_6, Conference on Lasers and Electro-Optics CLEO'07, Baltimore (MD), USA, 2007, paper JWA31, in: CLEO/QELS Tech. Digest CD-ROM.

[6] Tian. W, Wang. Z, Meng. X, N Zhang, Zhu. J, Wei. Z, "High-power, widely tunable, green-pumped femtosecond BiB_3O_6 optical parametric oscillator," Opt. Lett. 41, **2016,** 4851-4554.